1986

Nonphotochemical hole burning of organic dyes and rare earth ions in polymers and glasses: a probe of the amorphous state

Bryan Leo Fearey
Iowa State University

INFORMATION TO USERS

This reproduction was made from a copy of a manuscript sent to us for publication and microfilming. While the most advanced technology has been used to photograph and reproduce this manuscript, the quality of the reproduction is heavily dependent upon the quality of the material submitted. Pages in any manuscript may have indistinct print. In all cases the best available copy has been filmed.

The following explanation of techniques is provided to help clarify notations which may appear on this reproduction.

1. Manuscripts may not always be complete. When it is not possible to obtain missing pages, a note appears to indicate this.

2. When copyrighted materials are removed from the manuscript, a note appears to indicate this.

3. Oversize materials (maps, drawings, and charts) are photographed by sectioning the original, beginning at the upper left hand corner and continuing from left to right in equal sections with small overlaps. Each oversize page is also filmed as one exposure and is available, for an additional charge, as a standard 35mm slide or in black and white paper format.*

4. Most photographs reproduce acceptably on positive microfilm or microfiche but lack clarity on xerographic copies made from the microfilm. For an additional charge, all photographs are available in black and white standard 35mm slide format.*

***For more information about black and white slides or enlarged paper reproductions, please contact the Dissertations Customer Services Department.**

Fearey, Bryan Leo

NONPHOTOCHEMICAL HOLE BURNING OF ORGANIC DYES AND RARE EARTH IONS IN POLYMERS AND GLASSES: A PROBE OF THE AMORPHOUS STATE

Iowa State University PH.D. 1986

PLEASE NOTE:

In all cases this material has been filmed in the best possible way from the available copy. Problems encountered with this document have been identified here with a check mark __✓__.

1. Glossy photographs or pages _____
2. Colored illustrations, paper or print _____
3. Photographs with dark background _____
4. Illustrations are poor copy _____
5. Pages with black marks, not original copy _____
6. Print shows through as there is text on both sides of page _____
7. Indistinct, broken or small print on several pages __✓__
8. Print exceeds margin requirements _____
9. Tightly bound copy with print lost in spine _____
10. Computer printout pages with indistinct print _____
11. Page(s) _____ lacking when material received, and not available from school or author.
12. Page(s) _____ seem to be missing in numbering only as text follows.
13. Two pages numbered _____. Text follows.
14. Curling and wrinkled pages _____
15. Dissertation contains pages with print at a slant, filmed as received _____
16. Other _____

_____

_____

University
Microfilms
International

Nonphotochemical hole burning of organic dyes and rare earth ions in polymers and glasses: A probe of the amorphous state

by

Bryan Leo Fearey

A Dissertation Submitted to the
Graduate Faculty in Partial Fulfillment of the
Requirements for the Degree of
DOCTOR OF PHILOSOPHY

Department: Chemistry
Major: Physical Chemistry

Approved:

Signature was redacted for privacy.

In Charge of Major Work

Signature was redacted for privacy.

For the Major Department

Signature was redacted for privacy.

For the Graduate College

Iowa State University
Ames, Iowa

1986

TABLE OF CONTENTS

GENERAL INTRODUCTION

Historical Overview of Optical Hole Burning

To attain a full understanding of the topics to be covered within this thesis dissertation, one should first have a basic understanding of the generalized phenomenon of optical hole burning. Further, since optical hole burning can describe many quite distinct phenomena, the distinctions between different hole burning techniques need to be examined. To fully appreciate some of the advances and nuances of optical hole burning, a brief description of the historical development and advances of hole burning will be given.

The phenomenon of optical hole burning can be described generally as a localized population depletion, at a particular transition frequency, due to a monochromatic excitation into some optical transition. Since these holes are localized around the excitation frequency, the transition of interest must be inhomogeneously broadened. Thus, using this phenomenon, one can envisage the possibility of reducing or eliminating the inhomogeneous line broadening of spectral lines and in turn, obtain dynamical information about the system of interest.

Optical hole burning, within the above definition, can be divided into two types: one type associated with depopulation of the ground (or lower) state of a transition giving localized holes in the absorption spectrum and the other associated with excited (or upper) state population depletion also producing holes but in the emission spectrum.

The latter type of optical hole (in the emission spectrum) was first observed by Hughes [1] and Kisliuk and Walsh [2] in 1962, as an

intensity decrease of a ruby laser at the peak of the gain curve (ω_0). This was later interpreted [3,4] as being due to selective spatial depletion of excited states resonant with ω_0 at the positions of maximum amplitude of the standing wave defined by the laser cavity. Similarly, the laser intensity of a helium-neon laser also was found to decrease [5] and was explained [5,6] as the depletion of excited neon atoms with velocities near the peak of the Doppler profile for the laser transition. These holes or dips were first theoretically predicted by W. E. Lamb, Jr. in 1962 and was one of the primary results of his theoretical paper in 1964 [6]. Further, holes burned via this method have become known as "Lamb dips".

Although optical holes in the emission spectrum were the first to be observed, with the advent of more intense monochromatic sources, i.e. lasers, significantly more examples of hole burning due to ground state population depletion were discovered. The first example of this type of hole burning was seen by Lee and Skolnick [7] in 1967 for a neon absorption excited with a He-Ne laser detected by the Lamb-dip technique (see reference 8 for a basic review of the technique).

Saturation hole burning of the absorption spectrum in the solid state was first obtained by Szabo in 1975 for ruby [9]. Saturation hole burning was subsequently used to obtain high resolution absorption, Zeeman, Stark and hyperfine spectra of metal atoms in solid systems [9-13]. Saturation hole burning can also occur in solutions of organic dyes [14] (this technique is now widely used for the passive mode locking of dye lasers [15]), in solutions of aromatic hydrocarbons [16] and

in the zero-field spectra of triplet states [17], each providing dynamical information about the particular system studied. In addition, a related hole burning technique is population hole burning (or triplet bottleneck hole burning) in which the triplet state builds up at the expense of the ground state [18,19].

An important distinction between the above optical hole burning and persistent hole burning is that all of the above techniques are transient in nature. That is, the burned holes decay or fill rapidly, returning to the equilibrium populations before the application of the saturating beams.

Since the subject of this thesis is persistent hole burning, that is, the formation of permanent optical holes in frequency space (at least over the period of the experiment), a discussion of how to make this occur is in order. To create persistent holes, the processes which allow holes to fill must be removed. Permanent holes, which occur in the absorption transitions, are burned, as above, when the absorbing species are removed from a particular excitation frequency. This can occur either by the destruction of the species or by inducing their absorptions to be shifted away from the particular excitation frequency. In order to prevent the rapid refilling of these holes, the diffusion processes must be halted via rigid media and (with one exception [20]) low temperatures.

Basically, there are two manners which can lead to persistent hole burning: (1) photochemical hole burning (PHB) and (2) the subject of

this thesis, nonphotochemical hole burning (NPHB).[1] The former, perhaps, is the most easily understood since the photochemically induced product will have a new absorption at some different wavelength well removed from the excitation frequency. However, due to the required rigidity of the media, photochemistry requiring gross molecular rearrangements is inhibited except under severe conditions (i.e., extremely high laser flux). Thus, in general, PHB occurs only for species which can form stable photoproducts and do not require large structural changes. Photochemical hole burning was first observed by Gorokhovskii et al. in 1974 [21] and involved the molecular rearrangement of H_2-phthalocyanine in n-octane, where the inner protons of the porphin-like ring undergo photoinduced tautomerization. Many studies have since been performed on porphin-like molecules. PHB can also occur via photodissociation and was first observed by deVries and Wiersma [22] in 1976 for the system of s-tetrazine in a durene host crystal.

Another manner in which persistent optical holes can be formed is called nonphotochemical hole burning (NPHB), sometimes referred to as photophysical hole burning. This technique induces the absorption transition energy of the impurity to be altered slightly due to some excitation, leading to a hole coincident with the excitation frequency.

---

[1] Although the actual distinction between these two types of hole burning is often quite hazy, for purposes of this thesis they shall be referred to separately. It is possibly better to think in terms of a continuum of hole burning mechanisms, ranging from molecular photodissociation, molecular intramolecular photochemical changes, molecular intermolecular photochemistry to only matrix rearrangements, vide infra.

Importantly, this method is thought to change only the particular environment of the impurity and not the impurity itself, ergo, the name nonphotochemical. The mechanism whereby this occurs is discussed in the next section. NPHB was first directly observed by Kharlamov et al. in 1974 [23] in the absorption spectra of acridine and 9-amino-acridine in an ethanol glass at liquid helium temperatures. The hole production resulted from the narrow line laser irradiation into the impurity's vibronic absorption band associated with the lowest singlet (S_0) absorption system. The kinetics of the hole burning process were studied in order to determine the mechanism of NPHB [24]. The rate of formation was found to be nonexponential due to the fact that the hole burning sites burn with different hole burning rates. Modeling showed that the burning was a one-photon process. In 1978, little was understood about the mechanism of NPHB except the fact that it was a one-photon process [24]. A nonphotochemical mechanism for the production of holes was first proposed by Hayes and Small in a series of papers in 1978 and 1979 [25-27]. This general mechanism has been accepted in principal and has been examined in detail in several papers and reviews [28-30]. The basic mechanism is briefly discussed in the following section.

A review of many of the systems which have been shown to undergo either NPHB or PHB will be given below including much more current studies of the phenomenon of persistent hole burning.

Finally, to conclude this section, some of the important informational aspects of persistent hole burning need to be enumerated. First

and foremost is the fact that this is a site selective type of spectroscopy, vide infra. That is, when one burns with some excitation source, usually a laser, the hole that forms can be related directly to the homogeneous linewidth of a particular impurity molecule. From this linewidth, then, it is possible to obtain the dephasing times for these molecules at low temperature. Second, with this site selective technique, the homogeneous linewidth can be monitored as a function of temperature giving important dynamical information about the microscopic state. Third, this selective spectroscopy can be used to study a very small subset of the entire ensemble of sites since only those sites whose energies happen to overlap the excitation frequency are burned out. With this subset, one can then perform quite varied and diverse experiments studying the effects of electric (Stark hole burning) and magnetic (Zeeman hole burning) fields on the hole probing aspects of the amorphous medium. Further, the relationship of this subset to other subsets can be probed with both spontaneous hole burning and laser induced hole burning, vide infra.

Lastly, to give a couple of more practical applications for persistent hole burning, the technique has been considered as a possible optical communication filter and is presently being avidly pursued as a high density computer memory device. Thus, the techniques of PHB and NPHB both have significant portent in understanding and exploring a large variety of important physics and physical applications.

Basic Mechanism of Nonphotochemical Hole Burning

Before discussing in detail the mechanism of NPHB, the nature of the host materials needs to be discussed briefly. In persistent hole burning, the host material must be disordered in character and indeed this is what makes NPHB and PHB such powerful techniques to probe this media. The nature of disordered solids, e.g., glasses, polymers, etc., is fundamental to the understanding of the mechanism of nonphotochemical hole burning. That disordered solids are basically different from that of crystalline materials was evidenced first by Zeller and Pohl in 1971 [31] in measurements of specific heat and thermal conductivity of glasses at extremely low temperatures (i.e., $\lesssim$1 K). Their basic result was that the specific heat showed a linear temperature dependence, while the thermal conductivity showed a quadratic dependence. This result was in contrast to crystals in which both properties show quadratic dependences. In response to these results, Anderson et al. [32] and Phillips [33] proposed that glasses are characterized by atoms or sets of atoms which can exist in nearly isoenergetic configurations, called two level systems (TLS). Recent simulation studies by Stillinger [34], Weber and Stillinger [35], and Stillinger and Weber [36] indicate that indeed TLS are a general attribute of amorphous media.

Although the initial TLS model was proposed to explain only very low temperature phenomena (vide supra), the concept of two level systems has been extended to a variety of phenomena in glasses (and other amorphous media) where either the magnitude of the temperature dependence or the actual temperature dependence show anomalous behavior relative to

that observed for crystalline materials. Table 1 summarizes some of these anomalous glass properties. As indicated, vide supra, persistent hole burning is a probe of the properties and lends valuable information to the understanding of these phenomena.

In general, the absorption profile of impurities dissolved into amorphous (i.e., disordered) hosts or matrixes show very broad profiles due to site inhomogeneous line broadening. In other words, the site energies of the impurity are perturbed by the disordered environment. Then, in disordered media, there exists a distribution of transition energies (or equivalently, of homogeneous lines) giving broad linewidths relative to crystal-like hosts (this concept is illustrated in Fig. 1). Thus, for a particular absorbing impurity, the absorption energy is extremely sensitive to the solvent (host) structure around it. If this solvent cage shifts slightly, then it is apparent that the transition energy for that impurity is shifted also. A possible driving force for this process is the process of absorption itself. As is evident due to the linewidth broadening, there must be coupling between the solute and solvent. If, during the excited state of the impurity, a transition is induced between the minima of the TLS (vide supra), then the microenvironment around the impurity molecule also is altered which in turn, following deexcitation, changes the absorption energy. The coupling mechanism between the TLS and the impurity is electron-phonon coupling whose strength of interaction is evidenced by the nature of the hole.

Figure 2 illustrates schematically the mechanism of NPHB and uses the common symbols and terms used to discuss NPHB theoretically (vide

Table 1. Comparison of glass and crystal properties

Property	Crystal	Glass	Relative Magnitude[a]
specific heat	T^3	$cT + c'T^3$	larger
thermal conductivity	T^3	$\sim T^2$	smaller
ultrasonic attenuation		saturates	larger
sound velocity	T independent	ln T	10-100 times slower
dielectric constant	T independent	ln T	10-100 times larger
optical linewidth	T^7	$T \Rightarrow T^2$	10-100 times larger

[a]Glass value relative to crystal value.

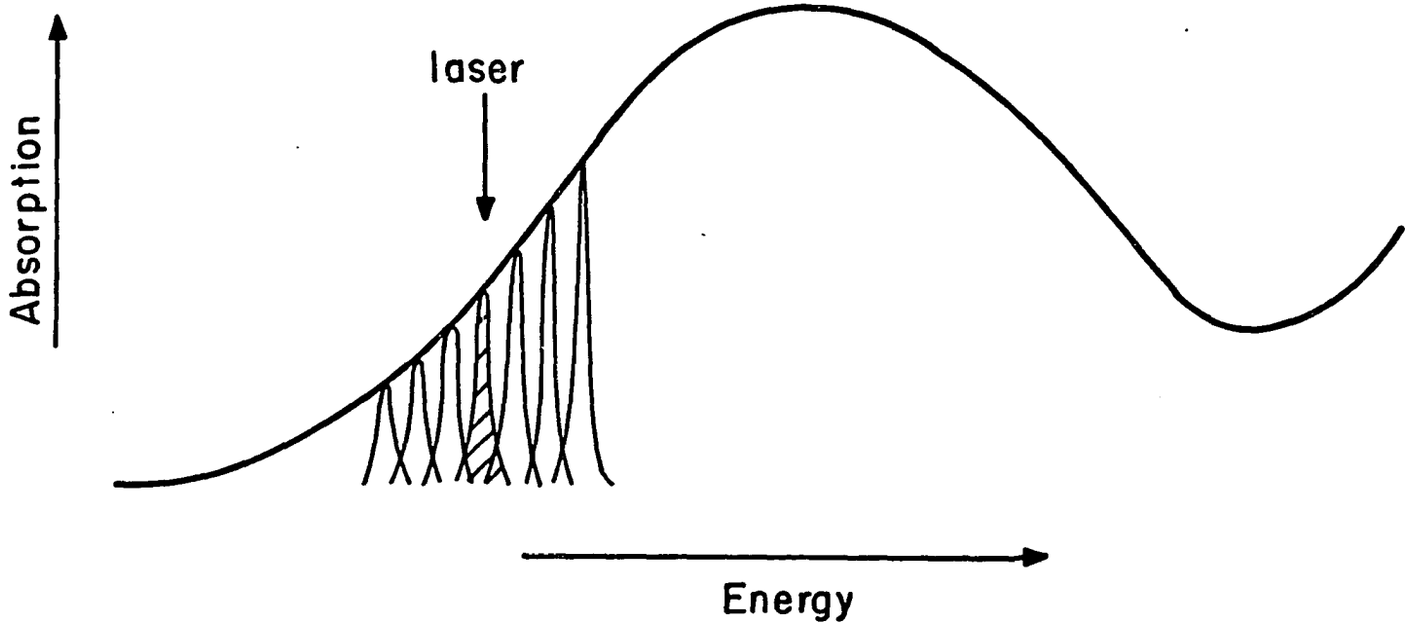

Figure 1. A schematic representation of an impurity doped glass absorption spectrum shows the many narrow site absorptions which are inhomogeneously distributed across the entire absorption band. Irradiation with a narrow frequency laser at the frequency shown results in only selective site excitation of the shaded sites

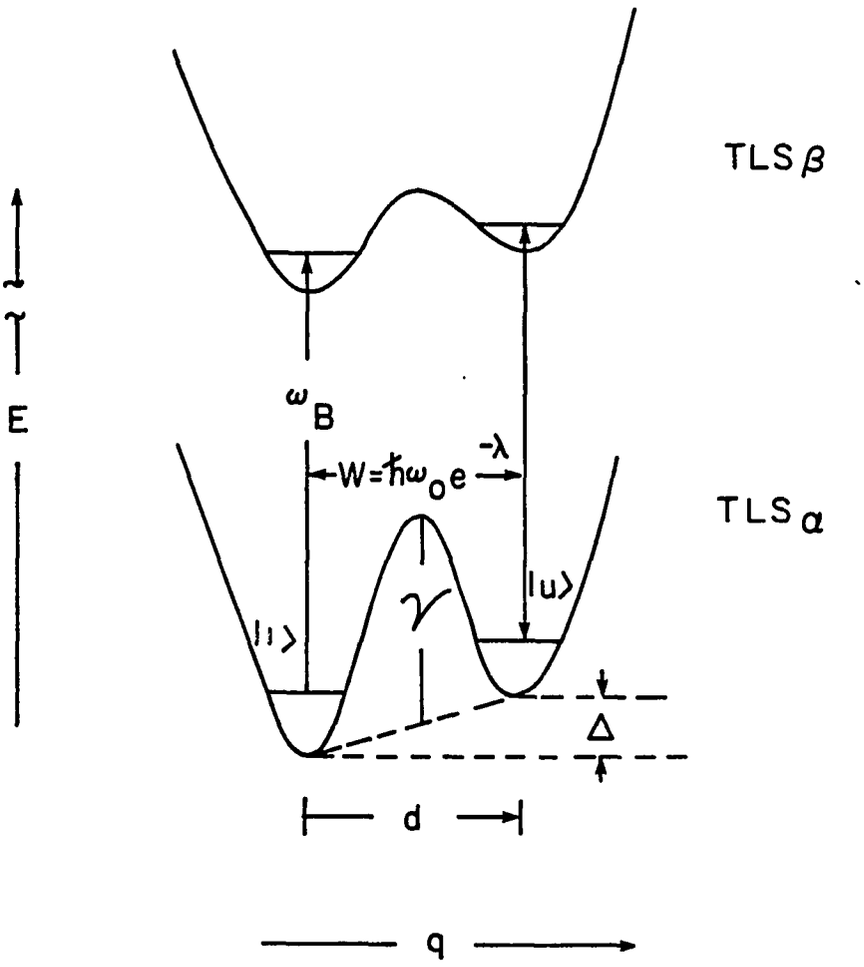

Figure 2. A schematic representation of the potential energy curves (asymmetric double well potential) for a TLS coupled to an impurity in the ground state, α, or excited state, β. The tunneling rate between the well is given by W

infra). This figure depicts the energy level diagram of an impurity coupled to a TLS (an assymetric double potential well). TLS_α represents the electronic ground state of a particular TLS coupled to the impurity molecule[1] while TLS_β represents the excited state, β. The TLS potential energy diagram depicted in Fig. 2 is characterized (similar to that in Refs. 28-30) by a barrier height, V, a zero-point splitting, D, and a potential well separation, d. Each of the parameters is expected to have a distribution of values within a glass. Further, there can be a variety of TLS coordinate values, q. The phenomenon of NPHB occurs due to the fact that, for a small subset of the TLS (at low temperature), the rate of phonon assisted tunneling in the ground state is slow on the time scale of the experiment, while for the impurity in its excited state, interconversion between the tunnel states is fast relative to the impurity's natural lifetime. The increase in the interconversion rate upon excitation is due to the marked decrease in the excited state potential energy barrier. So, in NPHB, an impurity coupled with the TLS can be considered to be located (i.e., trapped) in one of the wells of TLS_α, which upon excitation can convert to the opposite well of TLS_β and remain in that well after deexcitation.

The net effect is that the absolute transition energy of the impurity molecule has been shifted slightly. Now, examining Fig. 1, it becomes apparent that if the frequency linewidth of the excitation

---

[1]Note that from now on "impurity molecule" is used only for clarity and does not preclude other sorts of impurities, e.g., atomic ions, F-centers, etc.

source is less than the homogeneous linewidth of the impurity molecule, then the linewidth of the created hole is directly related to the true homogeneous linewidth of the impurity molecule in the host material.

Overview of Photochemical (PHB) and Nonphotochemical (NPHB) Hole Burning

Since the discovery of persistent hole burning [21], the number of systems known to exhibit either PHB or NPHB has become quite large. However, even though the theory of Hayes and Small would appear to suggest that virtually all amorphous systems should exhibit hole burning this has not been the case [28-30]. Several review papers examining the fundamentals of hole burning and systems which exhibit hole burning have been published [30,37,38]. For a current review, see the book chapter [39] by Hayes, Jankowiak and Small in "Persistent Hole Burning: Science and Applications", Topics in Current Physics, edited by W. E. Moerner (1986). Since there are many well written reviews in the literature on this subject, only an overview of some of the more interesting and important systems shall be presented in this thesis.

A partial cumulative list of the systems which have shown either PHB or NPHB in a variety of host materials is given in Ref. 40 (a more extensive table is given in the Appendix). It is important to point out that this table is by no means comprehensive and only attempts to show the extent and variety of persistent hole burning. The Appendix table also indicates the probable type of hole burning, although for many systems the delineation between NPHB and PHB is rather blurred [39]. In addition, the Appendix table also breaks down the host materials into

various categories in order to indicate some trends. Most apparent is the importance of the hydrogen bonding in the host matrix to NPHB. Although hydrogen bonding is not a requirement to NPHB, the efficiency of these systems is in general much higher than for those without.

Next, some of the more important types of host systems used in NPHB will be discussed, specifically, NPHB in hydrogen bonding crystals, in amorphous acenes, in organic glasses and in polymers. Some of the more unusual and new systems will be discussed in the section following.

Molecules in hydrogen bonding crystals

Although when considering amorphous materials one usually thinks of glasses or polymers, in fact, for NPHB to occur, it is only necessary to have disorder. NPHB has been shown to be operative for systems with impurities doped into the hydrogen bonding crystals of benzoic acid, vide infra. Benzoic acid and related carboxylic acid are known to crystallize as cyclic dimers linked by two hydrogen bonds. Rearrangement of the dimers occurs via simultaneous proton exchange into the tautomeric structure [40,41]. For isolated dimers, the potential energy curve is symmetric, however, in the benzoic acid crystal, the double well is asymmetric [42,43] and, thus, impurities can couple with the host TLS and NPHB can occur. Three different impurities have been doped into this disordered crystal and studied for NPHB; these are: pentacene [44-47], thioindigo [48] and tetracene [49].

The system of pentacene in benzoic acid is the best studied of these. Hole burning was found to occur with irradiation into either the origin or the first vibronic band of the lowest excited state. Burn

powers used were typically ~40-400 mW/cm^2 for up to 20 minutes. Hole widths corresponded to the fluorescence lifetime. Interestingly, several distinct (i.e., sharp) antiholes were observed, the largest of which contained ~70% of the burned away sites. Further, both spontaneous hole filling and laser induced hole filling were observed and were found to be site dependent. The spontaneous filling times (1/e) ranged from 6 minutes to over an hour. It is important to point out that the behavior in this system appears to quite different than that observed by Fearey and Small [50], and Fearey et al. [51] (see Papers 5 and 6) in regards to the hole filling results, vide infra. The effects of NPHB upon deuteration of benzoic acid's acidic protons have also recently been examined [46]. Basically, the efficiency is found to be an order of magnitude higher than for the protonated species, despite the apparent two orders of magnitude drop in efficiency. These results were determined via kinetic modeling of triplet bottleneck studies of this system where apparently, upon deuteration, the second triplet state is lowered below S_1. Additionally, the spontaneous hole filling rate decreases dramatically. Lastly, an alternate photochemical hole burning mechanism has also been proposed for this system [47], which involves hydrogen abstraction from the matrix by the photoexcited pentacene.

Thioindigo in benzoic acid shows two absorption systems assigned to two distinct orientations within the host crystal. Each orientation in turn has three sites with varying intensity which correspond to different tautomeric forms. Holes could be burned into all of these sites.

Burn powers were ~1 W/cm^2 for 30-50 seconds. The holes were found to refill rapidly in minutes. No antiholes were detected.

Now, in contrast, tetracene doped into benzoic acid show no detectable hole burning. However, a large Stokes shift was found (~800 cm^{-1}), which was interpreted as being due to rapid reorientation of the tetracene molecule upon excitation.

Thus, NPHB can occur with only slight disorder where the host tautomerization acts as the source of the TLS. In principle, these crystalline systems can be exactly defined quite easily, giving a source of information about distinctions between crystals and glasses. However, for the examples described, there is a strong impurity dependence in contrast to glasses where, in general, the effect is less pronounced.

Molecules in amorphous acene films

Recently, a new class of materials, the linear acenes and their various derivatives [52-55], has been found to undergo NPHB. Linear acenes are those molecules which consist of linearly fused benzene rings, e.g., naphthalene, anthracene, tetracene, pentacene, etc. These sorts of materials have long been used in spectroscopic single crystal studies, which do not show any optical hole burning. However, when these linear acenes are deposited onto a very cold substrate (~10 K), an amorphous material results [56]. Extensive studies of these amorphous acenes has been performed via electron diffraction [56], optical absorption [57] and most recently by NPHB [52-55]. These amorphous acene films differ from other NPHB systems in that when warmed slightly, to relatively low temperatures (still well below the melting point), con-

version can occur from the amorphous state to a polycrystalline state, thereby destroying their NPHB capabilities. In glasses, the NPHB properties are retained even if the system is raised to the glass transition temperature for several hours.

The impurities studied to date in the amorphous acene films have been other acenes which couple well to the host. The most studied impurity systems are tetracene in either anthracene or anthracene derivatives. Two predominant absorption sites, separated by ~200 cm^{-1}, have been observed [55] for tetracene doped samples. The relative populations between these sites changes with varying sample deposition rates and conditions. Each of these sites is subject to large statistical variations of intermolecular parameters evidenced by large inhomogeneous linewidths of 200-400 cm^{-1}. Only the lower energy site exhibits hole burning (burned with a N_2-pumped dye laser with ~2.6 mW/cm^2 for 10-90 minutes), due to greater short range disorder for the lower energy site versus the higher energy sites. The hole linewidths are ~10 cm^{-1} which is a factor of 10 times greater than in glasses (see, for example, Ref. 30). Additionally, the hole burning efficiency was also found to be $\gtrsim$10 times greater than in glasses. These differences were interpreted in terms of strong coupling between the impurity and host matrix [55].

Molecules in organic glasses

The organic glasses discussed in this section are monomeric, aliphatic and other organic substances or mixtures which are, in general, liquids at room temperature. To clarify, if one defines a glass as an amorphous solid which exhibits a glass transition point [58], then both

the materials in this section and the acene films of the previous section can be considered glasses. Nevertheless, due to the differences in the NPHB properties of each and to accentuate the acene films, each type of glass is discussed separately. Tabulations of glass forming materials [59-62] and structural details of glass forming properties [61,63] have been given in previous publications and shall not be discussed here.

As alluded to previously, until the advent of the laser as a strong excitation source, glasses were not useful for high resolution studies due to large inhomogeneous broadening of the impurity spectra. But with the laser, it was soon discovered that this large broadening could be eliminated with fluorescence line narrowing (FLN) [64-67] and with persistent hole burning [23,24], vide supra.

Although, as with other amorphous media, a precise atomic nature of the TLS in organic glasses is not known, by using NPHB as a probe some idea of the nature of the modes within the host glass may be deduced. From a considerable body of data (see Ref. 40 and Appendix table), NPHB is essentially observed only for impurities dissolved in glasses which can have significant hydrogen bonding. FLN, on the other hand, has been observed for both hydrogen and nonhydrogen bonding systems. Further, when the hydroxyl protons were exchanged for deuterons in a methanol/ethanol glass, the hole burning efficiency decreased by a factor of ~5, but the temperature dependence and measured holewidths did not vary significantly from the protonated glass [40,68] (see Paper 1 for details). Thus, the results tend to indicate that hydrogen bonding hosts

can provide parameters appropriate to allow for NPHB. However, the lack of strong linewidth or temperature dependences on deuteration suggests that there exist additional two level systems which control the dephasing processes.

Molecules in polymers

The difficulty of using inefficient hole burning systems in NPHB studies was overcome with the rediscovery [30,69] (see Paper 2 for details) of the very facile systems of ionic dyes (usually laser dyes) in hydrogen bonding hosts, in particular, hydrogen bonding polymers. The hole burning efficiency was estimated to be one to two orders of magnitude greater than that of neutral linear acenes, e.g., tetracene [28]. The ideal systems for the study of NPHB immediately became these ionic dyes in polymeric hosts. The hydrogen bonding polymers in which these dyes are reasonably soluble are poly(vinyl alcohol) and poly(acrylic acid). Although much of the increased efficiency could be attributed to the ionic dyes themselves, there did appear to be some increase due to the polymers themselves. Indeed, this discovery provided the systems for which the body of this thesis discusses. An illustration of the sort of information that can be easily obtained in a "basic" NPHB experiment is shown in Fig. 3. Here with an excitation high into the absorption profile, numerous holes (greater than 27) appear to lower energy corresponding to the vibronic transitions or overtones of cresyl violet perchlorate [69-71] (see Papers 2-4 for more examples). In general, this sort of information is extremely difficult to obtain by traditional techniques. See the figure caption for relevant conditions.

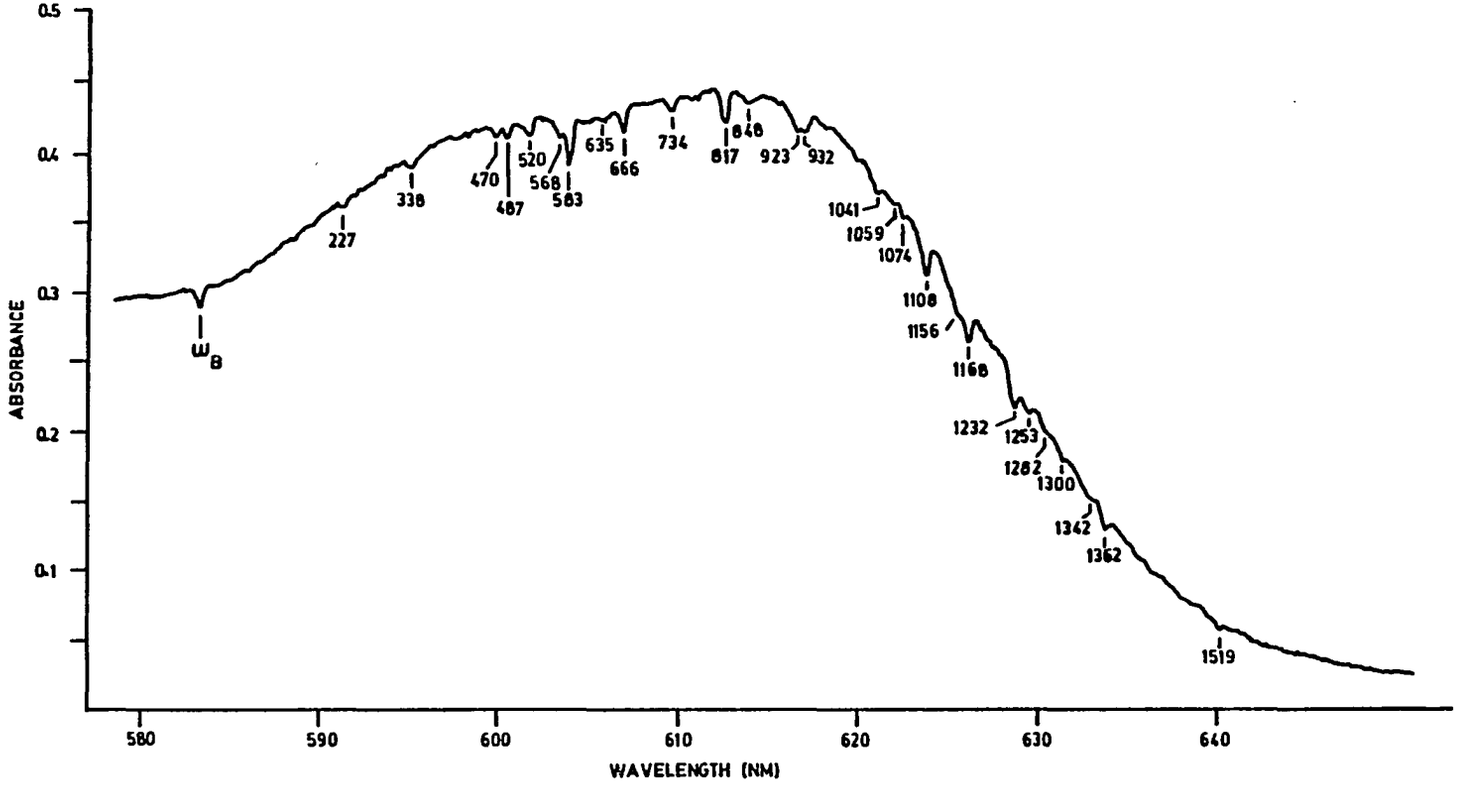

Figure 3. High energy hole burned spectrum of cresyl violet perchlorate (CV) in poly(vinyl alcohol) (PVOH). The sample was burned for 1 minute at 583.0 nm with a laser flux of ~100 mW/cm^2, T = 4.2 K

Nonhydrogen bonding polymers for which nonphotochemical hole burning has been observed are poly(vinyl butyral) [72], poly(methylmethacrylate) [60,73-75], polystyrene [76], and poly(vinyl carbazole) [40,77]. Interestingly, both chlorophyll and chlorophyll dimers have been found to hole burn [76], the import of which shall be briefly discussed in a following section.

Rare earth ions in glasses and polymers

In addition to molecular (polyatomics) impurities, NPHB has also been observed for rare earth ions as impurities in both hard inorganic glasses (e.g., silicates) [78,79] and quite recently in soft organic polymers [71,80].

Macfarlane and Shelby [79] have observed hole burning for Eu^{+3}, Pr^{+3}, and Nd^{+3} in inorganic silicate glasses. With the dopant of Eu^{+3}, the hole burning was into the $^3F_0 \leftrightarrow {}^5D_0$ transition and was due to a population redistribution of the nuclear quadrapole levels (rather than glass structural changes). The holes rapidly refilled in ~20 seconds via spin lattice relaxation. Due to the manner in which the burning takes place, it is perhaps more appropriate to refer to this as population hole burning and not NPHB.

In contrast to Eu^{+3} above, both Pr^{+3} and Nd^{+3} exhibit long lived holes in silicate glasses [78,79], and for the former, NPHB has also been observed in phosphate and berylium fluoride (BeF_2) glasses [79]. The hole burning mechanism was assumed to be of the type described earlier, vide infra. Holes were burned into the $^3H_4 \leftrightarrow {}^1D_2$ transition of Pr^{+3} in the silicate glass, where the linewidth of the burned hole

showed an increasing dependence with increasing excitation wavelength. The hole burning powers varied from ~10-500 W/cm^2 for ~10-500 seconds depending on conditions. The temperature dependence observed was roughly linear which was confirmed by accumulated photon echo experimental measurements. This is in marked contrast to the nearly quadratic dependence observed for many other rare earths as studied by fluorescence line narrowing.

NPHB has recently also been observed for the above two rare earths (Pr^{+3} and Nd^{+3}) in poly(vinyl alcohol) [PVOH] [50,71,79,80] (see Papers 4 and 5 for details). Only the lowest energy component of the J-J crystal field split transition of either rare earth ion profile indicated any hole burning (see Fig. 4). The inhomogeneous broadening of these transitions is found to be narrower (Fig. 4) than in hard inorganic glasses [78,79]. The hole burning efficiency was determined to be 1-2 orders of magnitude larger than in the hard glasses and the hole widths were found to be somewhat broader depending on the particular impurity. Additionally, the strong linewidth dependence seen for these ions in hard glasses, vide supra, was not observed in the soft polymers.

Recent Developments in Persistent Hole Burning

Since the discovery of the phenomenon of persistent optical hole burning, vide supra, there have been many systems studied over the years, some of which have been discussed above. Similarly, many developments have occurred and have been been described previously in several review papers [30,38,39]. However, quite recently, many new and interesting developments have occurred which deserve some discussion. In the

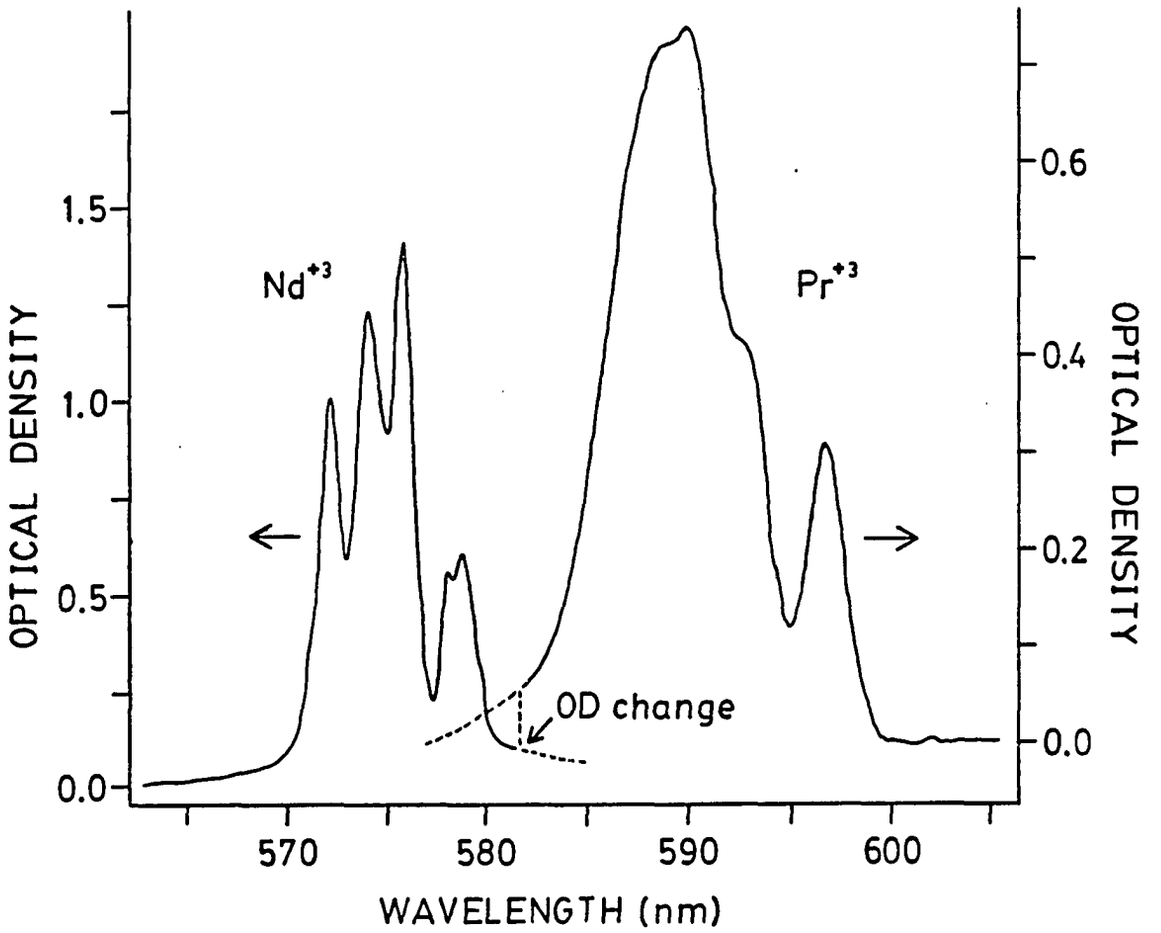

Figure 4. Absorption profiles of the $^1D_2 \leftarrow {}^3H_4$ transition for $PrCl_3 \cdot (6H_2O)$ (left axis) and of the $^2G_{7/2}$, $^4G_{5/2} \leftarrow {}^4I_{9/2}$ for $NdCl_3 \cdot (6H_2O)$ (right axis)

following discussion, only a brief summary of some of the most interesting developments in optical hole burning is given and is not intended to be comprehensive nor complete. Any important omissions are accidental.

New detection techniques

The development of several new detection techniques prompted by the need for much lower probe powers and significantly improved signal to noise has occurred since 1983. The goal of these techniques has been to remove many of the problems caused by more traditional techniques, i.e., absorption or fluorescence detection. These former techniques suffer from several problems: large background offset signals, lack of resolution (as with monochromator dependent systems), high probe intensities (causing distortion even though probes are usually $>10^3$ less than burn powers) and, often, slow time response. These new techniques are divided into two subsections: modulation techniques and alternate techniques (i.e., not modulation).

Modulation detection techniques Frequency modulation (FM) is a method of optical heterodyne spectroscopy which is capable of sensitive and rapid detection of absorption [81] and is also a zero-background technique. Basically, in FM, a light source, typically a laser oscillating at some optical frequency ω_c, is passed through a phase modulator driven at radio frequency ω_m producing an optical spectrum consisting of a strong carrier at ω_c with two weak sidebands at $\omega_c \pm \omega_m$. This beam is then passed through the sample containing the spectral feature of interest with the output impinging on a photodetector where the electrical signal is detected at ω_m. Since lasers have little noise at radio fre-

quencies, these beat signals can be detected with high sensitivity. This technique was first used to study hole burning by Lenth et al. [82] in 1981. However, in order to observe shallow absorption features with high sensitivity, high reading powers are required to overcome Johnson noise in the photodetectors, thus, limiting the power of simple FM.

Recently, Romagnoli et al. [83] solved this problem with a modified FM detection system that involves diagnostic procedures to reduce residual AM and the use of a more sensitive detector (with greatly reduced Johnson noise). Using this system, they have detected photochemical holes in free-base phthalocyanine-doped poly(ethylene) in times as short as 100 nanoseconds with 500 picojoules of energy. Results trom their study suggested that the hole burning bottleneck in phthalocyanine is due to population build up of the triplet state.

Another new type of FM detection, also developed by Romagnoli et al. [84] is frequency modulated polarization spectroscopy (FREMPOLSPEC), which again is a sensitive detection method, but in this case, the detection is of anisotropic absorption features. The use of FREMPOLSPEC has recently been demonstrated as an excellent technique for the detection of shallow holes [85] in otherwise isotropic solid media but which retain anisotropies when hole burned. This technique allows for very sensitive detection of weak anisotropic spectral features with essentially no intensity in the polarization that causes erasure. Residual AM is blocked with a polarizing prism. FREMPOLSPEC is similar to standard FM, except that not only is the laser frequency phase modulated but, also, the polarization is modulated giving another beat frequency.

Romagnoli et al. [85] have found that in appropriate materials holes can be both burned and probed many times without erasure using the same total optical power. Their best success was in the 607-nm color center in x-irradiated NaF due to persistent anisotropy where holes burned in 3-msec could easily be detected. The FREMPOLSPEC technique, however, works only marginally well for free-base phthalocyanine-doped poly-(ethylene) because its anisotropy is very weak.

Modulation techniques other than frequency modulation also have been found to be very sensitive for low absorption changes. One such technique developed by Lengfellner et al. [86], and Huston and Moerner [87] is high-resolution ultrasonic modulation [86] of persistent holes or HUMPH [87], which utilizes the fact that spectral holes are sensitive to strain fields within in the host matrix. The modulation is of an ultrasonic field applied to the sample at kilohertz to megahertz rates in order to create a corresponding modulation of the spectral hole. Only when the probing laser beam is near resonance to the burned hole is any amplitude modulation (AM) detected at the lock-in. This technique has been used for photochemical holes in 607-nm F_3^+ color centers in x-irradiated NaF [87] and in IR spectral holes in KI:ReO_4^- and RbI:ReO_4^- crystals [86]. The method was shown to be a high-sensitivity, zero-background, phase-insensitive technique. A major drawback for the HUMPH method is that the application of the ultrasonic field tends to broaden the probed hole [86,87] and, in fact, can totally erase the spectral hole at sufficiently high applied rf powers [86].

Another modulation scheme developed by Korotaev et al. [88] is the modulation of an applied Stark field upon a burned spectral hole. The technique combines hole burning with modulation Stark spectroscopy and is referred to as MSSH (modulated Stark spectroscopy of holes). MSSH was used to characterize octaethylchlorin in poly(methylmethacrylate), allowing detection of holes as small as 10^{-4} optical density units. In these studies, only low modulation frequencies (288.5 Hz) of the Stark field were used, suggesting that at higher frequencies, laser noise might be eliminated.

Lastly, another interesting modulation detection technique has been utilized by Thijssen et al. [89] for the study of spectra of crystalline samples and optical holes in amorphous samples at T = 1.65 K. In this case, the absorption change from a modulated laser is detected photoacoustically via resonant detection of second sound in superfluid helium. Photoacoustic (PA) methods are attractive in that many solid materials are not conducive to standard absorption or fluorescence spectroscopy due to high scattering opacity, very low optical density or low fluorescence quantum yields. As in conventional PA experiments, the signal is due to temperature pulses induced by modulation of the excitation source interacting with a sample, however, in conventional PA, this heat is usually detected in the form of acoustic signals by a microphone [90]. In this scheme, the induced periodic temperature variations (nonradiative energy transfer to the bath) in the superfluid helium (called second sound) are detected via a very sensitive resistance thermometer inside a Helmholtz cell (temperature variations of $\sim 10^{-8}$ K were easily

detected). Persistent photochemical holes were easily observed for free-base porphyrin and dimethyl-s-tetrazine in poly(methylmethacrylate). Besides the capability of simple absorption spectra of otherwise difficult samples, this technique may also allow for determination of energy transfer mechanisms and fluorescence quantum yields of solid samples [89].

Alternate detection techniques In addition to modulation methods of detection, two other kinds of detection systems have been developed. Renn et al. [91] recently demonstrated a CW holographic method for the detection of persistent photochemical holes in chlorin (2,3-dihydroporphyrin) embedded in poly(vinylbutyral) at 4.2 K. Basically, similar to other room temperature (RT) CW holographic studies [92], crossed laser beams are used to induce (burn) spatially periodic changes in the spectral hole depth for a sample, i.e., a frequency dependent grating is created at frequencies corresponding to the burned holes. To detect the spectral hole, one of the crossed laser beams is scanned (the other is blocked) which then only gives a signal, at the grazing angle, near the induced frequency grating. Renn et al. [91] showed that this holographic technique is a sensitive zero-background high-resolution method for detecting weak features associated with persistent optical holes. Also, the sensitivity of this technique compares favorably to some of the above FM techniques and has the additional advantage of fewer electronic elements and less complexity.

Lastly, a clever method for the detection of extremely narrow spectral features has been used by Rebane and Palm [93,94]. They have de-

veloped a spectrometer utilizing the Doppler effect to study narrow photochemical holes. Their apparatus operates by first passing a laser beam through the sample (twice to increase the Doppler shift), after which it reaches a rotator consisting of a rotating disk with several total internally reflecting prisms which, in turn, frequency shifts the laser beam by $\Delta\nu = 4\nu\ V/c$ (ν = laser frequency, V = linear velocity, and c = speed of light). Light shifted by $\Delta\nu$ is then passed through the sample and the intensity of the transmitted light detected by a photomultiplier tube. Instrumental broadening of the system was estimated to be ~0.005 $\Delta\nu$. Doppler shifts of up to 600 MHz were easily attained. Holes in H_2-octaethylporphyrin doped into polystyrene were accurately measured to be 0.017 cm^{-1} using this method. In principal, holes should be able to be measured from 1 MHz to 600 MHz [93]. Additionally, it has been demonstrated that using this Doppler spectrometer, holes near or less than the linewidth of the burn laser can be determined in certain samples [95].

New types of hole burning

Since the advent of persistent optical hole burning, only simple one photon hole burning mechanisms have been observed; further, the maximum hole depth usually has been below 50%. Recently, these conditions have been removed for certain systems. In addition, the phenomenon of hole burning has been extended to surfaces. These discoveries will be discussed briefly below.

Gated hole burning Two groups at IBM, Winnacker et al. [20] and Lee et al. [96], have recently observed two-color photon-gated spectral

hole burning, i.e., hole burning which occurs only in the presence of an additional gating light source, in both inorganic (20) and organic systems [96].

Winnacker et al. [20] found gating enhancement factors of $\sim 10^4$ for gated holes burned in BaClF:Sm^{+2} versus nongated burned holes. A 2-step photoionization mechanism of the Sm^{+2} ion is involved in the formation of persistent holes for both the $^7F_0 \rightarrow {}^5D_0$ (6879 Å) and $^7F_0 \rightarrow {}^5D_1$ (6297 Å) transitions. Narrow holewidths of 25 MHz at 2 K were observed to be much narrower than the inhomogeneous broadening (16 GHz). Studies indicated that Sm^{+3} acts as the electron trap. Perhaps, the most striking feature of their work was that the holes could be recovered <u>after</u> temperature cycling <u>300 Kelvin</u>.

Lee et al. [96] also have observed gated hole burning in organic systems. Specifically, two-color gated hole burning was seen for the system of carbazole in boric acid. This hole burning involves a stepwise biphotonic photoionization of the carbazole molecule. The exact mechanism was concluded to be photoionization of carbazole through the triplet state. Additionally, the quantum yield for the photoionization was found to increase exponentially with the energy of the gated photon. Importantly, this technique of gated hole burning allows for nondestructive reading of the burned hole which is a very important aspect for the application of frequency domain optical memory, vide infra.

<u>100% hole burning</u> High-efficiency photochemical hole burning for an infrared color center has been observed by Moerner et al. [97]. Specifically, the PHB properties of the 8892 Å zero-phonon-line (ZPL) in

electron irradiated samples of NaF:OH^- and NaF:Mn^{+2} at low temperatures were studied. The system displayed the highest reported hole burning efficiency to date of ~10^{-2}. Further, for the first time in persistent hole burning, holes could be burned to 100% (i.e., to baseline) suggesting the absence of strong reverse reactions. These systems were first analyzed by Kaipa and Luty [98] for possible hole burning processes. In addition to the above ZPL, they also found that the 10,720 Å IR color center is fully bleachable, although hole burning studies have not yet been undertaken. Due to the extremely high-efficiency hole burning for these color centers, burn powers and scanning powers had to be significantly reduced, in these studies scan powers were typically 100 nW/cm^2 [97] (in fact, holes rapidly burned with just the emission line from a pen lamp). As above, this high-efficiency aspect is important to optical spectral memory applications, vide infra.

Hole burning on surfaces Persistent spectral hole burning of submonolayers (0.1-0.01) of dye molecules adsorbed directly on surfaces has been observed by Bogner et al. [99]. Hole burning was reported for perylene and perylene butyric acid adsorbed on optically polished sapphire, γ-alumina, crystalline quartz powder and anodized aluminum. Hole widths were found to be generally broader than when these molecules were imbedded in glassy materials. These observations suggest that only disordered media with the ability to form asymetric double well potentials are necessary to observe optical hole burning.

New hole burning phenomena

Picosecond holography hole burning Recently, a new unusual type of hole burning, called dynamic picosecond holography produced by photochemical hole burning, has been reported by the Russian group of Rebane and co-workers [100,101]. They found that when an absorbing medium was burned with a picosecond laser with a repetition rate of 82 MHz, a Fourier transform of the time domain pulse train was reproduced in frequency space. This is created when a broad linewidth (relative to the dephasing time determined linewidth) high repetition picosecond laser interacts coherently with the dephasing molecules before they are completely dephased. In other words, a broad pulse source first coherently excites the molecules, then before these molecules can dephase, another pulse is absorbed and interferes with these coherent absorbers creating an interference frequency pattern corresponding to the pulse separation. The resulting optical persistent hole then consists of a broad hole, defined by the linewidth of the picosecond source, made up of many (up to 10^4-10^5) periodic holes separated by the frequency difference transform of the pulse separation.

Once this hologram has been created, then by exciting the sample with a weak picosecond pulses, the hologram now will act with a temporal response yielding easily detectable echoes. This technique is called photochemically accumulated stimulated light echo (PASLE). Possible applications of this technique are time-domain optical storage [100,102] along with other more traditional investigations of ultrafast phase relaxation studies.

Pressure effects in hole burning Richter et al. [103] have studied the effects of uniaxial pressure on the homogeneous linewidth of photochemical holes in free base phthalocyanine in both poly(ethylene) and poly(methylmethacrylate). They observed that holes began to show substantial broadening effects at pressures as low as 100 hPa and that at higher pressures (up to 3×10^4 hPa), irreversible line broadening occurred. This irreversible line broadening was attributed to irreversible site changes of the host-guest system. The authors also noticed a reversible component of the spectral hole upon pressure cycling which they could not explain. However, it seems that this reversible broadening is probably due to strain induced perturbations yielding slight frequency shifts which recover after the pressure is lowered. These reversible and irreversible broadening effects seem to be in close analogy to earlier temperature dependent studies by Hayes and Small [27].

Hole burning in new host materials or of new impurities

Since the discovery of NPHB [23], many new and quite interesting systems have been found, some of which have already been discussed. The intent of this section is to point out some of either the most unusual or the most important hole burning systems observed over the last few years.

Hole burning of organic impurities in amorphous silica gels For the first time, hole burning of an organic dye, 1,4-dihydroxyanthraquinone (DAQ or quinizarin), has been observed in inorganic amorphous media at low temperatures by Tani et al. [104] in 1985. Using a special technique of sol-gel alcoholate methodology (which uses significantly lower

preparation temperatures over conventional techniques) previously used to prepare oxide glasses [105,106], Tani et al. [104] were able to introduce the photosensitive organic dye, quinizarin, into an inorganic silica glass matrix (a-SiO_2). Specifically, when doping quinizarin into a-SiO_2, the temperature did not exceed 60°C [104]. For this system, the observed hole burning quantum yield was approximately equivalent to that observed in organic glasses. A rather broad intrinsic holewidth of 0.9 cm^{-1} was observed in the inorganic glass. In these studies, burn powers and times were 0.74 mW/cm^2 and 30 minutes, respectively. Annealing studies indicate that two kinds of mechanisms are operative in this system, one reversible and the other irreversible. It was conjectured that the nearest-neighbor structures around DAO consist of hydroxyl groups which are intimately involved in the hole burning process [104]. Lastly, it was also stated that many different organic molecules can be doped into a variety of inorganic glasses (e.g., SiO_2, GeO_2, B_2O_3, P_2O_3, TiO_2 and their mixtures) [107]. These systems not only offer new scientifically interesting possibilities (e.g., studying differences in coupling between the impurity and glass for either inorganic or organic host via LIHF), but also offer important technological advances in the possibility of optical memory due to the increase in host rigidity.

Hole burning of ReO_4^- in alkali halide crystals Recently, high efficiency NPHB has been observed by Moerner and co-workers in the spectra of ReO_4^- doped in inorganic alkali halide crystals [108,109]. The particular systems of study have been Czochralski-grown KI and RbI doped by the addition of 0.02-0.8 mole % of $KReO_4^-$ or $RbReO_4^-$ to the melt.

Holes were burned into various vibrational modes with low power (~100 $\mu W/cm^2$) for a few seconds. Hole burning efficiency was estimated to be $\sim 10^{-3}$ (at 922.91 cm^{-1}), significantly higher than most other systems. The mechanism for the formation of the long-lived hole, analogous to that of Hayes et al. [28,29], was determined to be intrinsic to single ReO_4^- molecules, based on concentration dependent studies [108,109]. Brief erasing studies (similar to laser induced hole filling [51], see Paper 6) were also performed, finding minimal erasing near Δf = 0 MHz (frequency displacement from burn frequency), maximum erasing at Δf = 10-15 MHz and decreasing erasing (~30% of maximum) at 50 MHz.

Another, quite interesting feature found for certain mixture of these systems, is the formation of persistent spectral antiholes (pegs) [110]. In these systems, in addition to holes coincident to the burn frequency, burns performed at certain frequencies induced increases in the absorption coincident to the burn frequency. This phenomenon was most predominant in the sample of doubly-doped KI with 0.05 mole % $KReO_4^-$ and 2 mole % NaI. The alloyed host produced a number of perturbed modes for the vibration of interest, each of which showed inhomogeneous broadening. Although, the relative magnitude of absorption change was larger for hole formation than for peg formation, the relative hole burning efficiencies of formation (n) showed opposite behavior with $\eta = 10^{-6}$ and 10^{-4} for hole and peg, respectively. A model which qualitatively accounts for the hole and peg phenomena was proposed (see Ref. 110 for details).

Hole burning of color centers in diamond Under the financial support of DeBeers Industrial Diamonds, Harley et al. [111] have demon-

strated persistent hole burning in color centers of diamonds. NPHB was observed for all tested zero-phonon lines of the defect centers in diamond. These results support the overall generality of persistent hole burning. Typical burn exposures to produce hole with depth of 10% varied considerably depending on the color center of interest, ranging from ~0.2 W/cm^2 to ~10 $\mu W/cm^2$. This brief experimental survey not only demonstrated the versatility of NPHB, but also that NPHB can be an important technique for the elucidation of color centers in diamond crystals.

Hole burning of chlorophylls in various host materials Over the last few years, there has been a considerable effort to attempt to understand biological systems using "high power" laser techniques (e.g., picosecond fluorescence and dephasing studies) previously reserved for more basic physical phenomena [112,113]. Thus, it is not surprising that the technique of hole burning has also begun to be used to study biological compounds in detail. Avarmaa et al. [114], and Avarmaa and Rebane [115] have reported hole burning for protochlorophyll-a and chlorophyll-a (chl-a) in ether attributed to NPHB. Recently, Hayes et al. [40] and Carter and Small [76] have studied persistent NPHB of chl-a and chl-b in polystyrene. In contrast to dyes and rare earths in PVOH or PAA [50] (see Paper 5), holes burned at pumped helium temperatures in the systems [76] did not exhibit any spontaneous hole filling (SPHF). However, the laser induced hole filling of the chlorophylls in polystyrene closely mimicked that observed in Paper 5. Holes were burned easily to ~13% (saturation ~20%) with 250 $\mu W/cm^2$ for 30 seconds. Also, Carter and Small [116] have reported hole burning in self-aggregated

chlorophyll-a dimers (chl-a_2). As in the monomers, no SPHF was observed. In the chl-a_2 (dimer), the saturated hole depths were significantly shallower (~4-8%) versus the monomer.

Two other groups have also been examining photosynthetic reaction centers, Meech et al. [117] and Boxer et al. [118]. In these cases, hole burning is of a transient nature, recovering very rapidly (i.e., <1 second). Interestingly, in the molecule studied, rhodopseudomonas sphaeroides [117,118], the measured linewidths, were on the order of 400 cm^{-1}, implying extremely fast relaxation processes (~25 femtoseconds). In both reports, various possibilities are discussed to account for the rapid relaxation and are beyond the scope of this overview. Additionally, neither group observed any persistent hole burning in contrast to the results of Carter and Small [76,116] for similar photosynthetic compounds. This inconsistency is presently being studied by the research group directed by Dr. G. J. Small.

Progress in frequency based optical memory

Cryogenic frequency domain optical memories [119,120] based upon either photochemical or nonphotochemical hole burning offer the possibility of storing data at densities of up to 10^{11} bits/cm^2 (significantly higher than in present memory devices). The basic concept of NPHB or PHB memory is that instead of the normal x-y type of memory storage, another dimension is added in the frequency regime via persistent hole burning [121]. Recalling that both NPHB and PHB are site selective techniques and that, in general, the holes width is homogeneous, then, one can then envision (in frequency space) burning a very narrow

hole for a data bit '1' and not burning a hole for a data bit '0'. Further, since $\Gamma_h \ll \Gamma_{ihm}$, it is then possible to have $\sim 10^3$-10^4 increase in data storage [122].

Technical aspects have been analyzed by Moerner to ascertain the system and material requirements needed to make frequency dependent optical memory feasible [123,124]. One of the limiting system requirements is the fast reading of the burned hole, approximately 30 nanoseconds per bit. This problem has largely been solved by Bjorkland et al. [81] and Pokrowsky et al. [125] with the sophisticated detection technique of frequency modulation (FM) spectroscopy (vide supra). However, materials requirements are a much more difficult problem [125]. Several properties need to be satisfied: (1) reversible hole burning, (2) long lifetime holes, and (3) fast burning times (30 ns/bit). Each of these properties have been accomplished in <u>different</u> materials, but to achieve all three simultaneously has yet to be accomplished for single-photon hole burning processes [124,125]. However, one possible solution is photon-gated hole burning (vide supra) which offers enhanced abilities since holes can be burned <u>and</u> probed nondestructively [20,96]. Thus, although many material problems still exist for the frequency domain optical memory, the reality of practical achievement has progressed significantly since its conception in 1975 [119].

Another interesting proposal for optical memory can, in principal, add a <u>fourth</u> dimension to the memory stage capability. Specifically, Bogner et al. [126] and Wild et al. [127] have suggested and demon-

strated the ability to multiplex the burned holes with electric fields (Stark effect) giving yet another dimension to the optical memory.

Lastly, the author would like to point out some complicating aspects apparently largely ignored in the practicality of frequency domain optical memory. First of all, as demonstrated in Paper 6 [51], the phenomenon of LIHF (vide infra), can be quite significant which could distort the data stored via persistent hole burning. In addition, for these systems to be very useful, a data bit (i.e., hole) must be easily erased so that the device change be dynamic rather than just static. How this particular problem could be solved is presently unclear. One possibility is rapid total erasure via either a white light irradiation burst [121] or a large acoustic burst [86] for a particular area in the x-y space, followed by rapid rewriting the entire data area. However, this seems somewhat infeasible since every time this occurs over 10^3 holes would have to be rewritten.

Summary of the Theories of Optical Dephasing

As mentioned early in this introduction, one of the photophysical properties of impurity molecules or ions in amorphous solids which is significantly different from that in crystalline solids, is optical dephasing (T_2). This anomaly was first noted by Hegarty and Yen in 1974 [128] for the $4f^n$ transitions of rare earth ions in inorganic glasses from resonant fluorescence line narrowing measurements. The dephasing times, determined by optical linewidths at low temperatures, were found to be 2-3 orders of magnitude shorter than in crystals. Also, the linewidth followed a quadratic linewidth dependence on T over a large tem-

perature range. Nonphotochemical studies of the $S_1 \leftarrow S_0$ transition of tetracene in an alcoholic glass by Hayes et al. [28,29] also led to the same conclusion for the first time in organic systems. However, unlike the inorganic system, a roughly linear temperature dependence was determined for the temperature range 2-20 K.

Since these early measurements, optical dephasing has been studied for a large variety of impurities in amorphous media. Techniques to probe the dephasing of impurities in disordered media include: nonphotochemical and photochemical hole burning, luminescence line narrowing (i.e., fluorescence or phosphorescence line narrowing) and photon echo experiments. The important early conclusions, that for amorphous solids, the magnitude of the optical linewidth and dephasing at low temperature and their T-dependence are markedly different from that in crystals, have not been altered since the advent of these more specialized methods.

To clarify the physical meaning of the term "dephasing", a short discussion of dephasing is in order. If one considers an ensemble of molecules (or impurities) excited by an incoherent light source (e.g., flashlight or arc lamp), then the only relaxation processes which lead to decay of the excited state of these impurities are natural lifetime (i.e., T_1) processes. However, if this ensemble is prepared in a coherently excited state, that is, each impurity excited state having the same phase, then the processes which lead to the loss of the phase coherence (i.e., memory loss of how the state was prepared) are called pure dephasing or T_2^* processes. Recall that $1/T_2 = 1/2T_1 + 1/T_2^*$. To

give a physical analogy to the dephasing process, the metaphor of Macomber [129] is borrowed. Consider a group of soldiers marching to a drill sergeant's call on a hot parade ground. While they march in cadence, the soldiers are in phase (i.e., coherent). If the sergeant then ceases cadence and the soldiers' memory of cadence is imperfect, then, the soldiers will eventually fall out of step until the unit is scattered over the entire parade ground. The unit has now lost its phase coherence and has been dephased; a T_2^* process. If after some longer time the soldiers collapse from heat exhaustion, the unit has undergone a T_1, lifetime, relaxation.

Since the above anomalous behavior for amorphous materials (e.g., glasses) could not be accounted for by existing dephasing theories developed for mixed crystals, early theories developed [28,29,130-132] to explain these results invoked phonon-assisted tunneling of two-level systems (TLS, vide supra) as a primary ingredient. More recently, several new theoretical developments have occurred [133-138] which assume that it is the TLS which provide the low energy ($\lesssim kT$) excitations responsible for dephasing at low temperatures. With these sort of excitations, it is not surprising that the exact treatment of the TLS distribution function is crucial to each theoretical prediction of the T-dependence of dephasing. The details of the differences between these various theories and their nuances are beyond the intended scope of this brief summary. The reader is referred to the book chapter by Hayes et al. [39] for a more complete discussion of each of these theories. Table 2 summarizes the predicted T-dependence behavior of the dephasing

Table 2. Theories of optical dephasing in glasses

Reference	Model Used[a]	Temperature Dependence of $\Delta\omega$[b]
Selzer et al. (130)	DM[c]; fast modulation	~ τ (TLS relaxation time); motional narrowing
Reinecke (131)	DM	T^1
Lyo & Orbach (132)	ODM[c]	~ T^1 (high T limit); ~ T^2 (low T limit)
Hayes et al. (28)	ODM	~ T^1 (high T limit); ~ T^2 (low T limit)
Reineker et al. (137)	ODM	~ T^1 (high T limit where $T << \theta_D$[d])
Lyo (133)	DM; slow modulation; short time limit	~ $T^{4+u-9/s}$[e] ($\rho(E) \propto E^{\mu}$, $V \propto r^{-s}$, W,E correlation)
Huber et al. (135)	DM; slow modulation; long time limit	~ $T^{(1+\mu)s/3}$ ($\rho(E) \propto E^{\mu}$, $V \propto r^{-s}$)
Small (139)	DM; slow modulation; short time limit	~ $T^{2+\mu-3/s}$ ($\rho(E) \propto E^{\mu}$, $V \propto r^{-s}$, no W,E correlation)
Jackson & Silbey (140)	ODM plus exchange coupling via low frequency impurity induced localized phonons	~ T^n with n ~ 1.3 for high T limit of ODM
Lyo & Orbach (138)	DM with fractons	~ $T^{1+d/4}$
Molenkamp & Wiersma (75)	equivalent to Lyo (129,130)	

[a] See section on dephasing for discussion of fast and short modulation and of short and long time limits.

[b] See section on dephasing for discussion of high and low T limits.

[c] DM ≡ diagonal modulation; ODM ≡ off-diagonal modulation, see section on dephasing for discussion of ODM & DM.

[d] Debye temperature.

[e] "s" is the coupling interaction of the system (e.g. s = 3 for dipole-dipole).

for each of the various theories. Concise statements in Table 2 refer to the type of model used for each theory. It is important to recall that a wide variety of T-dependences, $\Delta\omega \propto T^n$ ($1 \lesssim n \lesssim 2$), have been observed for a large number of impurity-amorphous host systems. This fact is exactly why a general theory to account for all observed T-dependences has been exceedingly difficult and as of yet not achieved.

Briefly, in order to examine Table 2, the fast and slow modulation limits are defined by $h\tau^{-1} > V'$ and $h\tau^{-1} < V'$, respectively, (were $V' = V\Delta/E$, V is the impurity-TLS coupling energy, Δ is the TLS asymmetry parameter and E is the TLS tunnel state splitting, see Fig. 2). The time limits refer to the time regime (t) being studied, that is, for long time $t > \langle\tau\rangle_{ave}$ and for short time $t < \langle\tau\rangle_{ave}$, where $\langle\tau\rangle_{ave}$ is an average relaxation for the system. For a more exact examination of the effects and justification of these different parameters for each theory, the reader is referred to reference 39.

The primary difference between the theories (besides the TLS averaging procedure) is how the impurity-TLS coupling is treated. The choice of how this coupling is handled depends on whether one assumes that the dephasing of an impurity site is dominated, on average, by a <u>single</u> (or a <u>small</u> number of) nearby TLS or by a "sea" of more <u>distant</u> and more weakly interacting TLS. These are referred to as off-diagonal modulation (ODM) (allows for mixing of the tunnel state functions) and diagonal modulation (DM) (no mixing), respectively. These are derived from the impurity-TLS diagonalized Hamiltonian (see Ref. 39 for details).

The dominance of the $T^{1.3}$ over an extended temperature range (0.3-~20 K) is quite apparent for many organic systems [141-144], although exceptions exist, notably, quinizarin in boric acid [145]. In fact, this dependence has been observed for Nd^{+3} in pure SiO_2 glasses for the temperature range 0.1 to 1.0 K [135,146]. Although at higher temperatures (T > 10 K), this same system follows a quadratic dependence [147]. The question as to which type of modulation (i.e., DM or ODM) is more in lie with experimental results if important. Recall that ODM is due to "local" TLS interactions, while DM is due to a sea of weakly interacting TLS. ODM predicts a linear T-dependence in the high temperature limit independent of the nature of the impurity-TLS interaction, while the DM predicts power laws indicated in Table 2 in the low temperature limit and does depend on the nature other impurity-TLS interaction (e.g., for dipole-dipole coupling, s = 3, $\Delta\omega \propto T^{1+\mu}$). Although the strength of DM coupling is significantly weaker than for DM, Lyo [133,134] argues, simply, that the large number of weakly interacting TLS provides a dominance of DM over ODM. The validity of this statement may be somewhat questionable, since the density of states normally referred to ($\sim 10^{17}$ TLS per cm^{-1} per cm^3) is determined from the 1 second time regime while dephasing occurs in ~1 ns, greatly reducing the effective density of states. Lastly, it can be concluded [39] that ODM, by itself, is incapable of predicting the power law of $T^{1.3}$ over an extended temperature range.

Thus, the DM theories offer a more appealing since their low T limits are able to account for the $T^{1.3}$ with s = 3 and μ = 0.3 (note

that μ refers phenomenological to the energy dependence of the density of state). Further, DM provides a link between the behavior of organic and inorganic systems via the glassy state. It is important to point out that both DM and ODM predict nonzero dephasing at 0 K [39]. Several persistent hole burning studies on organic systems which show a $T^{1.3}$, apparently exhibit a lifetime limited (T_1) value for $\lim_{T \to 0} \Delta\omega$ [144]. However, an extrapolation of the $T^{1.3}$ dependence to 0 K is most likely invalid. In fact, given the very nature of the glassy (amorphous) state, it is unquestionable that dephasing due to TLS relaxation must exist at 0 Kelvin.

As indicated above and in Ref. 39, the theories developed to date still have difficulty accounting for the observed temperature dependences over extended temperature ranges. One problem in each is the determination of the density of states (DOS) of the TLS. Generally, the DOS is either approximated as constant or determined only phenomenologically as required to fit theory to experiment. Obviously, this lack of a realistic determination of the DOS is a major difficulty. Many theories have been developed for the density of states [31-33,138,144-153], although many of the premises in their development have no physical basis or have since been shown to be inaccurate with the advent of more sophisticated experiments [39].

Very recently, to account for experimental discrepancies with the tunneling model, a more realistic DOS function for the TLS has been derived by Jankowiak et al. [154] (also see Ref. 39). Basically, the model is developed by only assuming Gaussian distribution functions

(GDF) for the site relaxation parameters in the tunneling process. It is again beyond the scope of this introduction to discuss these results in detail. However, suffice it to say that the DOS follows a increasing nonconstant temperature dependence of the form $\rho(E) \propto \rho_0(E)^{\mu(E)}$. Additionally, for the temperature ranges of 0.1-20 K, with a reasonable choice of parameters (determined experimentally), the determined value for this energy dependent DOS is $\mu \simeq 0.3\text{-}0.5$ (depending upon exact chosen parameters), in apparent agreement with most measured T-dependences.

Dissertation Format

The arrangement of this dissertation follows the alternate style format. First, a "general introduction" into the history, phenomenon, systems, progress, and basic theories of nonphotochemical hole burning (NPHB), is given. Additional theory can be found in the theory sections of the various papers. An "experimental" section follows which describes sample preparation, experimental apparatus including cryogenics, optics and lasers along with actual techniques used to study NPHB. Following these sections are the published or to be published papers. Paper 1 studies the effects of deuteration upon the efficiency of NPHB for tetracene in an ethanol/methanol mixture. Paper 1 was published in the Journal of Chemical Physics 78, 3590 (1983). Paper 2 describes the first studies of a new set of systems for NPHB. Paper 2 was published in Journal of Physical Chemistry 87, 3590 (1983). Paper 3 studies the optical dephasing in the above new systems in detail, in particular, for cresyl violet in PVOH. Paper 3 was published in Chemical Physics Letters 102, 272 (1983). Paper 4 discusses hole burning of rare earth ions

for the first time in soft organic polymers and also discusses some initial laser induced hole filling results. Paper 4 was published in the Journal of Luminescence 31&32, 792 (1984). Papers 5 and 6 examine some in depth studies of NPHB of dyes and rare earths in polymers. Specifically, Paper 5 examines studies of the phenomenon of spontaneous hole filling (SPHF). In Paper 5, a model is developed to account for the fact that no line broadening was observed in this process of SPHF. Paper 6 examines the phenomenon of laser induced hole filling (LIHF), including a tentative theoretical model of LIHF. Papers 5 and 6 have been published consecutively in Chemical Physics 101, 269 (1986) and Chemical Physics 101, 279 (1986), respectively. Finally, the dissertation ends with an overall "conclusion" which includes some personal thought into the future of optical hole burning.

EXPERIMENTAL METHODS

Sample Preparation

Several different samples, consisting of many different combinations of hosts and impurity molecules, have been studied over the course of this work. Typically, a sample consisted of some low concentration (usually $\lesssim 10^{-4}$ M) impurity molecule doped into an amorphous host. The samples studied are listed in Table 3, including the impurity's name, extinction coefficient, absorption maximum, fluorescence maximum, molecular weight, hosts into which it was doped, and the cooling rate required to obtain optically clear samples. Primarily, the hosts used were either soft organic glasses or polymers. In forming acceptable samples, many factors were important and will be discussed in turn: (1) impurity and host purity, (2) mixing of samples, (3) sample mounting, and (4) cooling of final sample.

(1) Impurity molecules were either synthesized at Ames Laboratory-ISU or were purchased from typical chemical suppliers as needed. The laser dyes were purchased from Exciton (laser grade) and were used without further purification. Tetracene and pentacene were purchased from Aldrich (>98%) and usually were purified further by vacuum sublimation. The rare earth ions used in all of these studied were prepared by associated of Dr. Frank R. Spedding in the hydrated chloride form ($ReCl_3$-H_2O) with a purity >99.99%. The host solvents were used either as purchased or distilled, if necessary. The deuterated samples of deuteroxy ethanol (EtOD) and methanol (MeOD) were used as purchased (Merck, Sharp and Dohme, deuteration >99%), making certain that all samples were re-

Table 3. Summary of new systems studied

Molecule	Mol. Wgt. (g/mol)	$\varepsilon_0 x10^4$	λ_{abs} (max) (nm)	λ_{fl} (max) (nm)	Host	Cooling Rate	Hole Burning	Burning Facility
Tetracene	228	1.0	476	512	EtOH/MeOH[a] EtOD/MeOD[b] PS[c]	very slow " fast	Yes Yes No	Weak Very Weak ------
Pentacene	278	1.3	575	520	PS	fast	No	------
Quinizarin	240	~ 0.8	470	520	Gly/H_2O[d] PS	moderate fast	Yes No	Medium ------
R560 (chloride)	367	7.4	506	532	PAA[e]	fast	Yes	Medium
R640 (perchlorate)	591	~ 5	575	605	PVOH[f] PAA	fast "	Yes Yes	Strong Strong
DCM	303	~ 5	481	644	PS	fast	No	------

[a] EtOH/MeOH ≡ protonated ethanol/methanol mixture.

[b] EtOD/MeOD ≡ hydroxy deuterated ethanol/methanol mixture.

[c] PS ≡ polystyrene.

[d] Gly/H_2O ≡ glycerol/water glass.

[e] PAA ≡ poly(acrylic acid).

[f] PVOH ≡ poly(vinyl alcohol).

Table 3. Continued

Molecule	Mol. Wgt. (g/mol)	$\varepsilon_0 x10^4$	λ_{abs} (max) (nm)	λ_{fl} (max) (nm)	Host	Cooling Rate	Hole Burning	Burning Facility
Cresyl Violet (perchlorate)	362	4.4	601	630	Gly/H_2O PVOH PAA PVK[g]	moderate fast " "	Yes Yes Yes Yes	Strong Very Strong Very Strong Very Weak
Nile Blue (perchlorate)	418	7.7	628	640	PVOH PAA	fast "	Yes Yes	Strong Strong
Oxazine 720 (perchlorate)	432	9.2	623	650	PVOH PAA	fast "	Yes Yes	Very Strong Extremely Strong
Oxazine 725 (perchlorate)	424	12.5	645	680	PVOH PAA	fast "	Yes Yes	Medium Medium
Oxazine 750 (perchlorate)	470	~ 9	662	705	PAA	fast	Yes	Weak
DECI-N[h]	455	~ 7	422	?	PVOH	fast	No	———

[g] PVK ≡ poly(vinyl carbazole).

[h] DECI-N ≡ 1,1'-diethyl-2,2'-aza-cyanine iodide (donated by Alfred Marchetti, Eastman Kodak Co.).

Table 3. Continued

Molecule	Mol. Wgt. (g/mol)	$\varepsilon_0 x10^4$	λ_{abs} (max) (nm)	λ_{fl} (max) (nm)	Host	Cooling Rate	Hole Burning	Burning Facility
DECI[i]	454	7.9	524	?	PVOH	fast	No	-------
MCI[j]	409	~ 8	572	?	PVOH	fast	Yes	Moderately Strong
Malachite Grn.	308	~ 5	614	?	PAA	fast	Yes	Weak
Methylene Blue	374	8.9	661	690	PAA	fast	Yes	Very Weak
Indigo Carmine	466	~ 0.6	608	?	PAA	fast	Yes	Medium
Pr^{+3} ($PrCl_3 \cdot 6H_2O$)	354	1.5 E-4	590[k]	many λ[l]	PVOH	fast	Yes	Weak
Nd^{+3} ($NdCl_3 \cdot 6H_2O$)	357	7 E-4	575[k]	many λ[l]	PVOH	fast	Yes	Weak

[i] DECI ≡ 1,1'-diethyl-2,2'-cyanine iodide (donated by Alfred Marchetti, Eastman Kodak Co.).

[j] MCI ≡ 1,1'-methylene-2,2'-cyanine iodide (donated by Alfred Marchetti, Eastman Kodak Co.).

[k] Wavelength of studied transition (see text).

[l] Depends on exact transition excited (fluoresces out of many transitions).

frigerated and were opened only under nitrogen atmosphere to preclude rapid proton exchange.

(2) Basically, the mixing of the sample solutions is quite straight forward. To clarify this section, it will be broken down into the subsections of glasses and polymers. For glasses, only the composition of the solvent mixture and the complete solvation of the dopant is important. The mixture is often an established recipe found after considerable trial and error [62]. However, it is extremely important to totally remove any particulate matter from the sample solutions, since even the smallest trace can cause the glass to crack and shatter upon cooling to liquid helium temperatures. To avoid this problem, the samples were filtered with a filter syringe to remove any particulate material. Additionally, just before cooling, the samples should be vigorously stirred and then deaerated. By following these techniques, the chances of achieving a glass is greatly enhanced.

In contrast to the soft organic glasses, the problem of cracking and shattering usually is not evident when cooling polymers. This ease in cooling, as well as the current broad interest in polymers, are the primary reasons that the major thrust of this thesis deals with polymer hosts. Unlike the glasses, little work had been performed previously in our group to determine the best preparation of various polymer formations. Thus, most polymers were prepared somewhat serendipitously. In this work, only four different polymers were studied in any detail: polystyrene [PS], poly(vinyl alcohol) [PVOH], poly(acrylic acid) [PAA] and poly(vinyl carbazole) [PVK].

For polystyrene, a teflon mold was made with a size of 1 cm x 1 cm. This holder then was placed on a hot plate where polystyrene pellets were added and then melted; the sample then was added and mixed until a homogeneous solution was attained. Importantly, this procedure was performed entirely under a nitrogen atmosphere, since polystyrene is known to undergo oxidation in air. The entire holder was immersed then into liquid nitrogen to quench the polymer. Next, the sample was placed into a vacuum tube so that freeze-pump-thaw cycles could be performed to remove bubbles and improve sample clarity. Finally, the sample was removed from the tube and cut to a thickness whose optical density was ~0.5. The samples prepared by this technique had the impurities of tetracene, pentacene and quinizarin.

PVOH and PAA were purchased from Aldrich Chemicals with average molecular weights of 14,000 and 250,000, respectively. PVOH was 100% hydrolyzed. Both polymers were prepared similarly. Each was dissolved into distilled and deionized hot water until a syrupy solution was attained; a relatively large amount was prepared so that identical samples could be made. Once the polymer solution was prepared, a small amount of impurity (usually laser dyes or rare earths) was added to approximately 15-20 ml of solution in small increments until the approximate concentration was attained. Since the extinction coefficient of the dye molecules is large (typically 10^{+5} 1/cm•mole), exact quantification was not practical. Next, this sample solution was poured through a filter syringe onto a glass plate (either 2" or 1 cm diameter) to a liquid thickness of ~2-3 mm (using the solution's surface tension to hold it on

the plate). The samples were allowed to air dry for 1-2 days. Finally, the prepared samples were checked for reasonable optical density, and the entire procedure was repeated until good samples were attained. For the optical studies, the prepared films were ~100-200 microns thick and samples were cut to a size of ~2 mm x 2 mm from the larger film, selecting for clarity and uniformity. For the dye dopants, the sample integrity remained good essentially indefinitely, thus, these samples were used repeatedly. However, the rare earth samples tended to become opaque over time, consequently, they were prepared fresh for each experimental run. The concentrations used were ~5 x 10^{-4} - 1 x 10^{-5} M for the dye molecules and roughly 1-2 M for the rare earths.

PVK (purchased from Aldrich) was dissolved into methyltetrahydrofuran (MTHF) until the consistency was appropriate, and then the impurity was added. The solution then was poured as above and placed into a desicator using a slow flow of nitrogen gas to evaporate the solvent; importantly, the flow had to be controlled carefully in order to obtain high quality samples (i.e., without opacity, cracking and shrinkage due to rapid drying).

(3) Sample mounting varied greatly depending upon the system under study and the type of experiment to be performed. In general, the polymer samples were held in intimate contact with a copper sample plate for maximum thermal conductivity using pressure sensitive tape. The soft organic glasses were either mounted onto a copper plate or inserted into a copper cylinder with optical access. For all samples, a silicon temperature diode with an accuracy of better than 0.05 K was used in direct

contact with the copper sample holder and, in cases of temperature studies, was affixed with G. E. Adhesive Varnish No. 7031. For the polymer sample holders, several small holes of ~1/8" diameter were drilled close together, allowing as many as 12 holes within the vertical diameter of the temperature diode and, thereby, allowing for accurate measurement of the temperature for multiple samples. One additional point is that in order to study some very low concentration films, a relatively high optical density was required, and was accomplished by the careful folding of a polymer film.

(4) As has been demonstrated previously [62], the cooling procedure can be extremely important in the study of the properties of glasses. Additionally, it has been shown that the rate of cooling is critical in the formation of a good clear glass. In particular, as stated in Paper 1 [68] (vide infra), the simultaneous preparation of the protonated and deuterated methanol/ethanol glass mixtures was exceedingly difficult. Typical cooling rate of this touchy glass was ~5° per hour and even slower near the glass transition point. In contrast to these liquid solvent glasses, formation of polymers at cryogenic temperatures does not have any of the same tedious problems since the glass is already formed at room temperature. To eliminate many of the problems induced by the different cooling rates used from sample to sample, the polymers usually were immersed directly into liquid helium at 4.2 K. Using this technique, no hysteresis effects were observed. Furthermore, by using this direct immersion technique, samples gave reproducible

results, thus, giving "identical" samples from one experimental run to another.

Cryogenic Equipment

For most studies, either a Janis Vari-Temp 8DT convection cooled cryostat or a Pope 4-liter immersion dewar was used for the low temperature studies. Samples were mounted as stated above and the temperature was measured by a calibrated silicon diode sensor (Lakeshore Cryogenics Model DT-500) with a precision of <0.05 K; this diode was connected either to a home built constant current supply with voltage output or to a Lakeshore Cryogenics Temperature Controller Model DTC-500. Samples were cooled in the Janis cryostat by passing cold helium over the sample.

Temperatures can be controlled by a variety of techniques; the three major procedures will be described here. First, the throttle valve can be varied slightly while having the sample chamber valve open and the reservoir closed or slightly open. This is the simplest technique, although it can be quite sensitive to these slight adjustments in the throttle valve setting. Second, the valves can be set as in the first case, except that the helium flow is allowed to be greater and the sample then is heated by a 50 Ω heating resistor controlled by varying the applied voltage. Lastly, another procedure is to open the throttle valve more, close the reservoir valve, and then control the temperature by changing the sample chamber valve back pressure slightly. Generally, in practice, one is required to use a combination of the above

techniques to achieve the desired temperatures and stabilities required.

Finally, to achieve temperatures below 4.2 K, the helium is pumped on by a standard high capacity vacuum pump, which then allows one to reach the lambda point (2.2 K) and temperatures below. Usually, temperatures of ~1.6 K are quite easily achieved, although temperatures of 1.2 K should be attainable. To achieve temperatures between 1.6 K and 4.2 K, both the throttle valve and the pumping valve must be varied.

Optics and Lasers

Several different laser systems have been used in this study of nonphotochemical hole burning. The primary systems used were:

(1) Nd-YAG pumped pulsed dye lasers:

Quanta Ray (DCR-1) Nd-YAG pumped (PDL-1) dye laser

$\Gamma_l = <0.7\ cm^{-1}$ Γ is the laser linewidth at FWHM.

Quantel 480 Nd-YAG pumped (TDL-III) dye laser

$\Gamma_l = <0.14\ cm^{-1}$

(2) Helium-neon CW lasers:

Spectra-Physics (134)

Melles-Griot (05 LLR 111)

$\Gamma_l = <0.004\ cm^{-1}$

(3) CW argon ion laser:

Coherent (Innova 90-5)

$\Gamma_l = <0.5\ cm^{-1}$

(4) CW ring dye laser (various configurations):

Coherent (699-03, 05, or 21)

$$\Gamma_1^{03} = <0.1 \text{ cm}^{-1}$$

$$\Gamma_1^{05} = <0.001 \text{ cm}^{-1}$$

$$\Gamma_1^{21} = <0.0001 \text{ cm}^{-1}$$

Basically, two experimental apparatuses were used in the study of NPHB. The general format was different for each; in one, the hole is measured via photoexcitation (i.e., the collection of total fluorescence while scanning the dye laser in frequency), while the other technique uses basic absorption in a double beam configuration. These two experimental setups will be discussed in turn and are shown diagrammatically in Figs. 5 and 6, respectively.

Photoexcitation detection system and pulsed burn laser

For the photoexcitation (fluorescence mode) experiments (see Fig. 5), a Quanta-Ray Nd-YAG pumped pulsed dye laser (vide supra) was used as both the burning laser and the excitation source; for scanning, the intensity of the laser was reduced by a factor of ~100, using a translating filter solution ($CuSO_4$-H_2O for tetracene) [155]. With this reduction in laser flux, no apparent broadening was observed when scanning with the laser. Burn powers, typically on the order of ~2 mW/mm^2, were measured with an accurate power meter (Scientech 361). Depending upon the actual experiment performed, either single or dual (i.e., two samples simultaneously) fluorescence detection was utilized. In either case, the laser beam was split by an ordinary quartz glass plate (re-

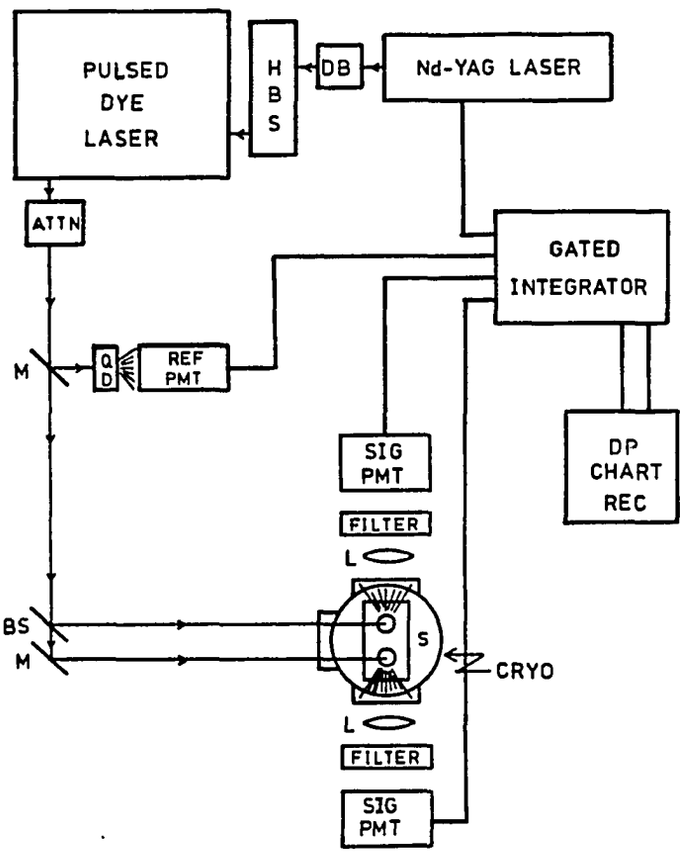

Figure 5. Photoexcitation experimental apparatus. DB - doubling crystal; HBS - harmonic beam separator; ATTN - attenuator; M - mirror; BS - beam splitter; REF - reference; SIG - signal; PMT - photomultiplier tube; DP - dual pen; REC - recorder; S - sample; CRYO - cryostat

flectance ~3%) into a reference quantum detector (saturated solution of rhodamine B in methanol, fluorescence detected at 90° with a photomultiplier tube (PMT)). For dual detection, the beam was split equally by a 50% broadband coated beam splitter (Klinger), so that both samples were burned and probed under identical conditions. The fluorescence was detected at 90° by either one (single detection) or two (dual detection) PMTs using the appropriate filters (Corning 3-69 and Corion 490 interference filters for tetracene). PMTs, usually RCA-1P28's or RCA-4832's, varied depending on fluorescence strength and PMT wavelength response, and typically were operated at 600-900 volts. For the single beam excitation, a tenth meter monochromator (Jobin-Yvon(JY) H-10) often was added to aid in rejection of stray light.

The PMT signals were input into either a Lambda Physik Laser Fotometer (LF-300) or a Quanta-Ray dual gated integrator (DGA-1); these provided ratio output to either a single pen (Heathkit SR-204) or a dual pen (Heathkit SR-206) chart recorder.

Absorption detection system and CW burning lasers

For the major portion of this work, a double beam (DB) absorption system (built primarily by T. P. Carter, Iowa State University, Ames, Iowa) was utilized as the detection system, while either a helium-neon laser, an argon ion laser or a ring dye laser was used as the burn laser. Figure 6 shows both the latter two lasers used for hole burning and the detection system. The detection system will be discussed first; the CW burning lasers, second.

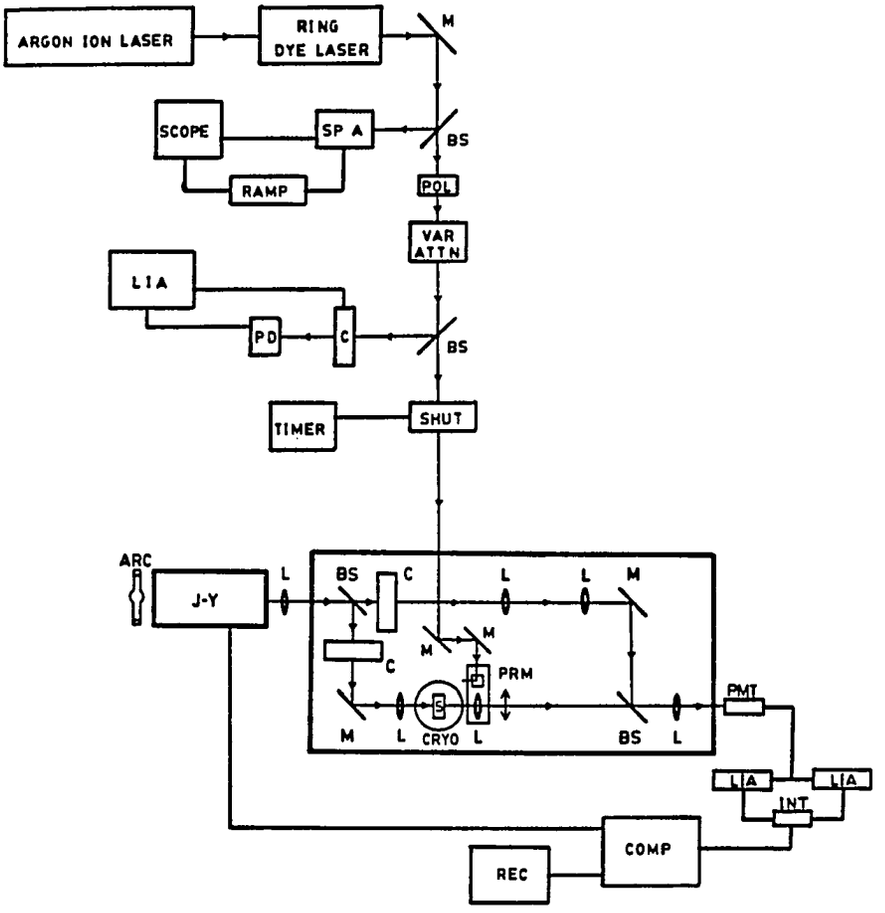

Figure 6. Absorption experimental apparatus. M - mirror; SPA - spectrum analyzer; POL - polarizer; VAR ATTN - variable attenuator; BS - beam splitter; C - chopper; PD - photodiode; LIA - lock-in amplifier; SHUT - shutter; PRM - prism; L - lens; ARC - arc lamp; J-Y - Jobin-Yvon monochromator; S - sample; CRYO - cryostat; PMT - photomultiplier tube; INT - integrator; COMP - computer; REC - recorder

Detection system The absorption system consists of a 500 Watt (small arc) high power Xenon arc lamp (Kratos model LX/500-1 arc lamp, Oriel 6102 housing powered by an Oriel C-72-20 power supply) whose output is focused and dispersed through a high resolution spectrometer, the output is collimate and split equally by a 50% beam splitter (Melles-Griot) into two beams. These beams then are mechanically chopped (Laser Precision CTX-534 choppers) at different frequencies and are passed through identical optics (Melles-Griot). One beam is the reference beam, while the other is the sample beam which is focused into the sample. Next, these beams are recombined and focused into the same cooled PMT (RCA-C31034) whose output is sent to two frequency referenced lock-in amplifiers (Ithaco model 397E0). These signals are sent to an integrator (Ithaco model 385E0) which integrates the signals for a certain number of periods. These signals then are sent either to a ratiometer (Evans Associates card no. 4122) or to a computer (vide infra), which calculates the logarithm of the ratio of the two signals, thus, yielding the absorbance. By using the same PMT, nonlinear response, wavelength dependencies and intensity fluctuations are essentially eliminated. Additionally, the reference beam has an iris attached to one lens which allows for the zeroing of the absorbance when there is scattering due to the sample. Finally, the ratio output is sent to a chart recorder (either a Texas Instruments model FS01W6D, Heathkit model SR-204, or a Houston Instruments model 4512) which then can expand and offset the output to full scale.

Two additional components were added to the DB system to facilitate the hole burning experiments. One of these was a translating mirror which allowed the burn laser to be sent through the monochromator to determine the burn frequency. The second, a turning prism mounted on a translator, was incorporated into the system so that the burn laser and probe beam would be on the same axis.

Perhaps, the most critical component of this entire system is the high resolution monochromator. The spectrometer was calibrated by using several of the lines from a low pressure neon penlamp (Oriel). The theoretical resolving power was 264,000, generally measured at better than 240,000. In practice, the resolution of the spectrometer was typically ~0.04 Å (as verified by the transition line of an iodine cell) or, in the wavelength range of most experiments, $<0.12\ cm^{-1}$.

Very recently, this entire apparatus has been interfaced to a computer (Digital Equipment Corporation 11/23+) so that essentially everything now is controlled automatically and the data are recorded permanently onto disk. Once the data are recorded, graphics terminals (Visual 550 and Visual 102/graphic) are used to analyze the data, and a digital plotter (Houston Instruments DMP4) is used to plot the output.

CW burn laser system The laser system is shown along with the detection system in Fig. 6. For convenience, only the most current version of the burn laser setup will be discussed, since no effectual changes occurred upon upgrades. The primary burn laser was a Coherent 699-21 ring dye laser ($\Gamma_1 < 0.0001\ cm^{-1}$) pumped by a 5 W Coherent Innova 90-5 argon ion laser ($\Gamma_1 < 0.5\ cm^{-1}$). To monitor and to measure the

laser frequency stability, a spectrum analyzer was used (for linewidth measurement, a Tropel 240 was used and for monitoring stability, i.e., mode hops, a Spectra-Physics 470-04 was used). The dye laser power output using R6G (Exciton) at 585 nm was usually ~500 mW in the stabilized configuration. Since, typical burning flux used in these experiments was <1 mW/cm^2, the laser power had to be accurately attenuated to reasonable powers. This was accomplished by the combination of a Glan-Thompson polarizer (KLC Corp.) and a NRC 935-5 variable attenuator. To give maximum flexibility, the polarizer usually was set to attenuate the laser beam to an easily measured power (~50 mW) and then was precisely attenuated with the variable attenuator. Further, to obtain an accurate measure of the power at the sample, the combination of a Coherent 210 power meter and a Molectron LP141 photodiode was used in conjunction with a PAR 124 lock-in amplifier. Using this technique, powers as low as 1 μW could be measured precisely. To determine an accurate measure of the actual laser flux (power density) used, a translating 70 μ pinhole (using a Burleigh Inchworm, CE-2000 controller and IW-601 micrometer) was utilized to measure the laser beam diameter at the $1/e^2$ point. Finally, the time period of the burn was controlled by a NRC 845 digital shutter controller.

Experimental Techniques

During the course of this research on NPHB, many different experimental techniques have been used to perform several different types of experiments. Some of these techniques and procedures have been described in generalities above, however, the exact protocol has not.

Since many of the actual details are presented in the actual papers (vide infra), only the most important aspects will be discussed here.

Firstly, it is important to emphasize the exact procedure used in the temperature dependent dephasing studies [68,70] (see Papers 1 and 3). In all of our studies, the linewidth measurements are performed at the same temperature that the burn was performed, i.e., not burned at some temperature and then allowed to warm to obtain the linewidths. Thus, each data point represents a newly burned sample, contrary to what often has been performed previously by other groups [141].

Secondly, as verified by separate experiments for all the polymer samples, the results obtained from one sample to another were identical. This leads to the ability to have many identical but "unique" samples at the same time, all "identically" prepared with the same thermal history. Thus, multiple experiments could be done in the same experimental run, greatly increasing the reliability and quantity of the data. These facts are exactly the reason that the phenomena of spontaneous and laser induced hole burning could be studied at all (see Papers 5 and 6) [50,51].

Finally, an important aspect of these studies is the actual measurement of the holes, i.e., hole depths and hole widths, as well as the fits used to analyze this data. Usually, the hole parameters were determined by hand, using a straight edge or french curve to find the baseline followed by tedious use of a precision ruler. Using this technique, the measurement error generally was kept below the signal to noise ratio of the spectra. More recently, due to the recording of the

data by computer, this portion can now be done with the aid of a graphics terminal, although it is still quite time consuming. For dephasing, SPHF and LIHF studies, the computer is used extensively to perform weighted linear or nonlinear least squares analysis of the data. These programs were developed by the author.

PAPER 1. NONPHOTOCHEMICAL HOLE BURNING IN A HYDROGEN BONDING GLASS: DEPENDENCE ON DEUTERATION

EXPERIMENTAL, RESULTS AND DISCUSSION

Photochemical and nonphotochemical hole burning (PHB, NPHB) spectroscopy of molecules imbedded in amorphous solids has been the subject of many recent investigations [1-9]. Although the hole production mechanisms for PHB and NPHB are different, with the latter a photoinduced guest-host cage structural deformation involving host two level systems (TLS), both can be used to study the fast dephasing of guest electronic transitions in glasses and polymers [5,7,9]. Amorphous solids are currently viewed as containing a distribution of TLS [asymmetric intermolecular double well potentials] [10,11]. Dephasing theories, by necessity, have had to take into account the TLS and the T dependence of the phonon assisted tunneling [5,6,12]. One such theory for NPHB provides a framework for understanding the low hole burning quantum yields and the fast (relative to crystalline hosts) dephasing in terms of the TLS [5]. In that work, the importance of recognizing that the characteristics of TLS distribution functions for "soft" organic solids may be very different from those for inorganic glasses was underscored. Hole burning data have been used to estimate that the width of the TLS distribution as a function of the zero-point splitting of the two wells is narrow (a few cm^{-1}) for organic glasses [5,7].

Further studies of dephasing in amorphous solids should lead to an improved understanding of disorder of the high density of very low frequency excitations in such materials. Thermal annealing of nonphotochemical holes should yield similar information, since by NPHB at different burn temperatures, one probes different subsets of the TLS dis-

tribution [5]. A great deal is to be learned by determining how general the NPHB phenomenon is. The question of generality has been under investigation in our laboratory for some time and led to the experiments described herein.

NPHB of π-electron molecules has been studied in a variety of polar hydrogen-bonding glasses, hydrocarbons glasses and polymers [13]. The polar glasses include 4:1 ethanol:methanol (EtOH:MeOH), 2:1:1 glycerol: dimethylsulfoxide:dimethylformamide (Gly:DMSO:DMF), 5:2:2 glycerol: water:ethanol (Gly:H_2O:EtOH) and 5:4 glycerol:water (Gly:H_2O). The glycerol containing glasses are particularly easy to form (without cracking) at liquid helium temperatures. The hydrocarbon glasses are decalin, o-terphenyl, a 2:3:3 mixture of pentane:2-methylpentane: methylcyclohexane (P:MP:MC) and benzophenone, all of which form readily at 4.2 K (see Ref. 13 for details). The polymers studied include polymethylmethacrylate (PMMA), polycarbonate (PC), and polyvinylcarbazole (PVK). The manner in which the experiments were performed is described elsewhere [5,13], but we note that a "burn" laser flux of $\lesssim$10 mW/mm^2 was generally used. On the basis of ~24 "survey" experiments, it appears that NPHB in polar hydrogen-bonding glasses is significantly more facile (efficient) than in hydrocarbon glasses or polymers. For example, tetracene in the EtOH:MeOH and Gly:DMSO:DMF polar glasses hole burns readily with a quantum efficiency of ~10^{-4} with zero-phonon holes easily discernible after an irradiation time of several minutes. On the other hand, no hole burning for tetracene in the three polymers or in the first three hydrocarbon glasses was discernible after an irradiation

time of 1 h. Exceptions exist, notably; NPHB is observed for 1,4-dihydroxyanthraquinone in P:MP:MC (but not in benzophenone) [13], R640 in PMMA [13], and dimethyl-s-tetrazine in PVK [14]. Very recently, NPHB more efficient than 10^{-4} has been observed for Pr^{3+} and Eu^{3+} in inorganic glasses [15] and tetracene in thin amorphous films of anthracene [16]. Clearly, even though our data indicate a trend, there are important exceptions and, thus, far more work is required before the microscopic aspects of disorder which lead to NPHB will be understood.

To ascertain whether hydrogen bond modes are instrumental for NPHB in the polar glasses, experiments were conducted on tetracene in 4:1 EtOH:MeOH and 4:1 EtOD:MeOD (Merck, Sharp and Dohme, >99% deuteration). The samples were contained in 4 mm NMR tubes with tetracene concentrations of ~5 x 10^{-5} M. Protonated and deuterated samples were prepared simultaneously in a Janis 8DT "supervaritemp" cryostat by cooling from room temperature to ~30 K over a 24 h period at a rate of ~12 K h^{-1}. Spectra were obtained in the photoexcitation (fluorescence) mode using a Quanta-Ray DCR-1 Nd-YAG laser which pumps a tunable Quanta-Ray PDL-1 dye laser (Coumarin 480, Exciton). The laser beam was split into a reference quantum detector for normalization before being split equally into both samples with a 50% beam splitter. All burns were performed at 475.0 nm (in the origin band of tetracene's S_1 state) with fluxes of ≈2 mW/mm^2 and laser linewidths <1 cm^{-1}. Photoexcitation scans were performed with a two order of magnitude reduction in laser power. Fluorescence from each sample was detected simultaneously and processed by a Lambda Physik laser photometer which provided simultaneous display of

photoexcitation spectra. Typical results are shown in Fig. 1 where the change in optical density (Δ[OD]) following NPHB is plotted as a function of wavelength. The horizontal axes locate Δ[OD] = 0 on the vertical axis for each spectrum. The zero-phonon holes occur at 475.0 nm accompanied by broad low and high energy phonon side band holes. Taking into account the difference in burn fluxes, the integrated Δ[OD] curves indicate that NPHB in the protonated glass is ~5x more efficient than in the deuterated glass (hydroxyl deuteration only). This establishes that hydrogen bond modes are important in the hole formation process. Earlier work on tetracene indicated in EtOH:MeOH that for T(burn) $\lesssim$10 K, the hole production proceeds via phonon assisted tunneling of TLS [17]. The above deuteration dependence is about a factor of 10 times weaker than that reported by Olson et al. [18] for NPHB of pentacene in single crystals of benzoic acid. The uncertainty in our data precludes our being able to assign the negative Δ[OD] region in Fig. 1(a) ($\lambda < 473.3$) to an antihole.

Finally, the dependence of zero-phonon hole width on burn temperature for the EtOD:MeOD glass was studied between 2 and 14 K (see Ref. 5 for analogous studies for EtOH/MeOH). Unfortunately, the low hole burning efficiency made these experiments very time consuming and the quality of the data was poor relative to that reported in Ref. 5. A least squares analysis indicates that the dependence of hole width as a function of burn temperature follows a T_n power curve with $n = 1.1 \pm 0.3$. Previous work with organic glasses has found the exponent (n) to be 1.0 [5,19], 1.3 [20], and 1.5 [21]. Also, the hole width dependence

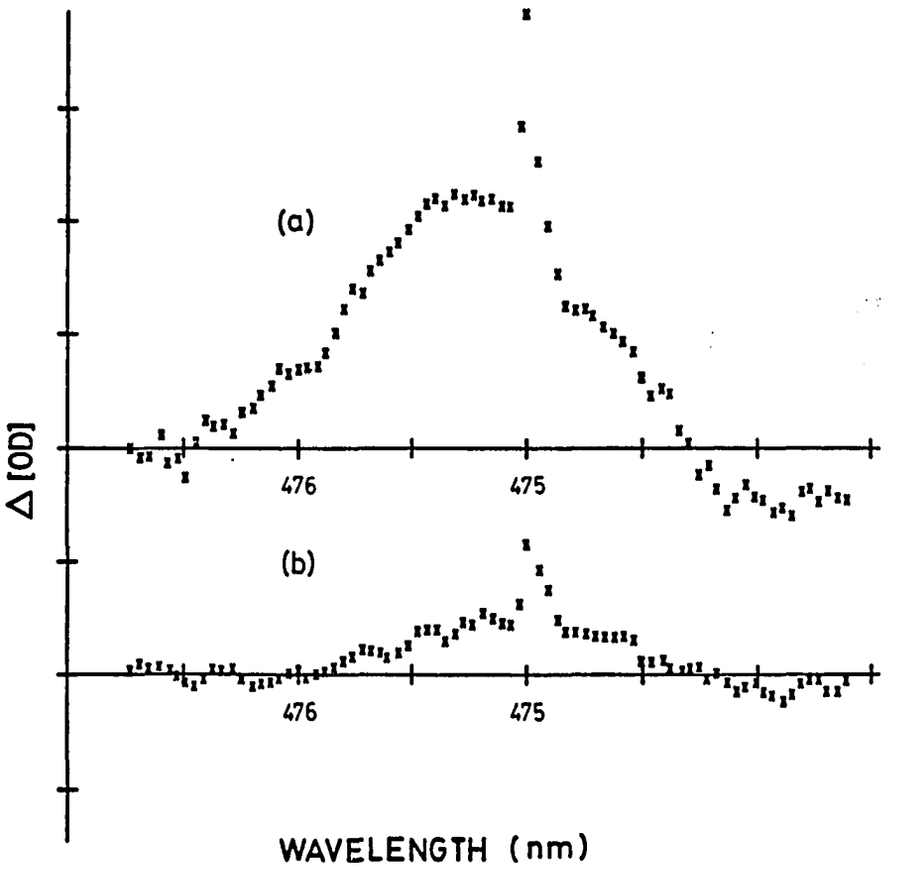

Figure 1. A plot of the change in optical density, Δ[OD], (arbitrarily scaled) vs. wavelength in nanometers of a nonphotochemical hole burned at 475.0 nm in ~10^{-5} M tetracene in an ethanol-metahnol glass; (a) EtOH-MeOH glass, 1.5 mW/mm^2, (b) EtOD-MeOD glass, 2.1 mW/mm^2. Sample temperature, 5.0 K; burn time, 1 hr

upon deuteration is weak relative to the hole burning efficiency, which is consistent with the theoretical model which proposes that the TLS involved in hole formation and in dephasing are distinctly different [5]. Friedrich et al. [7] have recently reported that for 1,4-dihydroxyanthraquinone in an ethanol glass, the zero-phonon hole width is essentially independent of deuteration over a wide range of temperatures.

REFERENCES

1. For a recent review see G. J. Small, in Spectroscopy and Excitation Dynamics of Condensed Molecular Systems, edited by V. M. Agranovich and R. M. Hochstrasser (North Holland, Amsterdam, 1983).

2. B. M. Kharlamov, R. I. Personov, and L. A. Bykovskaya, Spectrosc. 39, 137 (1975).

3. J. M. Hayes and G. J. Small, Chem. Phys. 27, 151 (1978).

4. J. M. Hayes and G. J. Small, Chem. Phys. Lett. 54, 435 (1978).

5. J. M. Hayes, R. P. Stout, and G. J. Small, J. Chem. Phys. 74, 4266 (1981).

6. R. Reineker and H. Morawitz, Chem. Phys. Lett. 86, 359 (1982).

7. J. Friedrich, H. Wolfrum, and D. Haarer, J. Chem. Phys. 77, 2309 (1982).

8. S. A. Kulagin and I. S. Osad'ko, Sov. Phys. Solid State 23, 2044 (1981).

9. A. A. Gorokhovskii, Ya. V. Kikas, V. V. Pal'm, and L. A. Rebane, Sov. Phys. Solid State 23, 602 (1981).

10. P. W. Anderson, G. I. Halperin, and C. M. Varma, Philos. Mag. 25, 1 (1972).

11. W. A. Phillips, J. Low Temp. Phys. 7, 351 (1972).

12. S. K. Lyo and R. Orbach, Phys. Rev. B 22, 4223 (1980).

13. R. P. Stout, Ph.D. Dissertation, Iowa State University, Ames, Iowa 1981.

14. E. Cuellar and G. Castro, Chem. Phys. 54, 217 (1980).

15. R. M. Macfarlane, IBM Corporation, San Jose, CA (private communication).

16. H. Bassler, Philips University, Marburg, West Germany (private communication).

17. J. M. Hayes and G. J. Small, J. Luminesc. 18/19, 219 (1979).

18. R. W. Olson, H. W. H. Lee, F. G. Patterson, and M. D. Fayer, J. Chem. Phys. 77, 2283 (1982).

19. In the high T limit of theories which attribute dephasing to phonon assisted tunneling of TLS, the hole width dependence on T_B is linear.

20. H. P. H. Thyssen, A. I. M. Decker, and S. Volker, Chem. Phys. Lett. 92, 7 (1982).

21. A. A. Goroklovski, Ya. V. Kikas, V. V. Pal'm, and L. A. Rebane, Fiz. Tverd. Tela Leningrad 23, 1040 (1981).

ACKNOWLEDGEMENTS

Ames Laboratory is operated for the U.S. Department of Energy by Iowa State University under Contract No. W-7405-Eng-82. This research was supported by the Director for Energy Research, Office of Basic Energy Science.

PAPER 2. EFFICIENT NONPHOTOCHEMICAL HOLE BURNING OF DYE MOLECULES IN POLYMERS

ABSTRACT

The nonphotochemical hole burning of ionic dye molecules in poly(vinyl alcohol) and poly(acrylic acid) polymers is shown to be efficient. Hole-burned spectra exhibit extensive intramolecular vibronic satellite structure which yields accurate S_1 vibrational frequencies. Data are presented which demonstrate that hole filling produced by a secondary burn at a frequency substantially removed from the primary burn frequency is highly selective. The class of ionic dyes in hydrogen-bonded polymers shows promise for detailed studies targeted at a better understanding of disorder and its associated relaxation processes in polymers.

INTRODUCTION

The connection between nonphotochemical hole burning (NPHB) of the optical absorption bands of impurities imbedded in amorphous hosts and the disorder of the latter was drawn by Hayes and Small [1,2] and Hayes et al. [3]. This and other work related to solid state hole burning spectroscopy has recently been reviewed [4]. A distribution of two-level systems (TLS) associated with asymmetric intermolecular double-well potentials [5,6] was used to model the disorder. Relaxation between TLS tunnel states, triggered by the impurity transition electron-TLS interaction, was proposed as the hole formation mechanism [1,2]. Because the hole burning process was too slow to account for the large homogeneous hole widths observed, it was further proposed that the impurity interacts with two "types" of TLS, distinguished by whether or not their tunnel states are in equilibrium when the impurity is in its ground state [3]. Those which are not can, at a given burn temperature T_B, give rise to persistent [7] holes. Those which are, are responsible for rapid optical dephasing by phonon-assisted tunneling (PAT) between tunnel states. The PAT accounted for the linear dependence of hole width on T_B observed for tetracene in organic glasses [3,8]. This dependence arises in the high T limit, kT > width of $f(\varepsilon)$, where ε is the zero-point splitting between local oscillators of a TLS and f is a distribution function. The problem of PAT dephasing in amorphous solids has not been considered by a number of groups [9-11]. With the exception of Ref. 11, the high and low T limits of these theories yield a linear and approximately quadratic dependence of dephasing on T, respec-

tively. In contrast with organic glasses and polymers, several experiments on rare earth ions in "hard" inorganic glasses have demonstrated, with one exception [12], the latter dependence in the low T regime [13]. In Ref. 11, the dephasing of the impurity is argued to be due to diagonal (vs. off-diagonal) modulation of the impurity optical levels. If the density of TLS states is constant, the theory finds the temperature dependence of the dephasing to be $T^{1.0}$, $T^{1.75}$, and $T^{2.12}$ for dipole-dipole, dipole-quadrupole, and quadrupole-quadrupole impurity-TLS coupling, respectively.

Importantly, NPHB has been observed in a wide variety of amorphous molecular solids [4,14-17], and very recently in Eu^{3+} and Pr^{3+} doped silicate glasses [12]. Thus, it is likely that NPHB will be added to the list of techniques [18] important for the study of disorder. Of course, photochemical hole burning of photoreactive species can also be used to probe dephasing in amorphous solids [19-21]. However, NPHB affords greater flexibility. For example, one can study the irreversible thermal annealing of holes burned at different T_B [3], the dependence of the integrated hole intensity on T_B [3], and the filling of a primary hole produced by subsequent burns at different frequencies located within the same inhomogeneously broadened profile [2].

Unfortunately, data from these latter types of experiments are limited because the experiments are very time consuming for low NPHB quantum yields. With one exception [15], the molecular systems studied have exhibited low yields, $\lesssim 10^{-5}$ [4]. For this reasons, we have been exploring the generality of NPHB and its efficiency in widely differing

(molecular) systems. Earlier results indicated that amorphous hosts with hydrogen bonding are promising, although it was noted that efficient NPHB has been reported for some nonhydrogen-bonding matrices [16]. This led to a study of a series of ionic dyes imbedded in poly(vinyl alcohol) and poly(acrylic acid) polymers. We report here some of our results because they indicate that such dyes in hydrogen-bonding polymers may form a class of efficient NPHB systems particularly convenient for future detailed studies. In addition, the NPHB spectra provide detailed vibronic structural information on the lowest excited singlet state of the ionic dye molecules.

EXPERIMENTAL SECTION

Holes were probed with a double-beam spectrometer. Light from a continuous 450-W xenon arc lamp is first dispersed by either a 1-m JA 75-150 Czerny-Turner fast spectrometer or a 1.5-m Jobin-Yvon HR 1500 spectrometer, and then split into two beams which are mechanically chopped (Laser Precision Corp. CTX-534) at different frequencies and passed through identical optics. Only air was present in the reference beam. After passage through the sample, the beams are recombined and monitored by the same photomultiplier tube whose output is provided to two identical lock-in amplifiers (Ithaco 391 A) referenced to the chopping frequencies. A logarithmic ratiometer displayed a signal proportional to sample absorbance. Extreme care was taken to ensure that the probe beam cross-sectional area at the sample was smaller than the area of the burn laser. A Janis variable temperature helium cryostat was utilized.

For the cresyl violet and hole filling experiments, the holes were burned with a Nd:YAG pumped dye laser with a linewidth less than 0.2 cm^{-1}. In all other experiments, a CW He-Ne laser was employed with a linewidth <0.02 cm^{-1}. Photon fluxes and burn times are given in the figure captions. The objectives of these experiments did not necessitate utilizing a narrow monochromator bandpass. The bandpass utilized was typically ~ 0.5 cm^{-1}.

Poly(vinyl alcohol) (PVOH) and poly(acrylic acid) (PAA) polymer films were prepared as follows: polymer powder (Aldrich) was dissolved in hot water to produce a syrupy consistency. Crystals of the dye (Ex-

citon) were added to the polymer solution and the mixture was stirred. Undissolved material was removed with a filter syringe. Aliquots of the solution were then poured onto 2-in. square glass plates and allowed to dry into thin (~0.1 mm) films which were subsequently removed from the plate. Film sections were then selected for optical density and high optical quality.

RESULTS AND DISCUSSION

The two lower traces of Fig. 1 are hole burned spectra obtained with a pulsed Nd:YAG pumped dye laser for cresyl violet in a PVOH polymer. Burning and recording were performed at T = 7 K. Spectrum a is the absorption prior to the burn. Its breadth and lack of structure should be noted. Spectrum b results from an initial burn, ω_{B1}, at 605.0 mn which is ~1000 cm^{-1} to higher energy of the absorption onset. The zero-phonon hole at ω_{B_1} is accompanied by a 32 cm^{-1} low-energy phonon side band hole [1,22] as well as about a dozen reproducible zero-phonon intramolecular satellite holes to lower energy of ω_{B_1}. The displacements of the satellite holes yield the optically active fundamental vibrational frequencies of the S_1 state of cresyl violet. For example, the 527 cm^{-1} hole is due to cresyl violet sites whose zero-point level lies at ω_{B_1} - 527 cm^{-1} and which absorb ω_{B_1} via their 527 cm^{-1} vibronic band. Thus, cresyl violet exhibits extensive vibronic activity of lower frequency fundamental which, along with inhomogeneous line broadening, is responsible for the structureless absorption spectrum a. Satellite activity to higher energy of ω_{B_1} is very weak because ω_{B_1} lies in a region where absorption by sites with zero-phonon origin absorption constitutes only a small fraction of the total optical density. It is interesting that the linear electron-phonon coupling, as judged by phonon side band hole intensity, is weak for an ionic dye.

That the holes are nonphotochemical is confirmed by spectrum c obtained following spectrum b with a second burn at ω_{B_2} (600.0 nm).

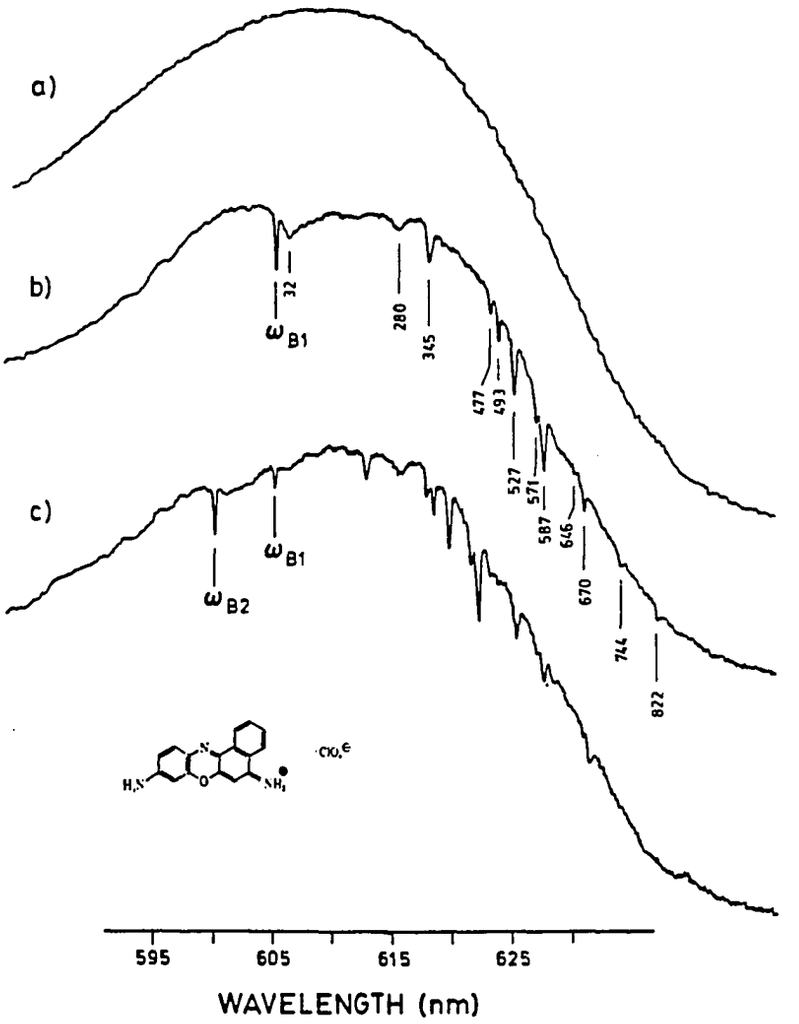

Figure 1. Hole burning and filling for cresyl violet perchlorate in PVOH at 7 K. Spectrum a is the inhomogeneous profile before hole burning; trace b shows the same sample after burning with the dye laser for 10 min with $\lesssim$5 mW/cm^2 at 605 nm. Frequency displacements of the satellite holes from the burn frequency are given in cm^{-1}; trace c is the spectrum of the same sample subsequently burned for 10 min at 600 nm with the same flux

This hole filling experiment [2] clearly shows how the holes in spectrum b are substantially filled by the ω_{B_2} burn lying ~150 cm^{-1} to higher energy of ω_{B_1}. Thus, it is demonstrated that, with NPHB, hole filling can occur when $\omega_{B_2} > \omega_{B_1}$ in addition to $\omega_{B_2} < \omega_{B_1}$ [2]. Given that inhomogeneous broadening in polymers is severe, a few hundred cm^{-1}, it is particularly interesting that a second burn so far removed from the first shows such a high degree of selectivity for producing impurity-TLS configurations which absorb at frequencies corresponding to those photobleached by the primary burn ω_{B_1}. If we note that the burn times for spectra b and c are identical and that their holes coincident with the burn frequency have nearly the same intensity, it seems unlikely that the selective filling is a result of bulk heating due to the laser. This possibility along with the interesting question of selective hole filling due to disorder induced cooperative effects are to be investigated further.

In comparing the satellite hole structure produced with ω_{B_2} with that in spectrum b, one can see that the two are essentially identical in frequencies and intensities. Given that ω_{B_2} and ω_{B_1} are so different, this may mean that the relative satellite hole intensities are a qualitative measure of the relative vibronic absorption cross sections. Further studies with a wide variety of burn frequencies are required to establish this with certainty. From spectra b and c, it can be seen that the linewidth of a number of vibronic satellite holes are considerably broader than the hole coincident with ω_B (see also Figs. 2 and 3).

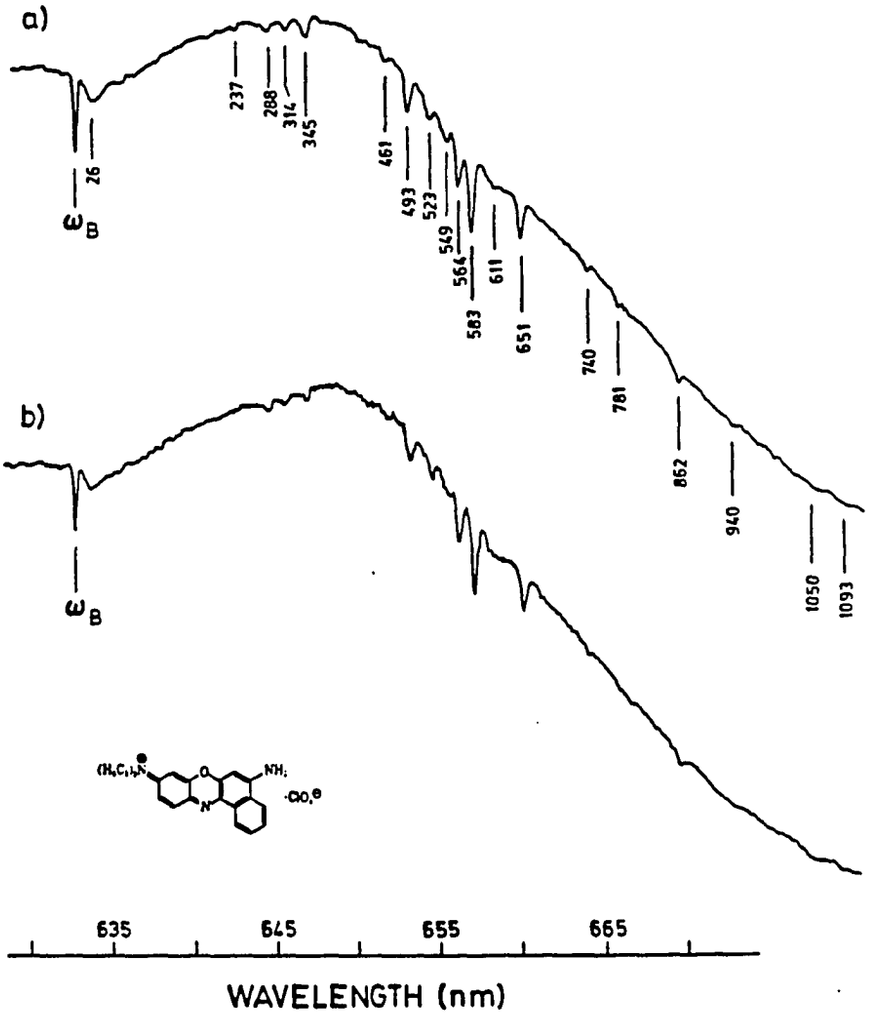

Figure 2. Hole burning for nile blue perchlorate at 5 K with a CW helium-neon laser. Spectrum a is in PVOH burned for 7 min at ~25 mW/cm^2. Displacements of the satellite holes from the burn frequency are given in cm^{-1}; spectrum b is in PAA burned for 12 min at ~25 mW/cm^2

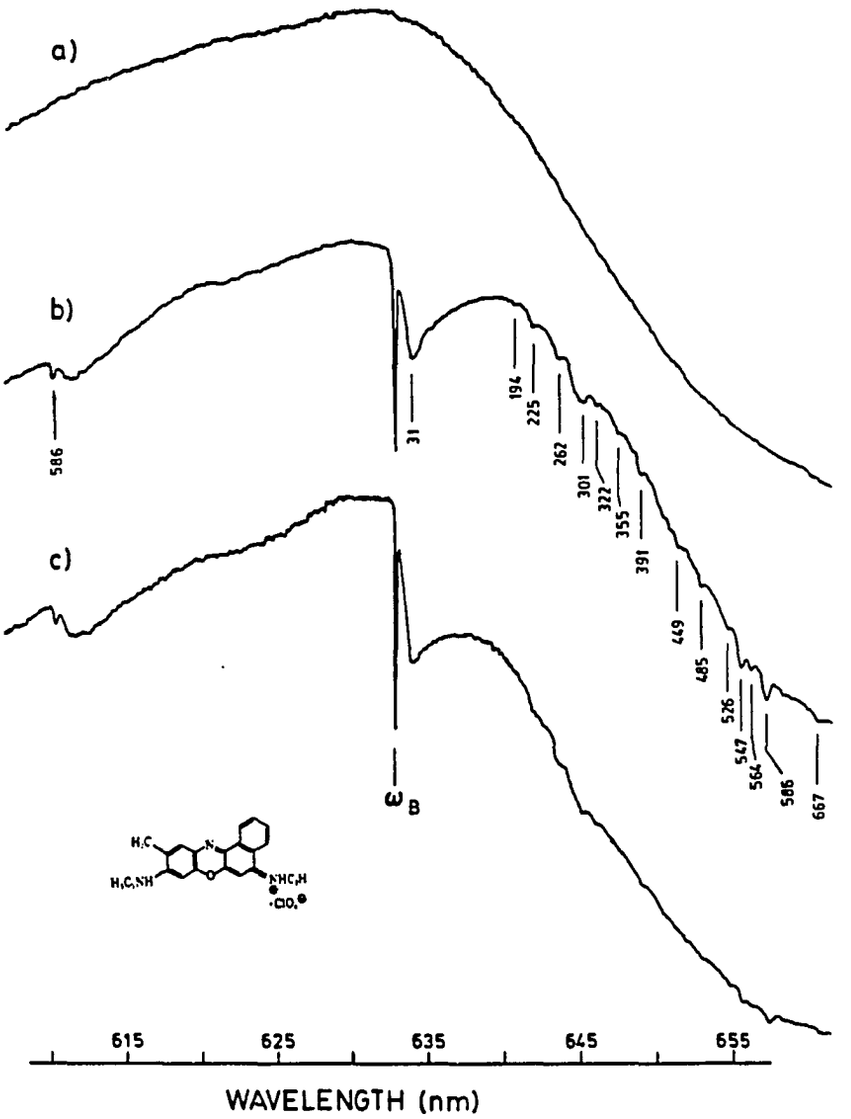

Figure 3. Hole burning for oxazine 720 perchlorate at 7 K with a CW helium-neon laser. Spectrum a is the unburned inhomogeneous profile in PVOH; spectrum b is the same sample burned for 7 min with ~25 mW/cm^2. Frequency displacements from ω_B are given in cm^{-1}. The host in spectrum c is PAA which was burned for 12 min at ~25 mW/cm^2

The reason for this has not been established, but one possibility is that the impurity site energy distribution function depends on the vibrational sublevel of S_1.

The optical dephasing of cresyl violet in PVOH has been studied with the HeNe laser at 6328 Å [23]. In the course of this work, we determined that at 6328 Å the saturated [24] hole intensity represents about a 50% optical density change. Using an approach identical with that in Ref. 15, we estimated the NPHB quantum yield (average) to be $\sim 10^{-2}$.

The hole burned spectra in Fig. 2 are for nile blue in PVOH (a) and PAA (b) at a burn and recording T = 5 K. Again, rich vibronic satellite structure is observed which is a signature for nile blue and essentially identical for the two polymers. The satellite holes labeled with vibrational frequencies are reproducible.

Finally, in Fig. 3, we show the NPHB spectra for oxazine 720 in PVOH (a and b) and PAA (c) burned with HeNe laser. At saturation, the optical density change associated with the ω_{B_2} zero-phonon hole is ~40%. The vibronic satellite structure is broader and less pronounced than in Figs. 1 and 2. Note, however, the pronounced zero-phonon hole 586 cm^{-1} to higher energy from ω_B, which is approximately 800 cm^{-1} from the onset of the inhomogeneous distribution.

CONCLUSION

Ionic dye molecules in hydroxylated polymers exhibit efficient NPHB and rich vibronic satellite hole structure. Further, the systems studied thus far are characterized by linear electron-phonon coupling sufficiently weak to permit temperature-dependent optical dephasing studies based on the zero-phonon hole profile. The observed efficiencies are sufficiently high to make this class of mixed polymer systems ideal for a wide range of studies targeted toward a better understanding of phonon-assisted tunneling processes and disorder in polymers. Because of the high optical quality of the polymers, it is hoped that photon echo experiments will prove feasible [25].

Although certain aspects of NPHB are fairly well-understood, the criteria for efficient NPHB are not. This is a difficult problem because at the very least, one must consider the microscopic disorder, electron-TLS coupling strength, the spatial extent and distribution of TLS, and specific intermolecular interactions. For the systems considered here, it may be that the ionic dye plays an important role, for NPHB of cresyl violet in a glycerol-H_2O glass is efficient [26]. On the other hand, NPHB of nonpolar impurities in nonpolar polymers, e.g., pentacene in polystyrene, has proven to be very inefficient [16,26]. Thus, it still appears to be that systems with extended hydrogen-bonding networks form a class which is promising for efficient NPHB.

REFERENCES

1. J. M. Hayes and G. J. Small, Chem. Phys. 27, 151 (1978).

2. J. M. Hayes and G. J. Small, Chem. Phys. Lett. 54, 435 (1978).

3. J. M. Hayes, R. P. Stout, and G. J. Small, J. Chem. Phys. 74, 4226 (1981).

4. G. J. Small, "Molecular Spectroscopy", edited by V. M. Agranovich and R. M. Hoschstrasser, in Modern Problems in Solid State Physics, V. M. Agranovich and A. A. Maradudin, General Eds. (North Holland, Amsterdam, 1983).

5. P. W. Anderson, B. I. Halperin, and C. M. Varma, Philos. Mag. 25, 1 (1972).

6. W. A. Phillips, J. Low Temp. Phys. 7, 351 (1972).

7. In a number of systems, holes have been observed to persist unchanged for many hours provided the sample is maintained at or below the burn temperature (see Ref. 4).

8. J. M. Hayes, R. P. Stout, and G. J. Small, J. Chem. Phys. 73, 4129 (1980).

9. S. K. Lyo and R. Orbach, Phys. Rev. B 22, 4223 (1980).

10. P. Reineker and H. Morawitz, Chem. Phys. Lett. 86, 359 (1982).

11. S. K. Lyo, Phys. Rev. Lett. 48, 688 (1982).

12. R. M. Macfarlane and R. M. Shelby, Opt. Commun. 45, 46 (1983).

13. A number of systems exhibit close to a T^2 dependence from very low T to $\gtrsim$300 K (see Ref. 12 for references to studies from M. A. El-Sayed's and W. M. Yen's laboratories).

14. E. Cuellar and G. Castro, Chem. Phys. 54, 217 (1980).

15. R. Jankowiak and H. Bassler, Chem. Phys. Lett. 95, 124 (1983).

16. B. L. Fearey, R. P. Stout, J. M. Hayes, and G. J. Small, J. Chem. Phys. 78, 7013 (1983).

17. And in a hydrogen-bonded single crystal, see R. W. Olson, H. W. H. Lee, F. G. Patterson, M. D. Fayer, R. M. Shelby, D. P. Burum, and R. M. Macfarlane, J. Chem. Phys. 77, 2283 (1982).

18. See Topics in Current Physics, edited by W. A. Phillips (Springer-Verlag, Berlin, 1981), Vol. 24.

19. H. Thijssen, S. Volker, M. Schmidt, and H. Port, Chem. Phys. Lett. 94, 53 (1983).

20. A. A. Gorokhovski, Ya. V. Kikas, V. V. Palm, and L. A. Rebane, Solid State Phys. 23, 1040 (1981).

21. F. Burkhalter, G. Suter, U. Wild, V. D. Samoilenko, N. Rasumova, and R. I. Personov, Chem. Phys. Lett. 94, 483 (1983).

22. J. Friedrich, J. D. Swalen, and D. Haarer, J. Chem. Phys. 73, 705 (1980).

23. T. P. Carter, B. L. Fearey, J. M. Hayes, and G. J. Small, to be submitted to Chem. Phys. Lett.

24. With NPHB, only a subset of the total number of impurity-TLS systems absorbing at ω_B undergo hole burning at any given T_B (see Ref. 4).

25. Such experiments are planned in collaboration with A. Zewail and co-workers, California Institute of Technology, Pasadena, CA.

26. B. L. Fearey, T. P. Carter, and G. J. Small, Iowa State University, Ames, Iowa, unpublished data.

ACKNOWLEDGEMENTS

Ames Laboratory is operated for the U.S. Department of Energy by Iowa State University under Contract No. W-7405-Eng-82. This research was supported by the Director for Energy Research, Office of Basic Energy Science. The authors gratefully acknowledge the technical assistance of Dr. John M. Hayes as well as discussions with him during the course of this work.

PAPER 3. OPTICAL DEPHASING OF CRESYL VIOLET IN A POLY(VINYL ALCOHOL) POLYMER BY NONPHOTOCHEMICAL HOLE BURNING

ABSTRACT

A new burn-probe sequence is utilized with nonphotochemical hole burning to study the optical dephasing of impurities in polymer films. For cresyl violet in polyvinyl alcohol, the temperature dependence of dephasing is close to linear in the range studied. A burn time dependence of hole widths is observed and discussed.

INTRODUCTION

It is now well-established that for molecular impurities in organic glasses and polymers [1-7] and rare earth ions in the relatively hard inorganic glasses [8], the dephasing at very low temperatures is anomalously fast relative to the dephasing in crystal hosts. In addition, the characteristic T dependences of the dephasing for amorphous and crystalline systems are distinctly different. This has led to several theories [9-11] which assume that the rapid dephasing is due to phonon-assisted tunneling (PAT) between the tunnel states of the so-called two-level systems (TLS). The TLS are associated with a distribution of intermolecular asymmetric double-well potentials which model the disorder. The high- and low-temperature limits for the T dependence of the dephasing are predicted to be linear and close to quadratic, respectively. These limits are roughly defined according to whether $kT >$ or $<$ width of $f(\varepsilon)$, where f is a distribution function and ε is the zero-point splitting between the two local oscillators of the TLS. The recent theory of Lyo [12] which accounts for impurity-TLS coupling, differs significantly from the above since the T dependence depends on the nature of the coupling, i.e., dipole-dipole, dipole-quadrupole, etc. He argues that it is the weakly interacting TLS far removed from the impurity which dominate dephasing. For the organic systems studied ($T \lesssim 20$ K), linear [10,13] or T^n (with $n \approx 1.3$) behavior [2-4] has been observed. For the later case, Jackson and Silbey [14] have considered, in addition to PAT, other mechanisms to explain the nonlinearity. For rare earth ions, a near quadratic dependence has in all cases but one [8]

been observed. It is tempting [1,10] to use such T-dependent data to estimate limits on the width of $f(\varepsilon)$ but, in doing so, it should be kept in mind that one is probing only TLS which dominate dephasing. Thus, it is desirable to study one and the same system by a variety of disorder probing techniques [15].

If the TLS tunnel states responsible for impurity dephasing are in thermal equilibrium when the impurity is in its ground state, the aforementioned theories predict that as $T \to 0$ K the dephasing should vanish. It would take a special set of circumstances for this to be otherwise as evident from Ref. 10.

In this paper, nonphotochemical hole burning (NPHB) is utilized to probe the optical dephasing of cresyl violet in polyvinyl alcohol (PVOH). This system is but one member of the class of ionic dyes/hydrogen-bonding polymers which appear very promising for NPHB studies [16]. Quantum yields (as calculated using the method of Ref. 5) for hole burning are ≈2-3 orders of magnitude higher [16] than in most systems studied previously [1], zero-phonon hole depths representing as high as a 50% optical density change have been observed, the linear electron-phonon interaction is weak and the NPHB spectra are rich in intramolecular vibronic satellite hole structure characteristic of the S_1 state of the dye molecule [16]. The method utilized here with NPHB to measure temperature-dependent dephasing is different than used in previous studies [5,10,13]. It avoids some potential problems or limitations associated with the latter approaches.

EXPERIMENTAL

Holes were probed (read) using a home-built double-beam spectrometer (see Ref. 16 for further details). Briefly, radiation from a 450 W xenon arc lamp is first dispersed using either a 1 m JA 75-150 Czerny-Turner fast spectrometer (used for hole filling experiment) or a 1.5 m Jobin-Yvon HR 1500 spectrometer (having a resolving power of 2.5×10^5 in first order and used for T-dependent experiments), then split into two beams which are mechanically chopped at different frequencies and passed through identical optics. Only air was present in the reference beam. After passage through the sample, the beams are recombined and monitored by the same photomultiplier tube whose output is provided to two identical lock-in amplifiers referenced to the chopping frequencies. A logarithmic ratiometer displayed a signal proportional to sample absorbance. Extreme care was taken to ensure that the probe beam cross-sectional area at the sample was smaller than the area of the burn laser. A convention-cooled variable-temperature helium cryostat was utilized. T measurements were made with a silicon diode sensor. When several polymer samples were mounted simultaneously for T-dependent studies, they were arranged horizontally in two rows on a sample holder with the sensor centrally located between the rows. Samples were cycled from room temperature to ≈4 K by plunging into liquid helium. Subsequently, T-dependent studies were performed beginning with the lowest temperature (≈1.7 K). The cool down procedure (fast versus slow) affects the zero-phonon hole widths as does temperature cycling over

several tens of degrees. The latter is not a factor for the T-dependent data reported here ($1.7 \lesssim T \lesssim 11$ K).

For the cresyl violet hole filling experiment, a pulsed Nd:YAG pumped dye laser was used (width <0.2 cm^{-1}) with a hole reading resolution of 0.5 cm^{-1}. A cw He-Ne burn laser (width <0.02 cm^{-1}) was employed for the T-dependent experiments with a hole-reading resolution of 0.1 cm^{-1}. Photon fluxes and burn times are given in the figure captions.

The preparation of the polymer films is discussed elsewhere [16].

RESULTS AND DISCUSSION

Traces b and c of Fig. 1 are hole-burned spectra for cresyl violet in PVOH. Spectrum a in the absorption prior to the burn. Our interest here is not the intramolecular vibronic satellite hole structure which builds to lower energy of the zero-phonon hole coincident with ω_B, the burn frequency. Such structure has been considered elsewhere [16]. Rather, we emphasize that spectra b and c establish that the hole burning is nonphotochemical. Spectrum c was obtained following b with the second burn at ω_{B_2} (600.0 nm). This hole filling experiment shows how the holes in spectrum b are substantially filled by the ω_{B_2} burn lying $\approx$150 cm^{-1} to higher energy of ω_{B_1}. Thus, with NPHB, hole filling can occur when $\omega_{B_2} > \omega_{B_1}$ in addition to $\omega_{B_2} < \omega_{B_1}$ [17]. Given that inhomogeneous broadening in polymers is severe, several hundred cm^{-1}, it is particularly interesting that a second burn far removed from the first shows a high degree of preference for producing impurity-TLS configurations which absorb at frequencies corresponding to those photobleached by the primary burn ω_{B_1} [16].

For the data which follow, the 6328 Å line of a He-Ne laser was used for burning. This coincides with a point on the low-energy tail of the absorption, Fig. 1. At this wavelength, a saturated (maximum) hole depth has been measured which represents a 50% change in optical density. Absorption at 6328 Å is believed to be dominated by transitions which involve no excitation of intramolecular vibrations since the saturated hole spectrum exhibited no satellite holes to lower or higher

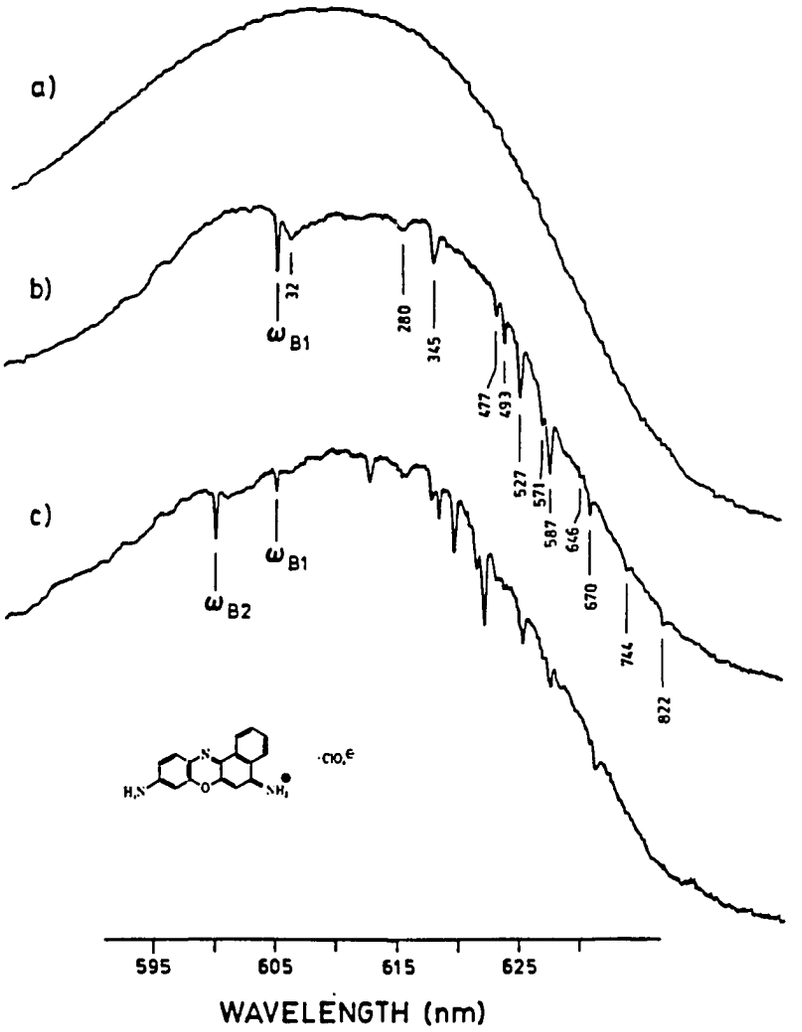

Figure 1. Hole burning and filling in cresyl violet perchlorate in PVOH at T = 7 K. Spectrum a is the inhomogeneous absorption profile before burning; spectrum b is of the same sample after burning for 10 min at 605.0 nm with ≈5 mW/cm^2. Frequency differences from ω_B for the satellite holes are given in cm^{-1}. Spectrum c is the same sample reburned at 600.0 nm for 10 min with the same flux

energy of ω_B. The absence of holes to higher energy indicates that the intramolecular Franck-Condon factors are small. This is not in contradiction with the rich satellite hole structure in Fig. 1 since the vibronic hole intensities there are governed by Franck-Condon factors weighted by the origin site energy distribution function.

The mechanism for NPHB based on TLS relaxation triggered by impurity excitation and the utilization of zero-phonon hole profiles to probe T-dependent dephasing have been recently reviewed [1]. The latter presents difficulties because generally a nonphotochemical hole undergoes irreversible thermal annealing [1,10]. Thus, one cannot generally study dephasing by burning at low T_B and reading the hole profile at higher temperatures. Thermal annealing can produce nonuniform filling [10]. Further, most organic glasses exhibit a propensity for cracking upon cool down. Because of this, Hayes et al. [10] determined Γ (hole-width) versus T_B data from measurements on a single glass sample. They utilized two approaches (sequences): (a) burn at $T_{B,1}$, (b) read at $T_{B,1}$, (c) thermally eliminate hole, (d) raise sample to $T_{B,2} > T_{B,1}$, burn at $B_{B,2}$ ...; and (a) burn at $T_{B,1}$, (b) read at $T_{B,1}$, (c) raise sample to $T_{B,2} > T_{B,1}$, (d) burn at $T_{B,2}$, etc. In the second sequence, the holes were burned to saturation. For tetracene in an EtOH:MeOH glass, both sequences gave the same results. The first sequence is preferable because it allows for the determination of the contribution to Γ from a population bottleneck or other effects [18]. Unfortunately, it is not generally applicable since temperature cycling can alter the TLS structure of the glass or polymer [10,19].

Utilization of polymers allows one to mount several sections from a given impurity-polymer films, cf. section 2. The sections can then be simultaneously and identically cooled to ≈4 K. In particular, we have used a different section for each T_B so that the advantages of the first sequence above are obtained without thermal cycling. For each polymer section (and T_B), we have studied the dependence of Γ on burn time. The overall procedure is viable when the sections are "identical". Thus, prior to its application we first established, in separate experiments, that following the initial cool down, each section gave the same Γ for identical T_B, photon flux and irradiation time.

The Γ versus T_B and burn time data are shown in Fig. 2. The cryostat liquid helium hold time limited us to three burn times (10, 20, 30 s corresponding to Δ, x, o data points). For T_B = 2.7 K, the 20 and 30 s data points are absent due to a temperature instability which occurred following the 10 s burn. For all T_B and burn times, the zero-phonon holes coincident with ω_B exhibit profiles which are close to Lorentzian, Fig. 3.

Returning to Fig. 2, the minimum Γ observed (1.75 K) is ≈0.4 cm^{-1}. We have considered the contribution of Γ from power broadening [18]. For the "worst case" situation ($T_2 = 2T_1$) and using for cresyl violet T_1 ≈ 1 ns, D ≈ 1 Å, the power broadening is several orders of magnitude smaller than 0.4 cm^{-1}.

In Fig. 2, the straight lines drawn through the data points serve as visual guides. The reading resolution utilized was 0.1 cm^{-1} so that a correction [20] to the T_B = 1.75 K linewidths was considered. A gaus-

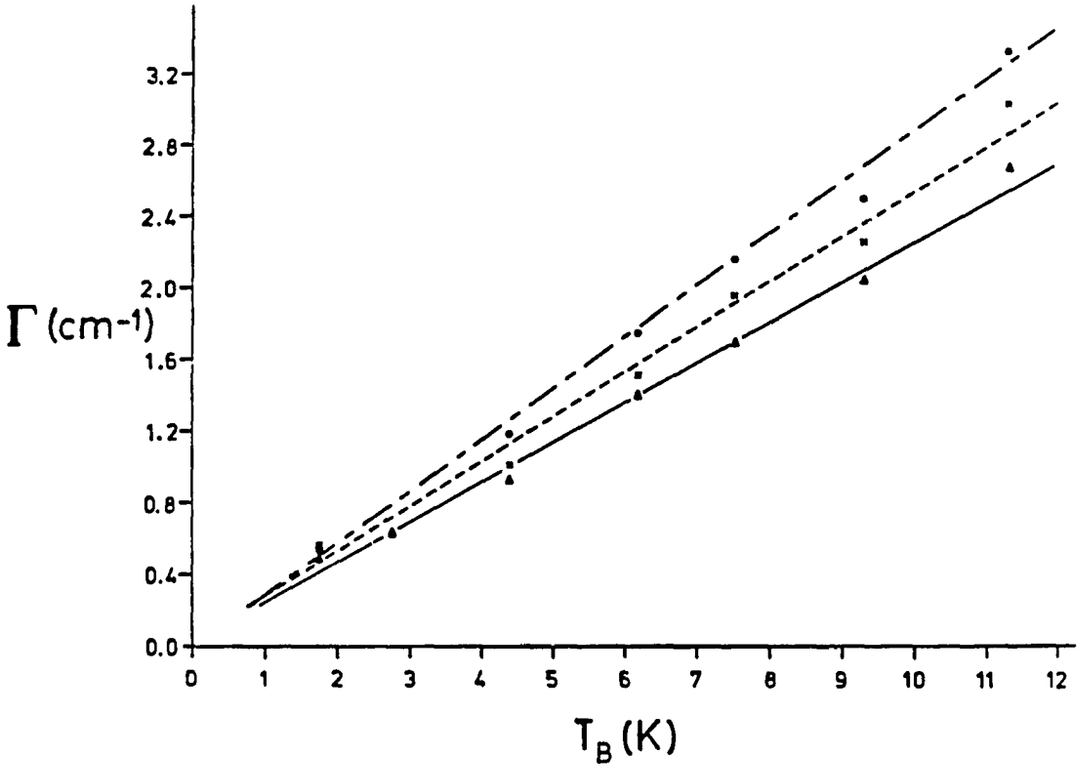

Figure 2. Observed hole width versus burn temperature for cresyl violet perchlorate in PVOH with burn times of 10 s (triangles), 20 s (crosses) and 30 s (circles). All holes were produced using a cw He-Ne laser at ≈25 mW/cm^2

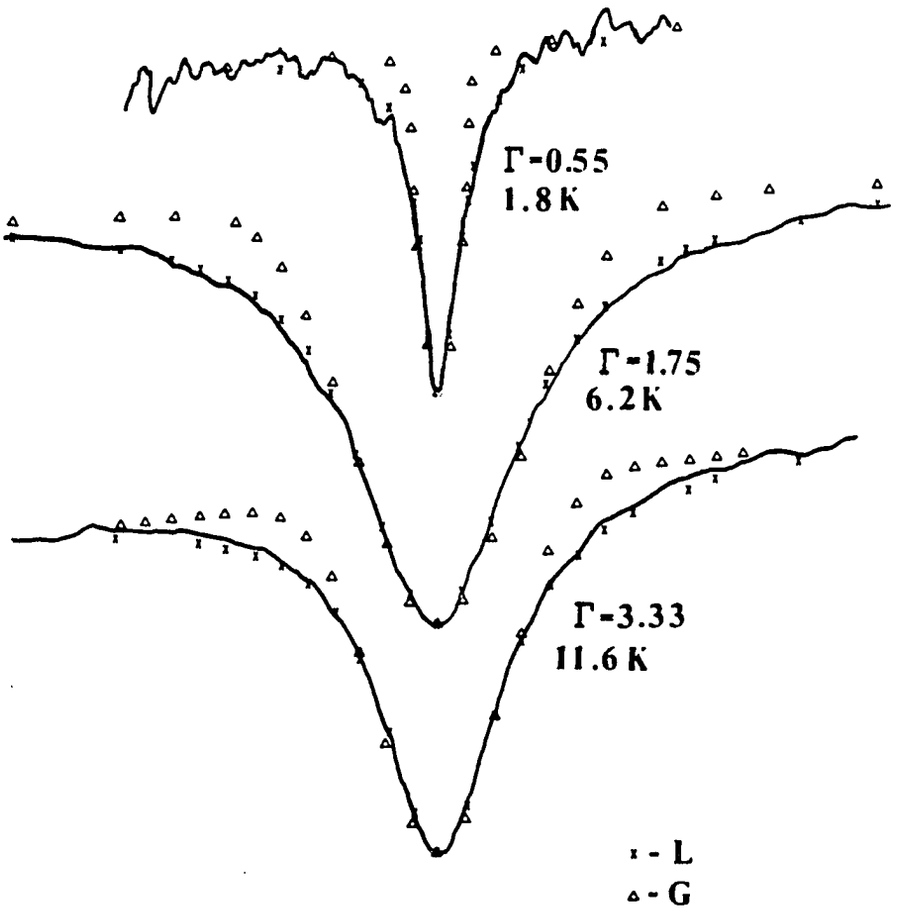

Figure 3. Hole profiles at various temperatures for cresyl violet perchlorate in PVOH for 30 s burns. Calculated Lorentzian (crosses) and Gaussian (triangles) fits to the data are shown. All linewdiths are in cm^{-1} (note the different scale for the lower trace). All hole depths represent an optical density change of ≈35%

sian instrument line-shape function was assumed which led to a reduction in the Γ values of 5-10%. Using only the 10 and 30 s burn time corrected widths for T_B = 1.75 K, a zero burn time width of 0.34 cm^{-1} results from linear extrapolation. Linear extrapolation of the Γ values for the five highest burn temperatures in Fig. 2 yielded zero burn time widths of 0.78, 1.22, 1.48, 1.82 and 2.36 cm^{-1}. A least-squares analysis of the zero burn time data, based on $\Gamma - \Gamma_0 \propto T^n$ in which the residual width Γ_0 is allowed to vary, led to a best fit for n = 1.1 and Γ_0 = 0.07 cm^{-1} (R^2 correlation factor = 0.998). The uncertainties in n and Γ_0 are estimated at ±0.1 and ±0.2 cm^{-1}. Clearly, further studies at lower T_B and higher resolution are required before the residual width Γ_0 can be meaningfully discussed.

The dependence of Γ on burn time may be due to a population bottleneck effect [18]. In this regard, the ionic dye-polymer systems we have studied exhibit some hole filling (≈10%) over a period of several minutes following termination of the burn. This effect is pronounced at first (first couple of minutes) and, thereafter, diminishes rapidly with time. Following this, the holes appear stable over long periods. The extent to which hole filling occurred during reading was small. The impurity-polymer sites which undergo ground state relaxation leading to the short-time filling may serve as bottlenecks. However, the existence of a distribution of TLS involving barrier height, zero-point splitting ε, etc. may be extended to include the hole formation rate constant even at a fixed T_B. Along this vein, if at a given T_B, the impurity-TLS sites which contribute to hole formation late in the burn (i.e., those

"harder" to burn) undergo faster dephasing on a average than those which burn at shorter times, then one has an alternative way of rationalizing the burn time dependence in Fig. 2. This and other possibilities will be investigated. The burn time dependence had not been observed in NPHB studies of tetracene in organic glasses [10,19], perhaps because the measurements were performed only at the lowest T_B = 1.8 K.

CONCLUDING REMARKS

Both NPHB [5,10,13] and photochemical hole burning [2-4,21] have been used to study the T dependence of impurity dephasing in organic glasses and polymers. Earlier NPHB studies [10,13] which employed either of the two burn sequences discussed above yielded data consistent with the high-T limit of PAT TLS theories, i.e., $\Gamma \propto T$. The other studies [2-5,21] employed the sequence: burn at T_B, read at T_B and read at $T > T_B$, vide supra. For quinizarin in ethanol/methanol [21] and tetracene in amorphous anthracene [5], a T^2 dependence was observed. For chlorin and free base porphin in a wide variety of polymers and glasses, a $T^{1.3\pm0.1}$ dependence was observed in all cases [4]. The extent to which ground state impurity-glass relaxation processes contribute to the T-dependences observed is not discussed in Refs. 2-5,21. The $T^{1.1\pm0.1}$ power law reported here for cresyl violet in the PVOH polymer is, within experimental uncertainty, the same as observed in Refs. 2-4,10,13. In comparing hole burning data from different laboratories, it seems particularly important to consider the burn-read sequences utilized.

A comment regarding the interpretation of NPHB holewidths in terms of existing PAT theories seems appropriate at this time. Nonphotochemical holes undergo thermal annealing [22] and so a hole burned at $T_{B,1}$ can anneal by $T_{B,2} > T_{B,1}$ but a hole can be burned at $T_{B,2}$[1,10]. Therefore, holes burned at different T_B appear to probe different subsets of the impurity-TLS sites capable of NPHB [10]. The application of the above theories assumes that these different subsets interact with TLS responsible for dephasing (but not hole burning [10]) which are

essentially identical. If the good agreement between the data and theory is not considered to be fortuitous, the assumption appears justified and its validity may mean that the dephasing interactions occur over distances large in comparison to impurity-nearest neighbor distances.

REFERENCES

1. G. J. Small, "Molecular Spectroscopy", edited by V. M. Agranovich and R. M. Hoschstrasser, in Modern Problems in Solid State Physics, V. M. Agranovich and A. A. Maradudin, General Eds. (North-Holland, Amsterdam, 1983).

2. A. A. Gorokhovskii, J. V. Kikas, V. V. Pal'm, and L. A. Rebane, Soviet Phys. Solid State 23, 602 (1981).

3. H. P. H. Thijssen, A. I. M. Dicker, and S. Volker, Chem. Phys. Lett. 92, 7 (1982).

4. H. P. H. Thijssen, S. Volker, M. Schmidt, and H. Port, Chem. Phys. Lett. 94, 53 (1983); H. P. H. Thijssen, R. van den Berg, and S. Volker, Chem. Phys. Lett. 97, 295 (1983).

5. R. Jankowiak and H. Bassler, Chem. Phys. Lett. 95, 310 (1983).

6. L. A. Rebane, A. A. Gorokhovskii, and J. V. Kikas, Appl. Phys. B29, 235 (1982).

7. F. A. Burkhalter, G. W. Suter, U. P. Wild, V. D. Samoilenko, N. V. Rasumova, and R. I. Personov, Chem. Phys. Lett. 94, 483 (1983).

8. R. M. Macfarlane and R. M. Shelby, Opt. Commun. 45, 46 (1983) and references therein.

9. S. K. Lyo and R. Orbach, Phys. Rev. B22, 4223 (1980).

10. J. M. Hayes, R. P. Stout, and G. J. Small, J. Chem. Phys. 74, 4266 (1981).

11. R. Reineker and H. Morawitz, Chem. Phys. Lett. 86, 359 (1982).

12. S. K. Lyo, Phys. Rev. Lett. 48, 688 (1982).

13. E. Cuellar and G. Castro, Chem. Phys. 54, 217 (1981).

14. B. Jackson and R. Silbey, Chem. Phys. Lett. 99, 331 (1983).

15. Topics in Current Physics, edited by W. A. Phillips, (Springer-Verlag, Berlin, 1981), Vol. 24.

16. B. L. Fearey, T. P. Carter, and G. J. Small, J. Phys. Chem. 87, 3590 (1983).

17. J. M. Hayes and G. J. Small, Chem. Phys. 27, 151 (1978).

18. H. de Vries and D. A. Wiersma, J. Chem. Phys. 72, 1851 (1980), and references therein.

19. R. P. Stout, Ph.D. Dissertation, Iowa State University, Ames, Iowa, 1981.

20. S. G. Rautian, Soviet Phys. Uspekhi 66, 245 (1958).

21. J. Friedrich, H. Wolfrum, and D. Haarer, J. Chem. Phys. 77, 2309 (1982).

22. J. M. Hayes and G. J. Small, J. Lumin. 18/19, 219 (1979).

ACKNOWLEDGEMENTS

Ames Laboratory is operated for the U.S. Department of Energy by Iowa State University under Contract No. W-7405-Eng-82. This research was supported by the Director for Energy Research, Office of Basic Energy Science.

PAPER 4. NONPHOTOCHEMICAL HOLE BURNING AND FILLING OF LASER DYES AND RARE EARTH IONS IN HYDROXYLATED POLYMERS

ABSTRACT

Laser dyes and rare earth ions in hydroxylated polymers undergo facile nonphotochemical hole burning. General aspects and laser induced hole filling are discussed.

INTRODUCTION

Nonphotochemical hole burning (NPHB) in glasses and polymers is a versatile probe for the dynamics of configurational relaxation governed by phonon assisted tunneling between the "glassy" tunnel states [1]. Quantum efficiency, optical dephasing, thermal annealing and laser induced hole filling measurements probe configurational relaxation ranging between picoseconds and many hours. NPHB is quite general, having even been observed for rare earth (RE) ions in inorganic glasses [2]. Recently, we have established that ionic dye molecules in hydroxylated polymers form a large class characterized by facile NPHB [3]. Over a dozen impurities doped into poly(vinyl alcohol) (PVOH) and poly(acrylic acid) (PAA) have been studied. Dopants include several dyes in the oxazine and rhodamine families as well as others and, for the first time in a "soft" organic host, RE^{3+} ions. Here, we present only a small fraction of our results. Experimental details are given elsewhere [3]. Briefly, hole reading was performed at a resolution of 0.05 Å with a double beam apparatus based on a JY HR1500 monochromator. Holes were usually burned with a Coherent 699-03 ring dye laser with an effective linewidth less than 0.002 cm^{-1}.

RESULTS AND DISCUSSION

Spectra in Fig. 1 are representative. The hole spectrum is characterized by a zero-phonon hole coincident with ω_B (burn frequency) and a large number of low energy vibronic satellite holes whose displacements from ω_B yield the active excited state vibrational frequencies (for oxazine 720 in this case). For cresyl violet in PVOH, we have analyzed the vibronic hole structure out to ~1600 cm^{-1}. Holes to higher energy of ω_B are observed to be broader and less pronounced. Their intensity depends, in part, on the optical density at ω_B due to zero-phonon origin transitions. Spectra like b), obtained with different ω_B, can be used to determine vibrational Franck-Condon factors and the site inhomogeneous line broadening.

Interestingly, it is always observed that the resonant hole at ω_B is sharper than the vibronic features. The widths of the latter exhibit considerable variation. This is consistent with a significant dependence of the site excitation energy distribution function on vibrational level in the S_1 state of the dye. Careful measurements have not yielded, for any of the dye-polymer systems studied, resonant zero-phonon holes significantly sharper than 0.4 cm^{-1} at 1.7 K. A close to liner dependence of the dephasing on temperature has been reported for cresyl violet in PVOH [3]. Phonon assisted tunneling between glassy configurations appears generally to provide anomalously fast impurity dephasing at low T in systems which undergo NPHB [1].

Optical dephasing and NPHB of RE^{+3} ions have only been studied in inorganic glasses. A key question is whether the different properties

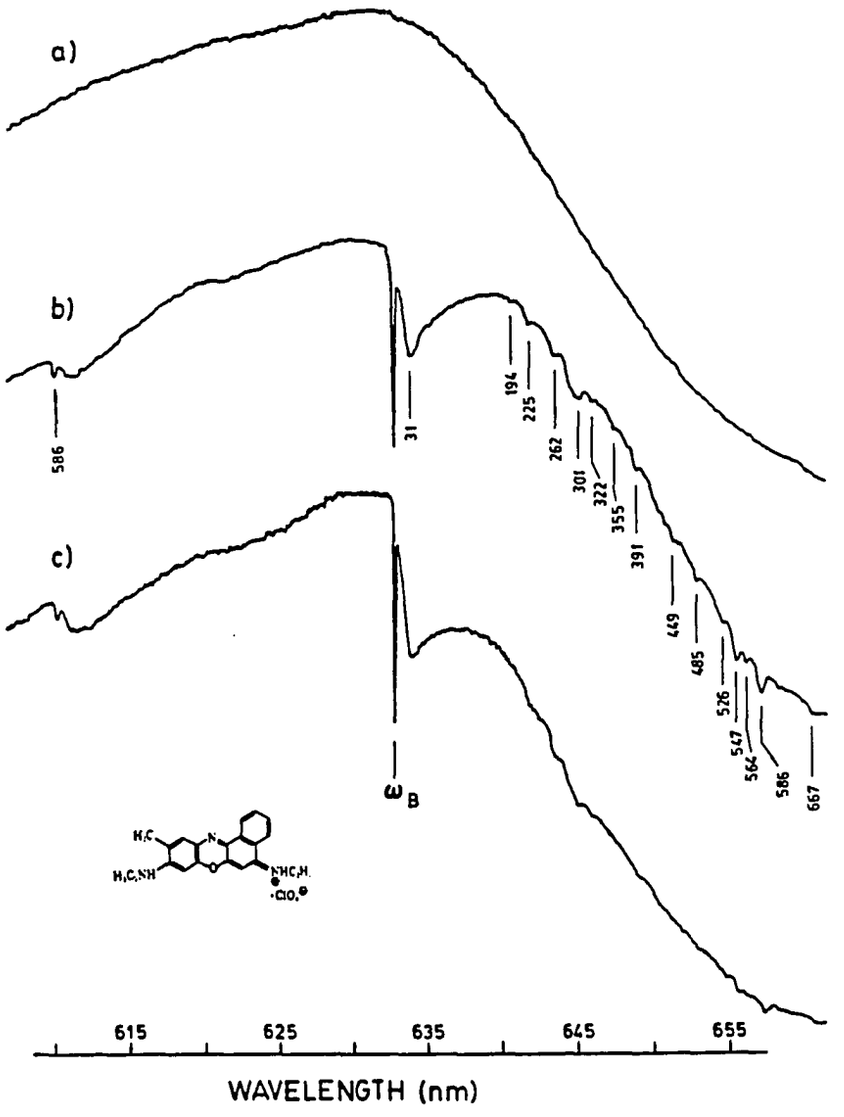

Figure 1. Hole burning for oxazine 720 perchlorate at 7 K with a CW helium-neon laser. Spectrum a is the unburned inhomogeneous profile in PVOH; spectrum b is the same sample burned for 7 min with ~25 mW/cm^2. Frequency displacements from ω_B are given in cm^{-1}. The host in spectrum is PAA which was burned for 12 min at ~25 mW/cm^2

(e.g., phonon dynamics) of an organic host will markedly affect the dephasing. Importantly, NPHB has been observed for Pr^{3+} and Nd^{3+} in PVOH, Fig. 2. For both, NPHB is only observed when ω_B is coincident with the lowest energy absorption component (associated with the ^1D state of Pr^{3+} and ^4G state of Nd^{3+}). Presumably, rapid radiationless decay of the higher energy J-levels markedly reduces their hole burning efficiency. However, low level laser irradiation of these levels effects complete filling of holes burnt in the lowest energy component. The hole burning efficiencies for Pr^{3+} and Nd^{3+} are 2 to 3 orders of magnitude higher in polymers than in inorganic glasses [2] and show about an order of magnitude larger holewidth than in inorganic glasses (at 1.7 K, Nd^{3+} yields a width of ~0.4 cm^{-1}). Thus, is is possible that their optical dephasing in "soft" amorphous hosts is correspondingly faster.

Hayes and Small (cited in Ref. 1) first observed that with NPHB, a primary hole burned at ω_{B_1} can be partially filled by burning secondary holes at ω_{B_2}. We have completed a detailed study of this for Pr^{3+}, Nd^{3+} and rhodamine 640 in PVOH in which, following the primary burn, $|\omega_{B_1} - \omega_{B_2}|$ was varied from a few to hundreds of cm^{-1}. Some observations follow: (1) hole filling is weakly dependent on the magnitude and sign of $\omega_{B_1} - \omega_{B_2}$ and remarkably efficient over the range of $|\omega_{B_1} - \omega_{B_2}|$ specified above; (2) hole filling can occur with surprisingly high efficiency for ω_{B_2} <u>outside</u> of the impurity absorption profile; (3) the width of the

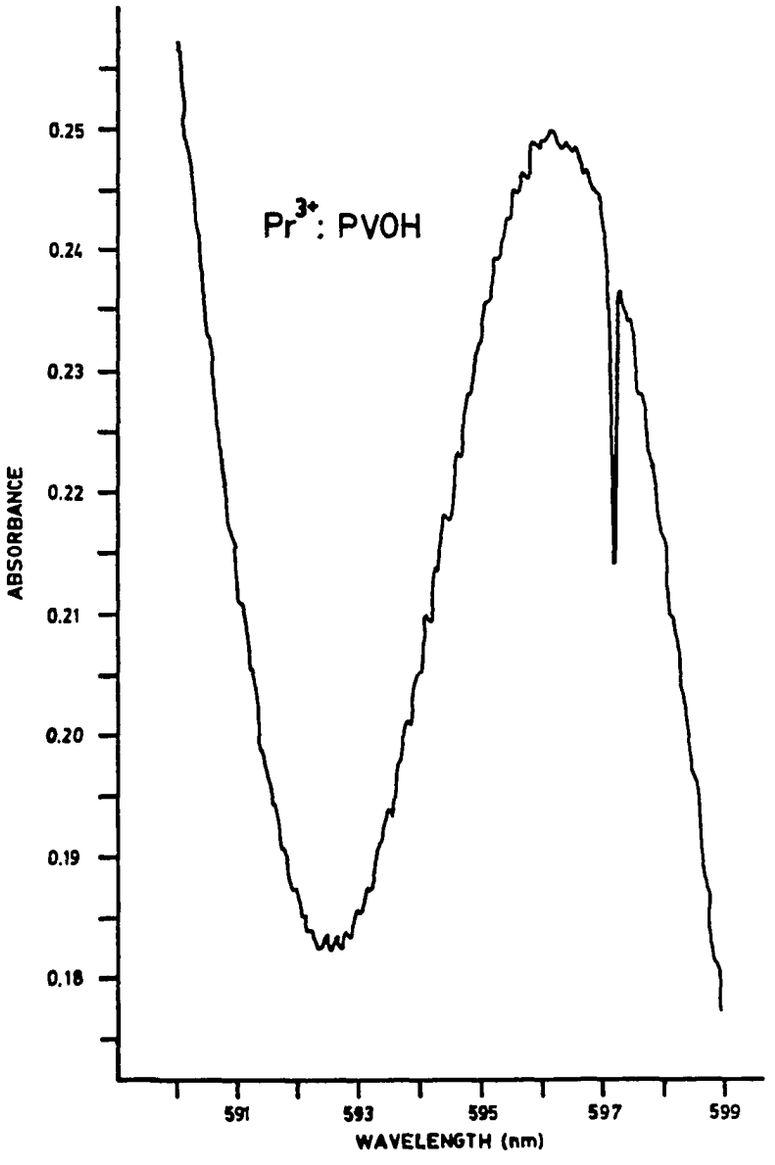

Figure 2. Hole burning of $PrCl_3(Pr^{3+})$ [~20% wgt equivalent] in PVOH at T = 6 K. Sample was burned 5 min at 5972 A ($^1D_2 \leftarrow {}^3H_4$ transition) with a flux of ~0.5 W/cm^2. The hole depth is ~10% with a FWHM of ~0.6 cm^{-1}

primary hole is not affected by filling; and (4) the extent of hole filling is not simply related to the absorbance at ω_{B_2}.

These observations and others indicate that: laser induced hole filling is due to spectral diffusion involving a wide distribution of impurity two level systems (TLS) and depends on long range connectivity (provided, perhaps, by spatially extended hydrogen bonding networks) and that at least two hole filling mechanisms are operative. One being investigated is that absorption by high O-H vibrational overtones of the polymer triggers TLS transitions which are relayed to impurity sites.

REFERENCES

1. G. J. Small, "Molecular Spectroscopy", edited by V. M. Agranovich and R. M. Hoschstrasser, in Modern Problems in Solid State Physics, V. M. Agranovich and A. A. Maradudin, General Eds. (North-Holland, Amsterdam, 1983).

2. R. M. Macfarlane and R. M. Shelby, Opt. Commun. 45 483 (1983).

3. T. P. Carter, B. L. Fearey, J. M. Hayes, and G. J. Small, Chem. Phys. Lett. 102, 272 (1983).

ACKNOWLEDGEMENTS

This research was supported by the Director for Energy Research, Office of Basic Energy Science, USDOE under Contract W-7405-Eng-82.

PAPER 5. NEW STUDIES OF NONPHOTOCHEMICAL HOLES OF DYES AND RARE EARTHS IN POLYMERS. I. SPONTANEOUS HOLE FILLING

ABSTRACT

Spontaneous hole filling data for rhodamine 640, Nd^{3+} and Pr^{3+} in poly(vinyl alcohol) films are reported. Over the time regimes studied, the time dependence of the filling can be understood in terms of a dispersive first order kinetic model based on some single two-level system tunneling coordinate. Alternatively, the filling can be explained equally well in terms of a model which invokes two "chemically distinct" two level system coordinates. The time dependence and the fact that the filling for all three dopants is not accompanied by spectral diffusion (e.g., broadening) of the hole appear to be connected. A theoretical model for this "uniform" filling is developed and based on feedback from the anti-hole sites into the zero-phonon hole region. The conditions for uniform filling are that the site excitation energies of the hole and anti-hole are correlated and that the probability for relaxation of anti-hole sites is slowly varying over the frequency profile of the anti-hole.

INTRODUCTION

The configurations of a glass which are thermally accessible from a glassy state are frequently modeled by a distribution of asymmetric intermolecular double well potentials (the two-level systems (TLS) model) [1-3]. Although the microscopic structures of TLS in glasses are not generally well understood, this model (with incorporation of phonon assisted tunneling between glassy configurations) has been remarkably successful in explaining the anomalous thermal and acoustic properties of glasses at low temperatures [4-7]. More recently, phonon assisted tunneling of TLS has been invoked as the mechanism responsible for the unusually fast dephasing of a variety of spectroscopic transitions in glasses [8-10]. The existence of disorder-induced tunnel states also imparts temperature dependences for optical dephasing which are distinctly different from those observed for impurities in crystals [11-17]. Several different theories, which are based on glassy tunnel state transitions, exist for dephasing [8,9,18-26].

Nonphotochemical hole burning (NPHB) of the electronic or vibronic absorption spectra of impurities in glasses and polymers has also been explained in terms of a TLS model [9,19,27,28]. A persistent hole produced at a particular burn temperature, T_B, is associated with a subset of the impurity-TLS isochromat at ω_B, the burn frequency. The phonon assisted tunneling frequencies of this subset are slow on the time scale of the experiment when the impurity is in its ground electronic state. Put another way, the transition electron-TLS coupling produces an impurity glass cage photoconfigurational transformation. It has been sug-

gested that the TLS associated with NPHB and optical dephasing are different; the TLS responsible for rapid dephasing on the picosecond time scale at ~4 K possess tunnel states which are in thermal equilibrium when the impurity is in its ground electronic state. It is reasonable to suggest that the TLS responsible for hole burning are, to a considerable extent, extrinsic while those responsible for dephasing are intrinsic [6].

Nonphotochemical hole burning spectroscopy was reviewed in 1982 [29]. In comparing the experimental data available then and now, it is clear that many exciting developments have occurred in three years. For example, NPHB has been observed for a wide variety of dye molecules in polymers [30,31], rare earth ions in inorganic glasses [32,33] and organic polymers [34], aromatic molecules in amorphous aromatic hydrocarbon hosts [35-37] and in organic mixed crystals in which the host is characterized by H-bonding [38]. We have observed NPHB for over 10 dye molecules in polymers like poly(vinyl alcohol) and poly(acrylic acid) [39]. Thus, NPHB can now be considered to be a quite common phenomenon. Although NPHB appears to be favored in H-bonding hosts, this is not a hard and fast rule.

Nonphotochemical hole burning is a versatile tool for studying the glassy tunnel states and their phonon assisted transitions. In addition to providing data on dephasing and the dependence of thermal annealing or hole erasure on T_B, NPHB yields the dependence of hole burning efficiency on T_B. Furthermore, the phenomena of laser induced hole filling and spontaneous hole filling (SPHF) can be studied. The former experi-

ment was first utilized to argue that the hole production for tetracene in the EtOH:MeOH glass is nonphotochemical rather than photochemical [27]. Spontaneous hole filling has been studied most extensively for quinizarin in alcoholic glasses [40,41].

In this paper, we report the results of SPHF experiments on non-photochemical holes of rhodamine 640 (R640), Pr^{3+} and Nd^{3+} in poly(vinyl alcohol). The observed characteristics of SPHF for all three systems are different than those observed for quinizarin in alcoholic glasses [40,41] and pentacene in poly(methyl methacrylate) [26]. Specifically, the SPHF is not adequately described by a logarithmic dependence on time and the hole filling is uniform (no spectral diffusion). A theoretical model which explains this behavior is presented.

EXPERIMENTAL

The basic procedural details for our recent hole burning experiments have been described previously [30,31]. In general, the same techniques were utilized for these experiments. However, for completeness and to point out certain important aspects, the procedures shall be reiterated briefly here.

The polymer samples were prepared as before [30]. The poly(vinyl alcohol) [PVOH] obtained from Aldrich was 100% hydrolyzed with an average molecular weight of 14,000. The laser dye dopants were purchased from Exciton. The rare earth (RE) impurities, $PrCl_3$ and $NdCl_3$, were prepared at Ames Laboratory with a purity of $\gtrsim$99.9%. All sample components were used without further purification. The dye samples were found to retain their integrity for an extended period of time, while the REs showed a degradation of optical clarity. To this end, the dye samples were used repeatedly and the RE samples were prepared fresh for each experimental run. Sample concentrations were adjusted such that an optical density of roughly 0.5 was obtained at the wavelength of interest. The sample thicknesses typically were 100 and 400 μ for the dye and RE samples, respectively.

Samples were cycled from room temperature to ~4.2 K by direct immersion into liquid helium contained in the sample chamber of a Janis Super Vari-Temp 8DT cryostat. This procedure allowed samples to be prepared reproducibly without hysteresis effects [31]. Temperatures were measured with a precision silicon diode sensor with an accuracy of <0.1 K.

Optical hole burning was performed with a Coherent 699-05 ring dye laser (linewidth $\lesssim 0.002$ cm^{-1}). The laser linewidth was measured and monitored with a Spectra Physics Model-470 spectrum analyzer. Powers used in burning were measured by a combination of a power meter (Coherent Model 210) and a photodiode (Molectron LP141) whose signal was chopped and locked-in (Par Model 124 Lock-in). Using this technique powers as low as one μW could be measured precisely. Beam attenuation was accomplished by a polarizer and a variable attenuator (NRC Model 935). To determine an accurate measure of the laser flux (power density), the laser beam diameter was measured after each run using a translating 70 μ pinhole. The $1/e^2$ point was used to determine the diameter.

The hole spectra were probed collinearly by a high resolution double beam spectrometer described previously [30]. The resolution used was 0.05 Å as verified by transition lines from an iodine cell. The critical component of the above instrument is the high resolving power ($\sim 2.5 \times 10^5$) of a 1.5 m Jobin-Yvon HR-1500 monochromator.

Spontaneous hole filling was monitored by repeated scans of the initially burned hole in time, where timing was initiated from the end of the burn. Times were recorded by a standard chronograph.

RESULTS

Nonphotochemical hole burning (NPHB) has been observed [30,31,39] in this laboratory for a large number of laser dye molecules imbedded in poly(acrylic acid) and poly(vinyl alcohol) (PVOH). In studying different facets of their NPHB, it was observed that spontaneous hole filling (SPHF) is a general phenomenon for these systems. Here, we report the results of detailed studies of SPHF for R640, Pr^{3+} and Nd^{3+} in PVOH. The associated optical transitions of interest are $S_1 \leftarrow S_0$ (~585 nm), $^1D_2 \leftarrow {}^3H_4$ (~590 nm) and $^2G_{7/2}, {}^4G_{5/2} \leftarrow {}^4I_{9/2}$ (~575 nm), respectively. For the rare earth ions, hole burning was performed on the lowest energy crystal field J-component which carries an inhomogeneous linewidth of ~90 and ~75 cm^{-1} for Pr^{3+} and Nd^{3+}, respectively. The laser dye R640 was selected because its inhomogeneously broadened absorption profile is composed primarily of molecular origin or (0,0) transitions. This is established by the NPHB spectra which exhibit only weak intramolecular vibronic satellite hole structure [30], cf. Fig. 1. In addition, pseudo-phonon sideband activity [27,42] is weak indicating that the electron-phonon coupling is also. Thus, R640 in PVOH provides a striking contrast with, for example, cresyl violet and nile blue in PVOH which exhibit prominent vibronic and phonon sideband structure for laser burn frequencies, ω_B, in the vicinity of their absorption maxima [30].

A typical NPHB spectrum for Nd^{3+} is shown in Fig. 2 with a hole depth corresponding to a 5.8% change in optical density. Based on a comparison of burn intensities, the hole burning facilities for Nd^{3+} and

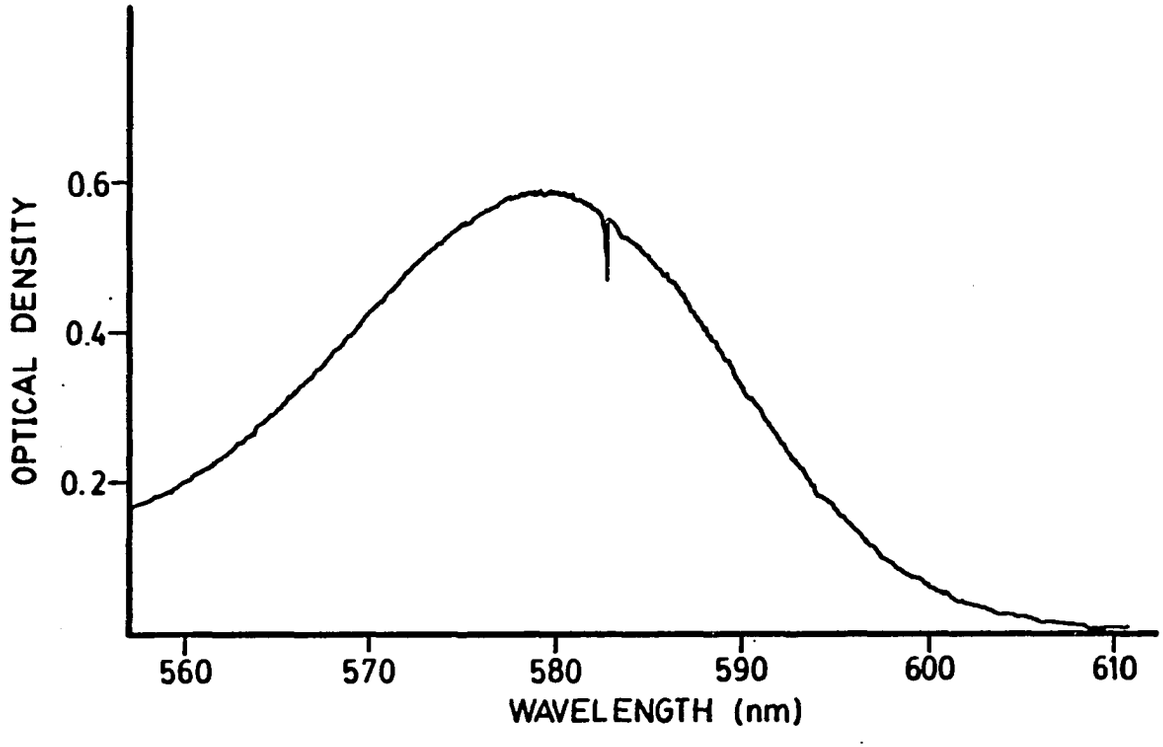

Figure 1. Hole burning for rhodamine 640 in PVOH, burned with ring dye laser for 1 minute at 583.0 nm, 50 mW/cm, T ≈ 5 K

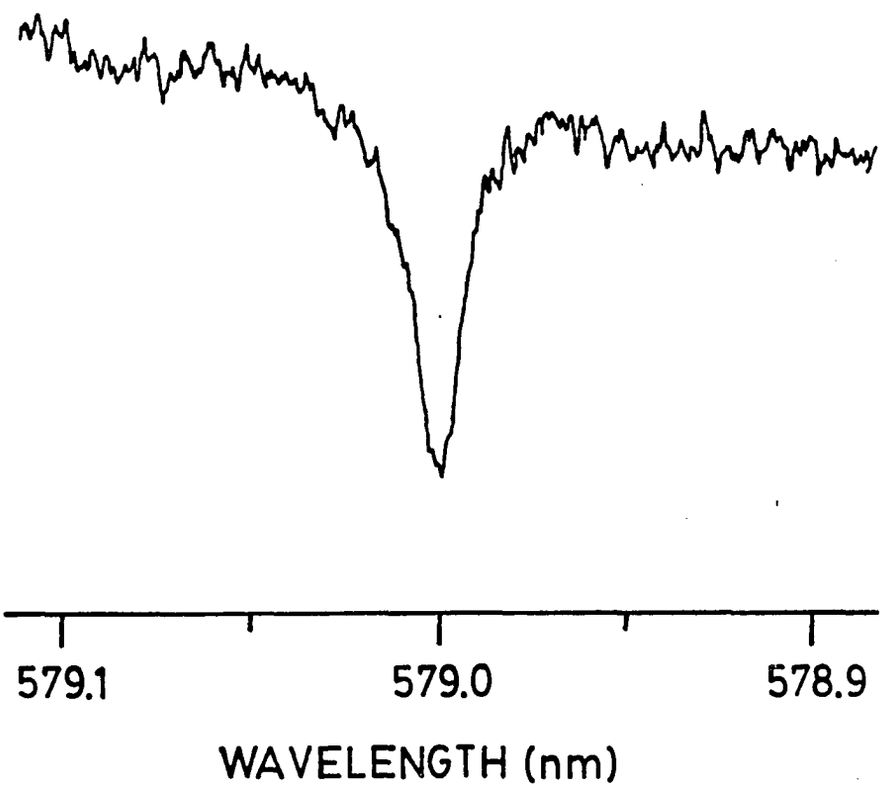

Figure 2. Hole burned profile for Nd^{3+} in PVOH, burned at 579.0 nm for 10 minutes with 100 mW/cm^2 in pumped helium, T = 1.7 K. Measured ~33 minutes after end of burn, with a hole depth of ~5.8% (% OD change) versus a ~6.6% hole just ~3 minutes after end of burn. Linewidth ≈0.45 cm^{-1}

Pr^{3+} in PVOH appear to be about two orders of magnitude higher than in inorganic glasses [32]. The narrowest holewidths (FWHM) measured at 1.7 K (burn and read) for Nd^{3+} and Pr^{3+} after deconvolution [43] are 0.30 and 0.090 cm^{-1}, respectively. The latter is significantly instrument limited while the former is not nearly so convoluted. The T_2 dephasing times corresponding to the former homogeneously broadened linewidth is 70 ps. If one assumes that this time is totally due to longitudinal relaxation (i.e., $T_1 = 2T_2$), then one has $T_1 = 35$ ps, which is within a factor of 1.5 of that which has been measured for a hole in the same transition in a silicate glass [44] attributed to a T_1 relaxation (natural lifetime) of 54 ps. A NPHB spectrum for Pr^{3+} in PVOH has been published [34]. It is similar to that of Fig. 2 in that no phonon sideband hole structure is observed.

In view of the simplicity of the structure underlying the inhomogeneously broadened absorption profiles of the aforementioned transitions, R640, Nd^{3+} and Pr^{3+} in PVOH are ideal systems for the study of SPHF. Typical results are shown in Figs. 3-4 for R640 and Nd^{3+}. Analogous results were seen for Pr^{3+} and shall not be shown here. For all three systems, the SPHF behavior was reproducible from sample to sample and can be fit to a simple exponential law of the form

$$[I(t) - I(\infty)] \quad \alpha \quad \exp[-Kt] \quad . \qquad (1)$$

Here, I(t) and I(∞) are the integrated hole areas at time t and infinite time. The parameter values determined from the least squares fit of Eq.

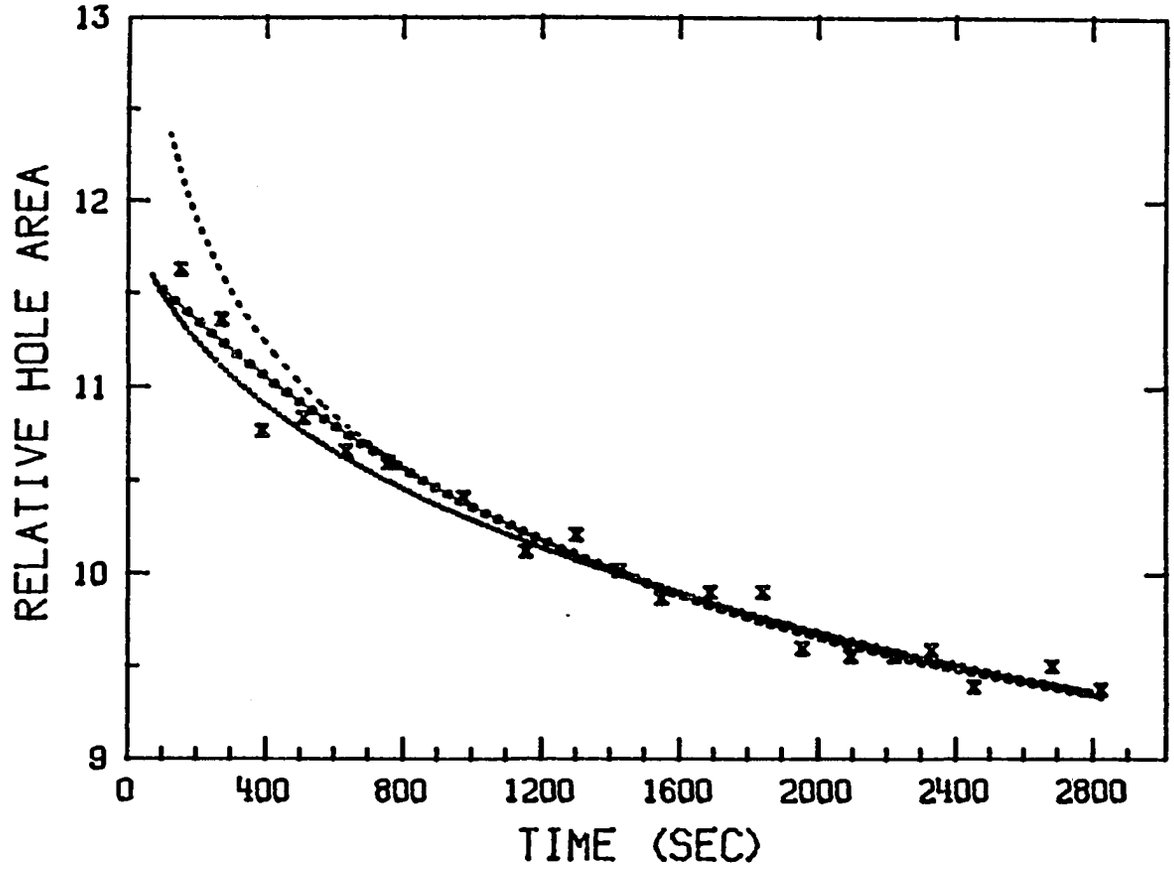

Figure 3. Spontaneous hole filling data for R640 in PVOH, X's indicate the relative hole area in time from the end of the burn (75 s at 582.5 nm with ~1 mW/cm^2) at T = 1.7 K. The curves indicated are based on three different kinds of fits (see text): (i) dashed (upper) curve is the logarithmic fit, (ii) solid line-filled circle (middle) curve is the exponential fit, and (iii) dotted (lower) curve is the dispersive fit

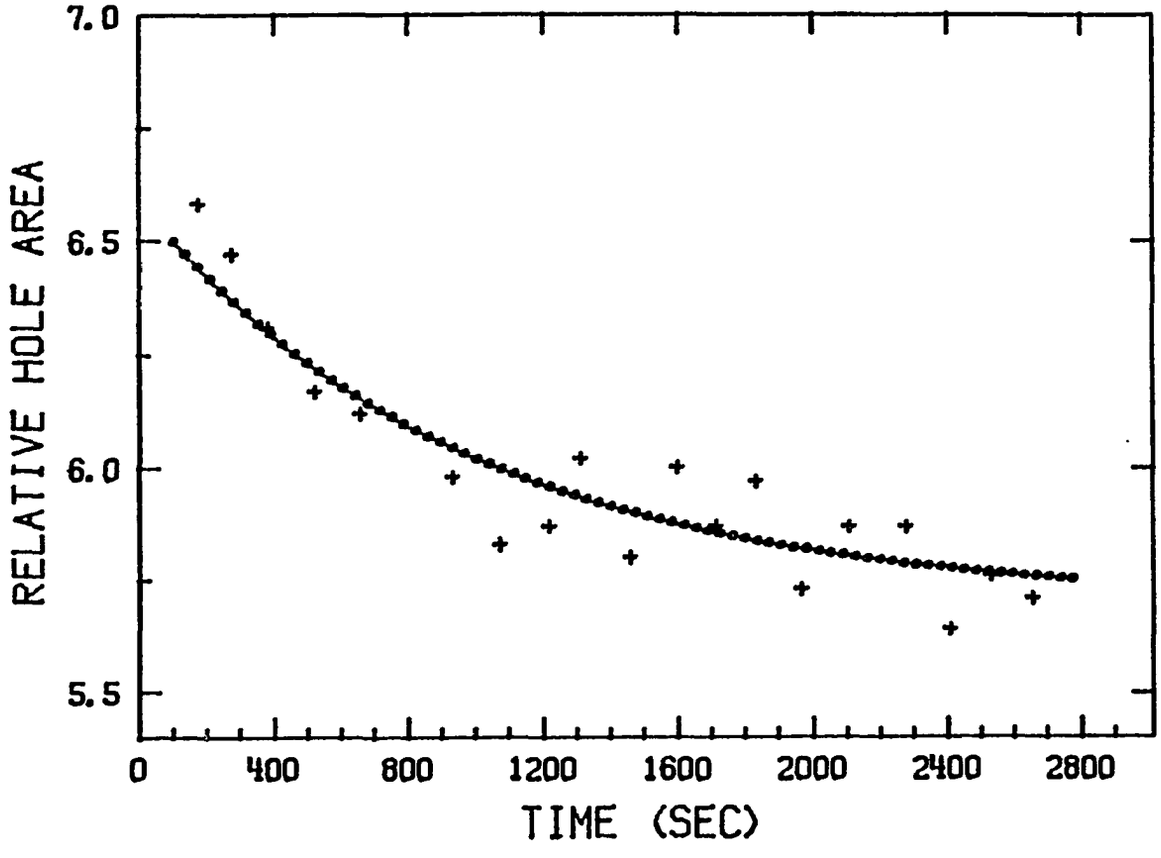

Figure 4. Spontaneous hole filling data for Nd^{3+} in PVOH, relative hole area versus time from end of burn. The sample was burned with ring dye laser at 579.0 nm for 10 minutes at 100 mW/cm^2, T = 1.7 K. The solid line-filled circle curve is an exponential fit as per text

(1) to the data are given in Table 1. The SPHF "lifetimes" (K^{-1}) range from ~10^3 - 10^4 s and for R640, Pr^{3+} and Nd^{3+} the percent spontaneous hole fillings [(I(0) - I(∞))/I(0)] are ~25, 75 and 14%, respectively. Discussion of Eq. (1) and the other two fits to the data shown in Fig. 3 is deferred until the following section. A second important characteristic of the SPHF for the above three dopants in PVOH is that no spectral diffusion accompanies the hole filling. The maximum error in our holewidth measurements is ~3%. The initial holewidths corresponding to Figs. 3-4 are 0.45 and 0.20 cm^{-1}. The absence of spectral diffusion here should be contrasted with the results of studies on poly(methyl methacrylate) [26] and quinizarin in an ethanol/methanol glass [40,41], where SPHF is accompanied by significant hole broadening. Furthermore, the SPHF for the latter system (as measured from the hole area) can be fit reasonably well to a logarithmic decay law [40,41]. This law does not provide a satisfactory fit to the data of Figs. 3 and 4.

Table 1. Pertinent data for systems studied for SPHF

Impurity	Concentration	$K_{(s^{-1})}$ [a]	$t_{(s)}$ [b]	% Spontaneous[c]
R640	10^{-4} M	6.5 E - 4	1.5 E + 3	25
Nd^{3+}	1.6 M	1 E - 3	1.0 E + 3	15
Pr^{3+}	2.5 M	8 E - 5	1.3 E + 4	75

[a]Decay rate constant as determined from Eq. (1).

[b]$t = 1/K$.

[c]The percent of nonpermanent holes (see text, i.e., $\frac{I(0)-I(\infty)}{I(0)} \cdot 100$).

DISCUSSION

Time Dependence of Spontaneous Hole Filling

The generally accepted mechanism for NPHB is based on phonon assisted tunneling between the tunnel states of two-level systems (TLS) which couple to the impurity [27,28]. The TLS are associated with asymmetric intermolecular double well potentials and in amorphous solids there is a wide and continuous distribution of TLS. The TLS are used to model the tunneling between different glassy configurations or states [1,2]. It is entirely possible that the TLS responsible for the observed inefficient [19] hole burning are distinct from those associated with the anomalously fast dephasing of impurity electronic transitions. Indeed, the former may be extrinsic (to a significant extent determined by the impurity) while the latter are intrinsic. The existence of the TLS distribution means that there will generally exist a distribution of hole burning efficiencies for each and every ω_B since the isochromat selected by ω_B can have a high degree of mechanical degeneracy associated with it [45]. Similarly, there will be a distribution of SPHF rate constants for the filling of a particular hole.

Very recently, Jankowiak et al. [46] have developed a dispersive first order kinetics model for interpretation of NPHB efficiency and SPHF data. Dispersion is accounted for by ascribing a distribution function, $g(\lambda)$, to the tunneling parameter λ associated with the phonon assisted tunneling frequency which is proportional to $\exp(-\lambda)$. In their calculations, a single Gaussian distribution function is employed. The arguments for doing so are similar to those given earlier in a theoreti-

cal study of optical dephasing in amorphous solids [35]. The theoretical expressions for growth of a hole or its filling due to SPHF can be written down immediately. For this and other reasons, we do not give them here. As expected, single exponential decay of the hole is obtained when the width σ of $g(\lambda)$ about the most probable λ-value, λ_0, is narrow relative to the dispersion of the exponential term which governs decay. Such behavior is not in accord with the data of Figs. 3 and 4. However, their theory with $\lambda_0 = 9.8$, $\sigma = 3.1$ and $K_t^0 = 1.0$ provides a fit to the data which is as good as the fit with Eq. (1). The parameter K_t^0 is the multiplicative factor of the $\exp(-\lambda)$ term.

The model of Jankowiak et al. [46] assumes a single TLS coordinate q and the above dispersion is associated with it. It predicts that the hole will eventually completely fill. It is, of course, reasonable to expect that, given sufficient time, such should occur. Equation (1), however, predicts that only partial filling will occur. This is a consequence of it being an incomplete representation of the following idea. Basically, the idea is that there may be more than one "chemically distinct" impurity-TLS coordinate involved in NPHB and SPHF, say q_a and q_b. Due to intrinsic disorder, each has an associated distribution of phonon assisted tunneling rates and different distribution functions, $g(\lambda)$, vide infra. Let λ_0^a and λ_0^b be their most probable values for the tunneling parameter λ. Then, if $\lambda_0^b \gg \lambda_0^a$, it is possible that the SPHF being observed in Figs. 3 and 4 is due predominantly to coordinate q_a. That is, the hole remaining at the longest times in the present experiments is associated to a significant extent with the q_b coordinate.

With reference to the dispersive first order kinetic model of Jankowiak et al. [46], the theory could be simply modified to take this into account. With the assumption that the SPHF of Figs. 3 and 4 is due to the coordinate q_a, the observed time dependence dictates that the associated distribution function $g(\lambda^a)$ is narrow ($\sigma^a \ll \lambda_0^a$). Clearly, SPHF experiments extended to much longer times would be required to test this idea, however, as can be seen from Fig. 3; even less sophisticated fits are essentially indistinguishable at relatively short times and would be difficult to separate even at extremely long times (>8 hours) making these experiments impractical except to determine whether spectral diffusion onsets at much later times. A more informative set of experiments would be to study the short time response and then attempt to understand these dynamics. Both types of experiments are planned for R640 and Nd^{3+} in PVOH.

Finally, we note that the data of Figs. 3 and 4 are not adequately fit by a logarithmic decay law. This law emerges when the distribution function, $g(\lambda)$, is assumed constant for $\lambda_{min} < \lambda < \lambda_{max}$ and zero otherwise [40,41].

Absence of Spectral Diffusion in Spontaneous Hole Filling

For R640, Nd^{3+} and Pr^{3+}, it has been mentioned that SPHF is not accompanied by spectral diffusion. In what follows, we present a theoretical model which can account for the absence of spectral diffusion or uniform SPHF. The notation and symbols used are similar to those employed by Friedrich et al. [47] who have studied the problem of temperature induced spectral diffusion of photochemical holes in glasses.

Therefore, it was not necessary in their work to take into account an anti-hole. An example of an anti-hole is shown in Fig. 5 for oxazine 720 in poly(acrylic acid). Note that it lies to higher energy of ω_B and that its shape must be determined to a considerable extent by the intense pseudo-phonon side band hole lying to the red of ω_B. The latter precludes the possibility of detecting a broad anti-hole to lower energy of ω_B. In our studies of R640, Nd^{3+} and Pr^{3+} in PVOH, no attempt was made to burn holes well past saturation of the zero-phonon hole in order to detect anti-holes. It is clear, nevertheless, that the anti-holes must be very broad relative to the zero-phonon holes.

We let

$$N_i(\omega') = N_{inh}(\omega') - a\frac{\gamma/\pi}{(\omega'-\omega_B)^2 + \gamma^2} + N_{ah}(\omega') \qquad (2)$$

be the site excitation energy distribution function at the termination of the burn. In addition, $N_{inh}(\omega')$ is the inhomogeneously broadened distribution profile of the impurity prior to burning and $N_{ah}(\omega')$ is the result of an increase in the number of absorbers at ω' due to production of the anti-hole. The shape of the ω_B hole in the distribution function is governed by the second term of Eq. (2) where the parameter "a" determines the hole depth. For mathematical simplicity, a Lorentzian profile for the hole is assumed. Without loss of generality, we consider that there is only a single anti-hole displaced to higher energy of ω_B by an amount Ω. Since we are primarily interested in the effect of SPHF on

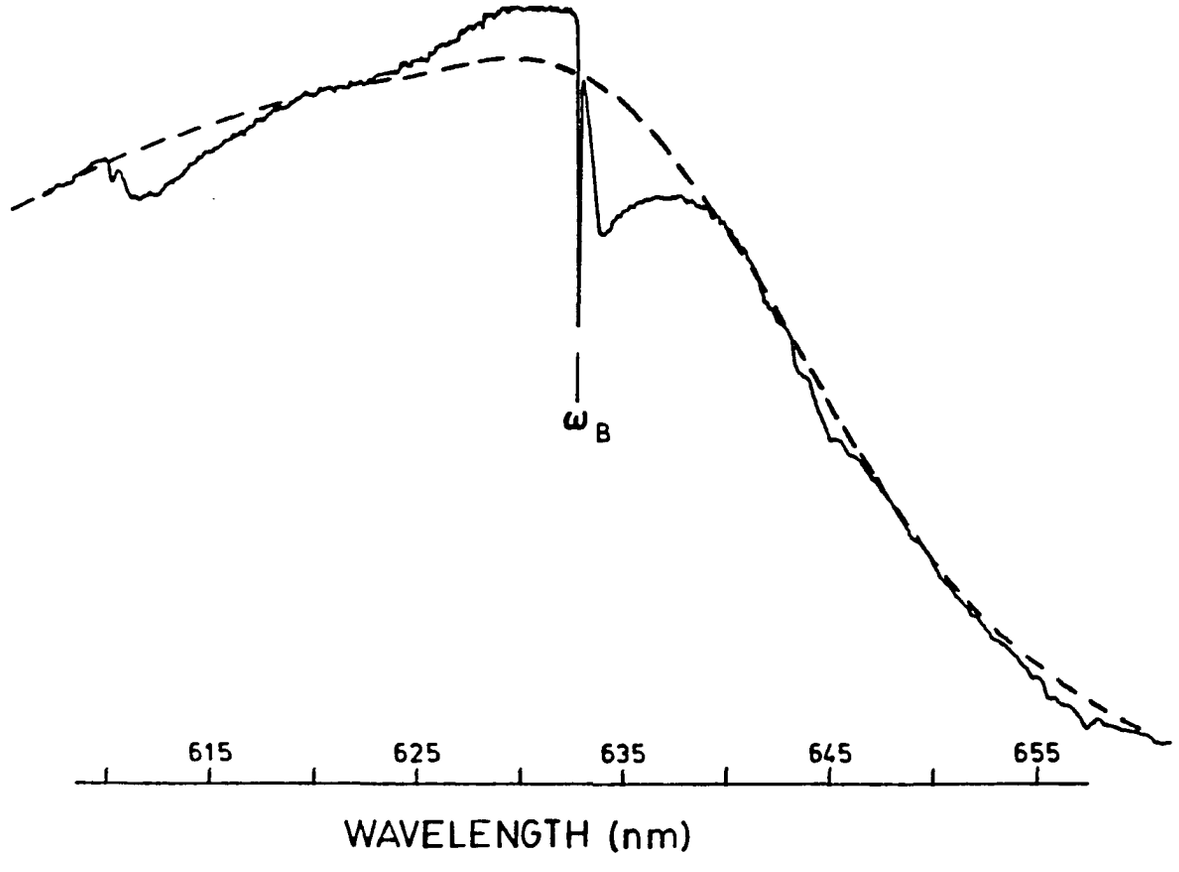

Figure 5. Hole burning and anti-hole formation of Oxazine 720 perchlorate in PAA. The dashed line is the unburned inhomogeneously broadened profile. The solid line is the burned spectrum after burning for 12 minutes with a cw helium-neon laser at 632.8 nm with a flux of ~25 mW/cm^2, T = 7 K

the linewidth of the hole at ω_B, it suffices to write

$$N_{ah}(\omega') = a \frac{\beta/\pi}{(\omega' - (\omega_B+\Omega))^2 + \beta^2} \quad . \tag{3}$$

Note that Eqs. (2) and (3) imply that the total number of absorbers is constant.

The basic premise of the model is that SPHF is the result of feedback from $N_{ah}(\omega')$ into the zero-phonon hole region. This is consistent with the local impurity-TLS model for NPHB. The model represents, therefore, a departure from that employed by Friedrich et al. [47]. In this present work, spectral diffusion due to a temperature increment above the burn temperature is not applicable. Thus, spectral diffusion due to tunneling of impurity-TLS not directly involved in the burn has to be taken into account. Defining $N_f(\omega')$ as the distribution function following some degree of SPHF and $\delta N_f(\omega') = N_{inh}(\omega') - N_f(\omega')$ [with an analogous definition for $\delta N_i(\omega')$], we write

$$\delta N_f(\omega') - \delta N_i(\omega') = -\sum_{\Delta\omega} P(\omega'+\Delta\omega \rightarrow \omega') N_{ah}(\omega' + \Delta\omega) \quad . \tag{4}$$

Here, P is the probability for an anti-hole site with excitation frequency $\omega'+\Delta\omega$ tunneling to a site with frequency ω'. Strictly speaking, Eq. (4) is applicable only in the limit of a small degree of SPHF since tunneling into the anti-hole region is not taken into account. In what follows, however, it will be seen that the conditions for the absence of

spectral diffusion would not be altered by inclusion of tunneling from the hole to the anti-hole. We note that the line shape of the measured hole is given by

$$L_f(\omega) = \int d\omega' \delta N_f(\omega') g(\omega-\omega') \tag{5}$$

with

$$g(\omega-\omega') = \frac{\gamma/\pi}{(\omega-\omega')^2 + \gamma^2} \tag{6}$$

the Lorentzian profile for an absorber at ω'. Thus, for <u>uniform</u> SPHF, we require that

$$\int d\Delta\omega \; P(\omega'+\Delta\omega \to \omega') N_{ah}(\omega'+\Delta\omega) = \frac{\kappa\gamma/\pi}{(\omega-\omega_B)^2 + \gamma^2} \quad , \tag{7}$$

since

$$\kappa \int d\omega' \frac{\gamma/\pi}{(\omega'-\omega_B)^2 + \gamma^2} \, g(\omega-\omega') = \kappa \frac{2\gamma/\pi}{(\omega-\omega_B)^2 + (2\gamma)^2} \quad . \tag{8}$$

It follows, then, that

$$L_f(\omega) = (a-\kappa)\frac{2\gamma/\pi}{(\omega-\omega_B)^2 + (2\gamma)^2} \quad , \qquad (9)$$

so that $L_f(\omega)$ has the same half-width (2γ) as the initial hole $L_i(\omega)$. Equation (7) is satisfied when the site excitation energies of the hole are correlated with those of the anti-hole and when the probability function P of Eq. (4) is constant. To see this, consider that $x = \omega_h - \omega_B$ and $y = \omega_{ah} - (\omega_B+\Omega)$ are the deviations from the most probable frequencies ω_B and $\omega_B+\Omega$ for the hole and anti-hole. Correlation demands that $y = \alpha x$ [$dy=\alpha dx$] with $\alpha > 0$ or < 0. Without loss of generality we take α to be positive in what follows. Since the anti-hole is broad relative to the hole, $\alpha \gg 1$. Equation (4) can now be written as

$$[\delta N_f(\omega') - \delta N_i(\omega')]d\omega' = -\alpha N_{ah}(\omega_B+\Omega-\alpha(\omega'-\omega_B)) \times P(\omega_B+\Omega-\alpha(\omega'-\omega_B) + \omega')d\omega' \quad . \qquad (10)$$

Provided P is taken to be constant, κ, Eqs. (3), (5) (and the analogous one for $L_i(\omega)$) and (10) and $\alpha = \beta/\gamma$ lead immediately to Eq. (9), the desired result for uniform SPHF. Inclusion of a low energy anti-hole would not, of course, alter the above conditions for uniform SPHF.

The condition $P = \kappa$ deserves some comment. First, it is consistent with the temporal decay of the zero-phonon hole discussed above. In addition, the anti-hole $N_{ah}(\omega')$ is determined by the site excitation energy while SPHF is the result of tunneling associated with the impurity in its <u>ground</u> electronic state. With little or no correlation

between the TLS parameters (zero-point splitting, barrier height, tunnel frequency, etc.) associated with the ground and excited states of the impurity and with a high degree of mechanical degeneracy associated with the isochromat at ω_B, the above condition is reasonable. That is, with reference to Eq. (4), there would be no reason to expect P to be determinable from $\Delta\omega$ above.

Nevertheless, we have explored (in the spirit of Ref. 47) the consequences of endowing P with such a dependence. Specifically and with reference to Eq. (10), we considered that

$$P(\omega') \quad \alpha \quad \frac{\sigma/\pi}{[\omega_B+\Omega-\alpha(\omega'-\omega_B)]^2 + \sigma^2} \tag{11}$$

because an analytic expression for $L_f(\omega)$ is readily obtainable. The resulting expression is lengthy and so we do not give it here. Not surprisingly, the result shows that SPHF can be accompanied by hole broadening and asymmetric filling. In the limit where $\sigma >> \beta$ (half-width of the anti-hole), deviations from uniform SPHF would not be observed. For the limit $\beta > \sigma$, the prediction is that SPHF would be asymmetric and would lead to an apparent narrowing of the hole.

CONCLUDING REMARKS

A theoretical model has been developed to explain "uniform" spontaneous filling of nonphotochemical holes. It involves feedback from the anti-hole sites into the zero-phonon hole region and, with correlation between the site excitation energies of the hole and anti-hole, the model predicts uniform filling. This means, for example, that hole broadening (or narrowing) does not accompany filling, as is found for the systems studied. We hasten to add, however, that alternative SPHF mechanisms may exist which do allow for hole broadening but for which the broadening could be imperceptible. It is, in our opinion, important in future SPHF experiments to focus on the effect of SPHF on the entire hole profile (in particular the wings) rather than just the width.

REFERENCES

1. P. W. Anderson, B. I. Halperin and C. M. Varma, Philos. Mag. 25, 1 (1972).

2. W. A. Phillips, J. Low Temp. Phys. 7, 351 (1972).

3. J. Jäckle, Z. Phys. 257, 212 (1972).

4. S. Hunklinger and W. Arnold, in Physical Acoustics, edited by R. N. Thurston and W. P. Manson (Academic, New York, 1976), Vol. 12, p. 155.

5. S. Hunklinger, J. Physique C6-1444 (1978).

6. B. Golding, M. v. Schickfus, S. Hunklinger and K. Dransfeld, Phys. Rev. Lett. 43, 1817 (1979).

7. A. K. Raychaudhuri and S. Hunklinger, Z. Phys. B - Condensed Matter 57, 113 (1984).

8. S. K. Lyo and R. Orbach, Phys. Rev. B 22, 4223 (1980).

9. J. M. Hayes, R. P. Stout and G. J. Small, J. Chem. Phys. 73, 4129 (1980).

10. P. Reinecke and H. Morawitz, Chem. Phys. Lett. 86, 359 (1982).

11. F. P. Burke and G. J. Small, Chem. Phys. 5, 198 (1974).

12. F. P. Burke and G. J. Small, J. Chem. Phys. 61, 4588 (1974).

13. T. J. Aartmsa and D. A. Wiersma, Chem. Phys. Lett. 42, 520 (1976).

14. K. E. Jones and A. H. Zewail, in Advances in Chemical Physics, edited by A. H. Zewail, Springer Series in Chemical Physics (Springer, New York, 1978).

15. C. Harris, J. Chem. Phys. 67, 5607 (1977).

16. G. J. Small, Chem. Phys. Lett. 57, 501 (1978).

17. P. deBree and D. A. Wiersma, J. Chem. Phys. 70, 790 (1979).

18. T. L. Reinecke, Solid State Commun. 32, 1103 (1979).

19. J. M. Hayes, R. P. Stout, and G. J. Small, J. Chem. Phys. 74, 4266 (1981).

20. H. Morawitz and P. Reinecke, Solid State Commun. 42, 609 (1982).

21. S. K. Lyo, Phys. Rev. Lett. 48, 688 (1982).

22. S. K. Lyo, in Electronic Excitations and Interaction Processes in Organic Molecular Aggregates, edited by P. Reinecke, H. Hoken, and H. C. Wolf, Springer Series in Solid State Sciences, Vol. 49 (Springer-Verlag, Berlin, 1983).

23. B. Jackson and R. Silbey, Chem. Phys. Lett. 99, 381 (1983).

24. P. Reinecke, H. Morawitz, and K. Kassner, Phys. Rev. B 29, 4546 (1984).

25. D. L. Huber, M. N. Broer, and B. Golding, Phys. Rev. Lett. 52, 2281 (1984).

26. C. W. Mollenkamp and D. A. Wiersma, J. Chem. Phys. 83, 1 (1985).

27. J. M. Hayes and G. J. Small, Chem. Phys. 27, 151 (1978).

28. J. M. Hayes and G. J. Small, Chem. Phys. Lett. 54, 435 (1978).

29. G. J. Small, "Molecular Spectroscopy", edited by V. M. Agranovich and R. M. Hoschstrasser, in Modern Problems in Solid State Physics, V. M. Agranovich and A. A. Maradudin, General Eds. (North-Holland, Amsterdam, 1983).

30. B. L. Fearey, T. P. Carter, and G. J. Small, J. Phys. Chem. 87, 3590 (1983).

31. T. P. Carter, B. L. Fearey, J. M. Hayes, and G. J. Small, Chem. Phys. Lett. 102, 272 (1983).

32. R. M. Macfarlane and R. M. Shelby, Opt. Commun. 45, 46 (1983).

33. R. M. Macfarlane, R. T. Harley, and R. M. Shelby, Radiat. Eff. 72, 1 (1983).

34. B. L. Fearey, T. P. Carter, and G. J. Small, J. Lumin. 31/32, 792 (1984).

35. R. Jankowiak and H. Bassler, Chem. Phys. Lett. 95, 124 (1983).

36. R. Jankowiak and H. Bassler, Chem. Phys. Lett. 95, 130 (1983).

37. R. Jankowiak and H. Bassler, Chem. Phys. Lett. 100, 274 (1983).

38. F. G. Patterson, H. W. H. Lee, R. W. Olson, and M. D. Fayer, Chem. Phys. Lett. 84, 59 (1981).

39. J. M. Hayes, B. L. Fearey, T. P. Carter, and G. J. Small, Int. Rev. Phys. Chem., 1986 (in press).

40. W. Breinl, J. Friedrich, and D. Haarer, Chem. Phys. Lett. 106, 487 (1984).

41. W. Breinl, J. Friedrich, and D. Haarer, J. Chem. Phys. 81, 3915 (1984).

42. F. Drissler, F. Graf, and D. Haarer, J. Chem. Phys. 72, 4996 (1980).

43. S. G. Rautian, Sov. Phys. Usp. 66, 245 (1958).

44. R. M. Shelby, Opt. Lett. 8, 88 (1983).

45. H. W. H. Lee, C. A. Walsh, and M. D. Fayer, J. Chem. Phys. 82, 3948 (1985).

46. R. Jankowiak, R. Richert, and H. Bassler, J. Phys. Chem. 89. 4569 (1985).

47. J. Friedrich, D. Haarer, and R. Silbey, Chem. Phys. Lett. 95, 119 (1983).

ACKNOWLEDGEMENTS

This work was supported by the National Science Foundation, Grant No. DMR-8400905.

We are grateful to R. Jankowiak for performing calculations based on Ref. 46 and for stimulating discussions. We wish to thank H. Bassler for making Ref. 46 available to us prior to its publication. In addition, we would like to thank T. P. Carter and J. M. Hayes for assistance in this work.

BLF would like to thank the IBM Corporation for fellowship support during the performance of this research.

PAPER 6. NEW STUDIES OF NONPHOTOCHEMICAL HOLES OF DYES AND RARE EARTHS IN POLYMERS. II. LASER INDUCED HOLE FILLING

ABSTRACT

The phenomenon of laser induced hole filling (LIHF) is reported and discussed in detail for rhodamine 640, Nd^{3+}, Pr^{3+} and the mixed system of rhodamine 560 and cresyl violet. Importantly, LIHF does not show any spectral diffusion (i.e., broadening). Possible mechanisms (thermal heating, site reversion and energy transfer) involved in LIHF are discussed and are argued to have insignificant contribution. A tentative model is developed to explain these results. The model basically invokes a connectivity between spatially removed extrinsic (impurity) two-level systems (TLS) via an ensemble of intrinsic (host) TLS (the glassy state). Additionally, correlation between impurity excitation energies and absolute glassy state energies is imposed.

INTRODUCTION

In the preceding paper, spontaneous hole filling (SPHF) data for nonphotochemical holes of rhodamine 640 (R640), Nd^{3+} and Pr^{3+} in poly(vinyl alcohol) (PVOH) were presented and discussed [1]. Here, we are concerned with the phenomenon of laser induced hole filling (LIHF) as it occurs in the same and other systems. By LIHF, we mean the partial or complete filling or erasure of a hole burnt at ω_{B_1} which results from subsequent laser irradiation at frequencies removed from ω_{B_1}. Interestingly, LIHF is the least studied aspect of hole burning in amorphous hosts even though it may be the most intriguing. The first LIHF experiment was performed on tetracene in an ethanol/methanol glass in order to argue that the hole burning mechanism is nonphotochemical (photophysical) rather than photochemical in nature [2]. It is conceivable that LIHF can also occur for photochemical holes burned in glassy hosts. Undoubtedly, LIHF and hole erasure due to white light irradiation are related phenomena. Gutierrez et al. [3] have studied the latter for quinizarin in the ethanol/methanol glass. White light erasure has also been observed by us [4] for cresyl violet perchlorate (CV) in PVOH. It is important to note that we do not ascribe LIHF or white light erasure to a bulk heating effect. It is easy to identify and, consequently, prevent interference due to thermal erasure since it is generally accompanied by spectral diffusion and hysteresis whose T-dependences can be characterized by separate thermal erasure (cycle) experiments [5,6].

Returning to the tetracene in ethanol/methanol glass system, it was reported that significant LIHF occurs only when the secondary irradiation frequency lies within ~2 cm^{-1} of the primary hole at ω_{B_1} [2]. Although a mechanism for LIHF was not given, it might be inferred that the LIHF is due to reversion of originally burnt impurity-TLS sites back to their configurations prior to the burn (presumably due to excitation of anti-hole sites). LIHF due to reversion following excitation of anti-holes has been firmly established for pentacene in benzoic acid crystals [7,8].

Following the observation [9,10] that LIHF for cresyl violet perchlorate (CV) in PVOH is facile for secondary irradiation frequencies (ω_{B_2}) far removed from ω_{B_1} ($|\omega_{B_2} - \omega_{B_1}| \sim 100$ cm^{-1}), it was decided to study the phenomenon in far greater detail. Given the large inhomogeneous absorption linewidths of dyes in polymers (~500-1000 cm^{-1}) and apparent large widths of the anti-holes (~100 cm^{-1} [1]), the above observation for CV/PVOH suggested that reversion resulting from anti-hole excitation may not be the dominant mechanism for LIHF in dye/polymer systems. Other possibilities include a mechanism based on spectral diffusion which depends on connectivity between the different two level systems (TLS) of the polymer which couple to the impurity. That is, secondary irradiation (or the resulting hole formation) may trigger configurational changes at impurity-TLS sites which are spatially removed from those involved in the primary burn or secondary light absorption process. Another possibility is that LIHF can result from inter-

molecular energy transfer. To begin to understand the LIHF process, it was judged important to first determine relative LIHF efficiencies as a function of the sign and magnitude of $\omega_{B_1} - \omega_{B_2}$ while, at the same time, to ascertain whether LIHF is accompanied by broadening of the primary hole. The results of such studies on R640, Nd^{3+} and Pr^{3+} in PVOH are reported. These data prompted us to perform LIHF experiments on the mixed dye system of rhodamine 560 and CV in PVOH. These experiments speak to the question of intermolecular energy transfer and the results of such are also reported and discussed.

EXPERIMENTAL

Experimental details are given in Paper 5. Here we present the protocol for the LIHF experiments. The basic procedure for studying LIHF is quite analogous to the SPHF experiments. First, the initially burned hole (B_1) was repeatedly scanned as in Paper 5 with the timing initiated from the end of the burn. This, then, was followed by the fill burn (B_2) (noting the time at the end of the burn) and again the initial hole (B_1) was repeatedly scanned. Typical results following the above procedure are shown in Figs. 1 and 2. Once the quantity of spontaneous hole filling is established (and shown to be a constant from sample to sample (see Paper 5)), then by ensuring that further LIHF experiments follow a set sequencing and time scale, the SPHF can be easily removed from any additional studies of LIHF for each system. It should be pointed out that, in most cases, each set of data represents an "identical" (samples reproducibly prepared and cooled were found to yield identical results from sample to sample [1,9]) unique sample, which allows for many similar experiments to be performed in a single run, such as where one burns a new initial burn at ω_{B_1} for each sample followed by a different ω_{B_2} for each.

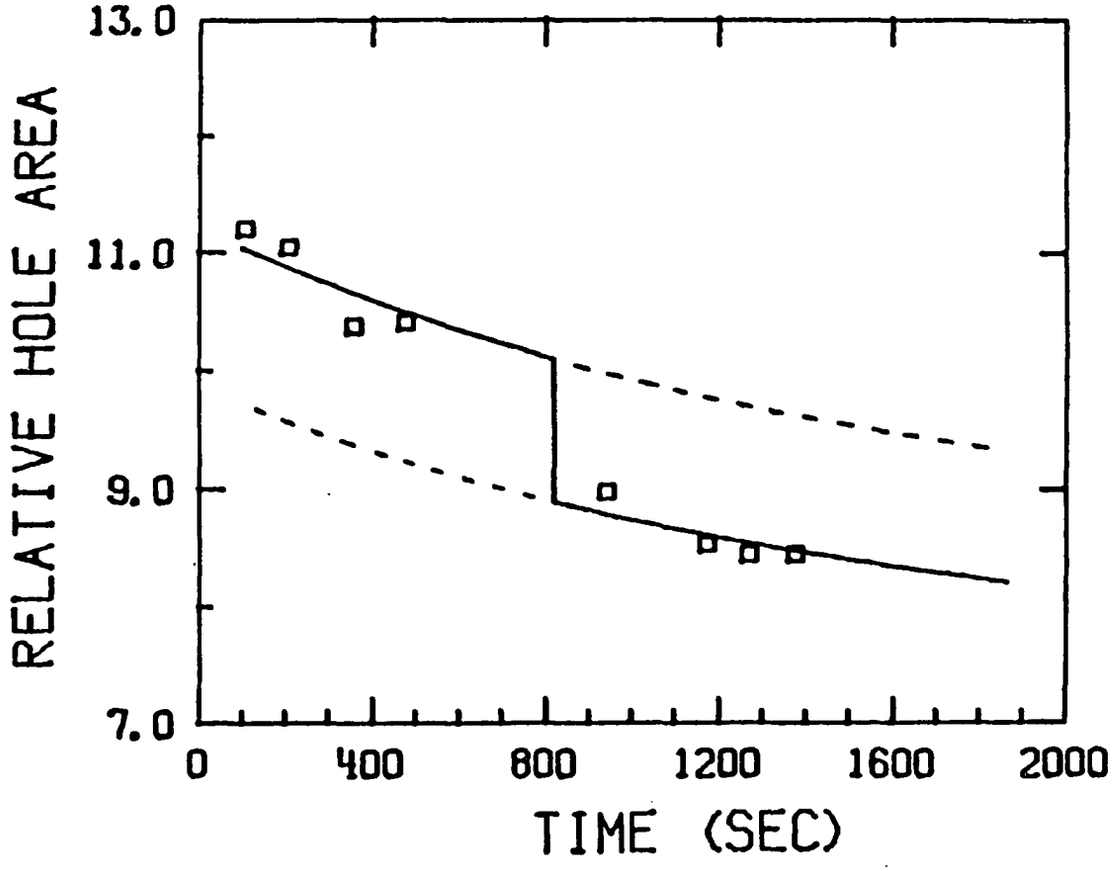

Figure 1. Laser induced hole filling (LIHF) of R640 in PVOH in pumped helium (T = 1.7 K). Burns were performed with a ring dye laser with a flux of 1 mW/cm^2 for 75 s at ω_{B_1} = 582.5 nm (initial burn) and for 250 s at ω_{B_2} = 576.2 nm. The data points ( ) show the measured holes in time, to which are fit the spontaneous hole filling (SPHF) curves as per paper 1. The vertical line indicates the <u>end</u> of the fill burn where the percent laser induced hole fill is 12%

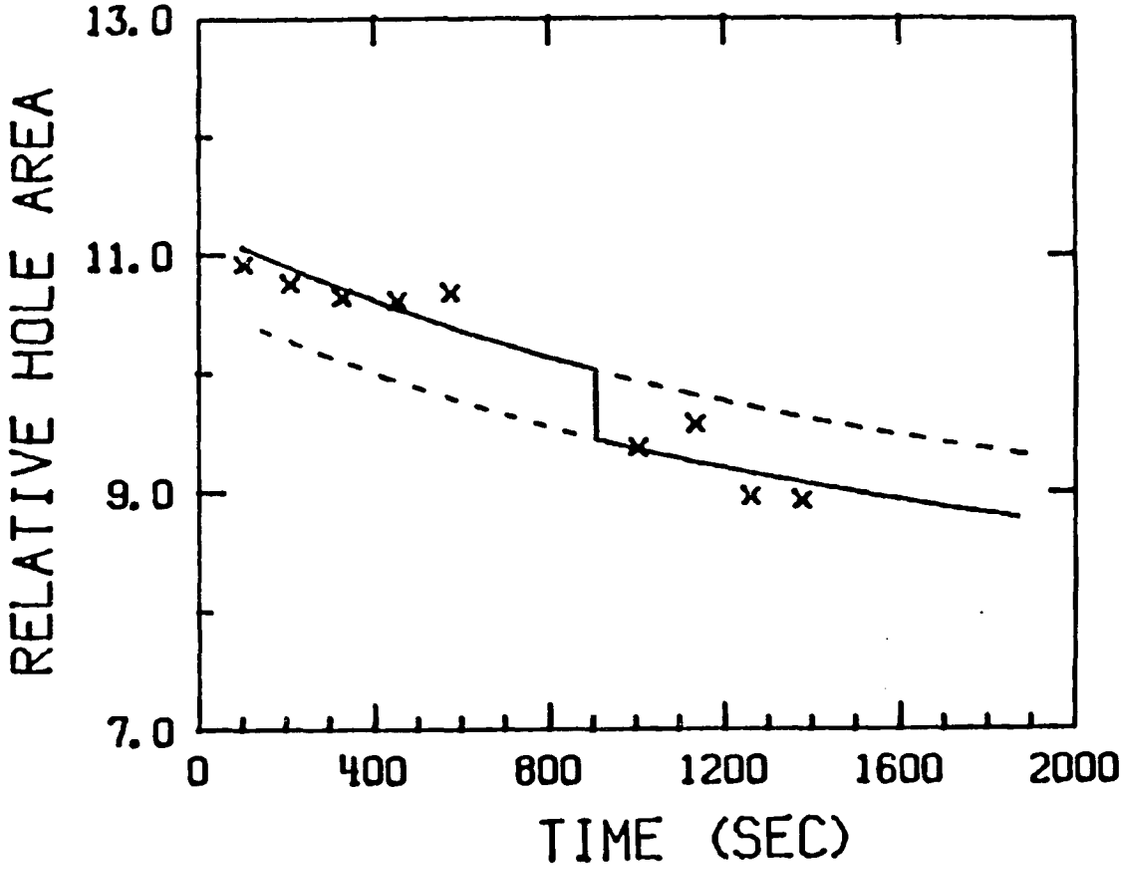

Figure 2. LIHF of R640 in PVOH in pumped helium (T = 1.7 K) with ω_{B_1} = 582.5 nm and ω_{B_2} = 588.9 nm. The data points (x) indicated the measured holes. All else is as stated in Fig. 1. The percent laser induced hole fill is 6%

RESULTS

Rhodamine 640 in Poly(vinyl alcohol)

A nonphotochemically hole burned spectrum of R640 in PVOH is shown in Paper 5 where SPHF data are presented and discussed. Because SPHF hole filling occurs during the time scale of the LIHF experiments, it was essential to subtract out the contribution of SPHF to the filling. The results of Paper 5 allow this to be done in a reliable manner. Two examples of how this was accomplished are shown in Figs. 1 and 2. Both figures are derived from a primary burn at ω_{B_1} = 582.5 nm with secondary irradiation frequencies at ω_{B_2} = 576.2 and 588.9 nm, respectively. Burn times and intensities are indicated in the figure captions. It should be noted that the vertical segment of the solid line in each figure indicates the time at which the ω_{B_2} irradiation terminates. Prior to and following the ω_{B_2} irradiation, the SPHF is monitored and the primary hole decay fit to Eq. (1) of Paper 5. Good agreement for the SPHF parameters with those reported in Paper 5 was found. Thus, the dashed line extensions, for example, are calculated. The difference between the upper and lower curves of Figs. 1 and 2 yield the percent hole filling due only to LIHF. These percentages are 12 and 6% for Figs. 1 and 2, respectively. Thus, LIHF for R640/PVOH is significantly more facile for $\omega_{B_2} > \omega_{B_1}$ than for $\omega_{B_2} < \omega_{B_1}$. Still, the observation that LIHF does occur for the latter case is important.

Figure 3 summarizes the results of our 1.7 K LIHF studies on R640/PVOH. The at from ω_{B_1} locates the primary burn frequency (582.5 Å) and the smaller arrows locate the secondary irradiation frequencies, ω_{B_2}. For each and every ω_{B_2}, a fresh primary hole at ω_{B_1} was burned (cf. experimental) for 75 s and with a burn flux of 1 mW/cm^2. A flux of 1 mW/cm^2 was also used for all ω_{B_2} irradiations. Focusing on the small arrow near 594.5 nm, the x, o and + percent hole area change (filling) data points correspond to ω_{B_2} irradiation times of 75, 150 and 225 s, respectively. We note that for the burn flux and times utilized, the zero-phonon holes were not saturated (i.e., were not burned to maximum depth) and that phonon sideband and vibronic satellite holes were not observed. Separate thermal annealing and cycle experiments confirmed that hole filling from bulk heating does not contaminate the data [11].

The absence of bulk heating is also consistent with one of the two most striking aspects of the data in Fig. 3, the "discontinuity" or step in LIHF efficiency which occurs at ω_{B_1}. The second is the apparent insensitivity of the LIHF facility to ω_{B_2} on both the low and high energy sides of ω_{B_1}. Clearly, LIHF facility is not obviously related to optical density. A third important observation is that LIHF of the primary hole occurs without hole broadening. Our linewidth measurements are accurate to ~6% and the FWHM of the initial primary holes burned at 582.5 nm was constant at 0.45 cm^{-1} for T = 1.7 K.

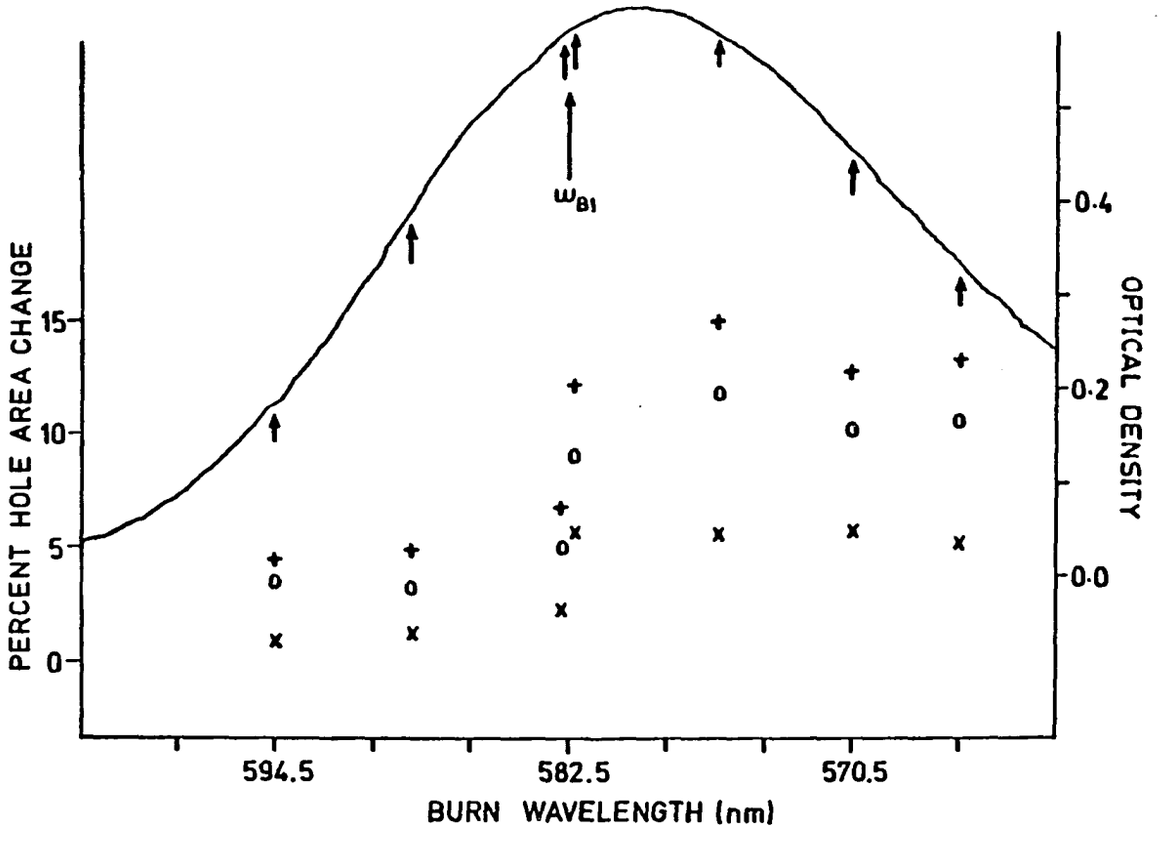

Figure 3. LIHF of R640/PVOH as a function of filling frequency. The initial burn at 582.5 nm (ω_{B_1}) was performed by a ring dye laser with 1 mW/cm^2 for 75 s. The observed percent hole area charge versus secondary burn frequency (marked with small arrows) is shown. The irradiation times used for filling were 75 s (x), 150 s (o) and 225 s (+) with the same flux. Each data set represents a different "identical" sample. T = 1.7 K

An obvious question is whether the LIHF of the primary hole is the result of the secondary hole formation at ω_{B_2} itself (rather than just absorption of ω_{B_2}). The data in Fig. 4 speak to this question and were obtained with a burn flux of ~1 mW/cm^2 and a burn time of 75 s. The dependence of the zero-phonon hole burning efficiency on ω_{B_1} is shown to decrease in a linear fashion with increasing ω_{B_1}. In comparing Figs. 3 and 4, ω_{B_1} = 582.5 nm corresponds to 17167 cm^{-1}. In the LIHF experiments, the secondary holes at ω_{B_2} were also monitored and these results along with those of Fig. 4 show that LIHF efficiency is not simply related to the intensity (depth) of the secondary hole. This point will be returned to later. One final point is that the hole profiles corresponding to the different data points in Fig. 4 exhibited the same FWHM (0.45 cm^{-1}).

Because of their possible connection with the data of Fig. 3, the data of Fig. 5 are presented. Figure 5 shows the percent hole depth (ω_B = 594.5 nm) for R640/PVOH as a function of burn flux at a constant fluence. The manner in which the hole depth initially decreases with increasing flux and then plateaus is similar to that observed by Romagnoli et al. [12] for phthalocyanine. In their work, the flux dependence was nicely explained in terms of a population bottleneck due to the lowest triplet state. Intersystem crossing from S_1 of phthalocyanine has a very high quantum yield. This is not the case for R640. A likely candidate for the bottleneck of R640/PVOH is the subset of R640-TLS sites

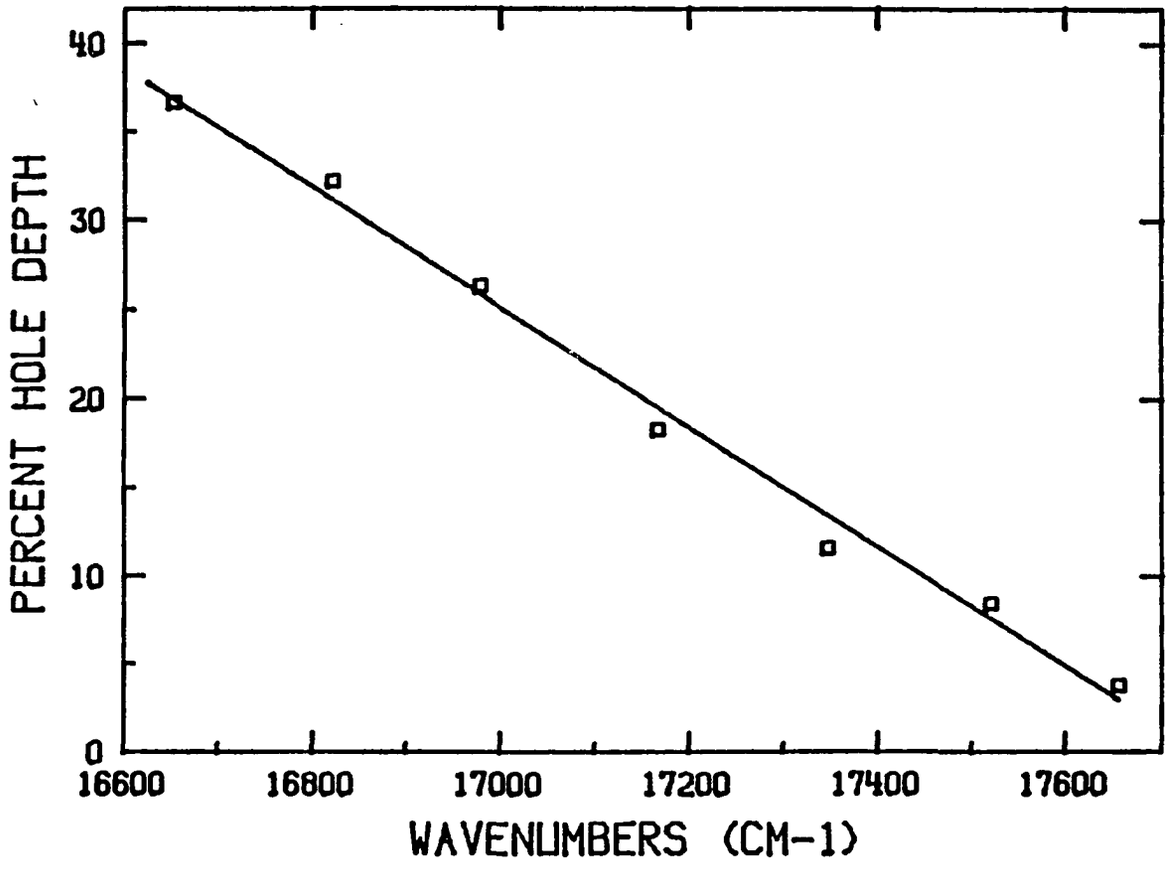

Figure 4. Hole burning efficiencies as a function of energy in wavenumbers for R640 in PVOH. Burns were performed with 1 mW/cm^2 for 75 s. T = 1.7 K

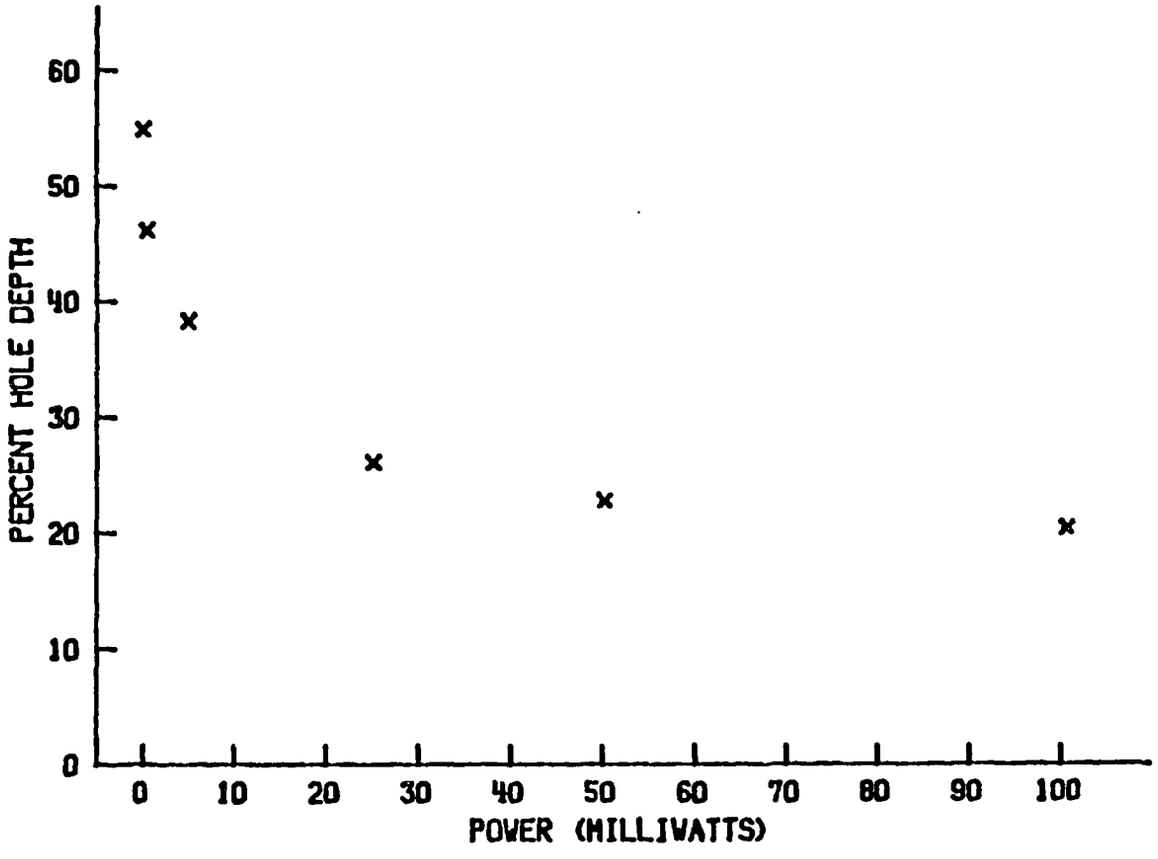

Figure 5. Hole depth of R640 in PVOH as a function of flux with a constant fluence of 75 millijoules

which undergo the initial step of hole burning in the excited electronic state but which undergo ground state tunneling back to their original configurations during the course of the burn. That this might occur is not surprising in view of the SPHF results of Paper 5. It would be worthwhile to determine whether the saturation behavior of Fig. 5 can be explained by a simple dispersive kinetic model.

Binary Dye Mixture in Poly(vinyl alcohol)

The data in Fig. 3 for R640/PVOH and similar data for Pr^{3+} and Nd^{3+} in PVOH (vide infra) show that LIHF occurs for $\omega_{B_2} < \omega_{B_1}$. The mechanism for LIHF when $\omega_{B_2} < \omega_{B_1}$ cannot be due to intermolecular energy transfer (spatial diffusion) between R640 sites. The step function behavior at ω_{B_1}, Fig. 3, might suggest that a second mechanism for LIHF is operative for $\omega_{B_2} > \omega_{B_1}$. One possibility is intermolecular energy transfer from sites at ω_{B_2} to lower energy anti-hole sites produced by the ω_{B_1} burn. Within the TLS model [6,13,14], this means that reversion (by phonon assisted tunneling) from the excited state of the anti-hole tunnel state to that of the precursor tunnel state occurs. LIHF would then be viewed as an excited electronic state process.

We have explored this possibility by performing LIHF on a binary mixture of cresyl violet perchlorate (CV) and rhodamine 560 (R560) in PVOH. Their absorption spectra exhibit minimal overlap [λ_{max}(CV) = 610 nm; λ_{max}(R560) = 510 nm] but the fluorescence spectrum of R560 provides an excellent match for the absorption spectrum of CV. Thus, for the

concentrations involved, the probability for Forster energy transfer is maximized [15].

The results of the experiments are given in Table 1. The conditions used to obtain the data are similar to those used for the R640 experiments. Samples were immersed in pumped helium (1.7 K) and all burns were performed with a flux of ~1 mW/cm^2. The burn times are indicated in the table. The primary (ω_{B_1}) burn times for R560 are higher than for CV because the NPHB facility of the latter is lower. In order to obtain good results, a reasonably deep primary hole is required. For clarity, the order in which the primary and secondary burns were performed is depicted in the crude spectra included in Table 1. The four sections of the table will be referred to as rows 1-4 (starting with mixed dye at the top and ending with R560 dye at the bottom). Further, numbers in circular brackets refer to the percent hole depth following a burn while numbers in square brackets refer to the percent fill due to LIHF caused by secondary (ω_{B_2}) irradiation.

Inspection of the data in rows 1 and 2 show that energy transfer is not involved in LIHF for the mixed dye system. Note that the protocols for rows 1 and 2 are identical except that for row 2 the R560 dye is absent. That is, the 15% LIHF is the same whether or not this dye is present. We hasten to add that for both samples the optical density of CV at ω_{B_2} = 514.5 nm was 0.08.

Consider next rows 3 and 4 which correspond to a sequence opposite to the above. For both rows, the primary burn (ω_{B_1}) is in the R560

Table 1. Binary dye mixture data

System Studied \ Lambda Burn	(R560) 514.5 nm	(CV) 617.0 nm	Schematic Spectrum
Mixed Dye ω_{B_1} = 617.0, t_1[a]		(27)[b]	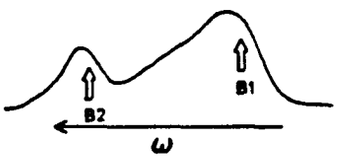
ω_{B_2} = 514.5, t_1	(10)	[15][c]	
CV Dye ω_{B_1} = 617.0, t_1		(27)	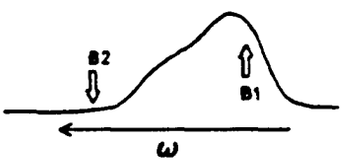
ω_{B_2} = 514.5, t_1		[15]	
Mixed Dye ω_{B_1} = 514.5, t_2[d]	(16)		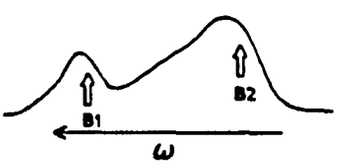
ω_{B_2} = 617.0, t_1	[7]	(28)	
R560 Dye ω_{B_1} = 514.5, t_2	(13)		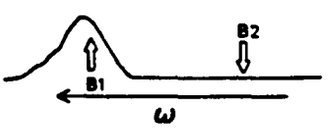
ω_{B_2} = 617.0, t_1	[13]		

[a] t_1 = 75 second burn time.

[b] () = percent burn hole depth.

[c] [] = percent fill of initial hole.

[d] t_2 = 225 second burn time.

profile. The only difference between rows 3 and 4 is that the sample used for the latter contained no CV. Thus, the presence of CV appears to reduce the LIHF for the primary hole of R560. One additional point from Table 1 is that the presence of the second dye does not seem to affect the hole burning efficiency of the other.

Nd^{3+} and Pr^{3+} in Poly(vinyl alcohol)

The optical transitions of Nd^{3+} and Pr^{3+} studied were $^2G_{7/2}$, $^4G_{5/2} \leftarrow {}^4I_{9/2}$ and $^1D_2 \leftarrow {}^3H_4$, the same as in Paper 5. Hole burning was performed on the lowest energy J-component of each transition. In fact, attempts to hole burn the higher energy components were not successful, presumably due to their rapid radiationless decay [16].

The experimental procedure used for LIHF was essentially identical to that used for R640/PVOH. Figure 6 shows the results of one LIHF run for Nd^{3+} which are of the type shown in Figs. 1 and 2 for R640. We note that high RE^{3+} concentrations corresponding to a number density of $\sim 10^{21}$ cm^{-3} or to an average interionic separation of ~10 Å were employed. The LIHF results for Pr^{3+} and Nd^{3+} are shown in Figs. 7 and 8. The indicated LIHF (filling) percentages are corrected for SPHF. Numbers in square brackets correspond to the percent optical density change due to hole burning at the indicated burn frequencies. Numbers without brackets correspond to the percent filling of a hole due to subsequent irradiation at a displaced frequency. With reference to trace b) of Fig. 7, irradiation at ω_{B_2} produces a 17% hole at ω_{B_2} while filling the ω_{B_1} hole by 4%. Similarly, trace c) shows that irradiation at ω_{B_3} fills the hole

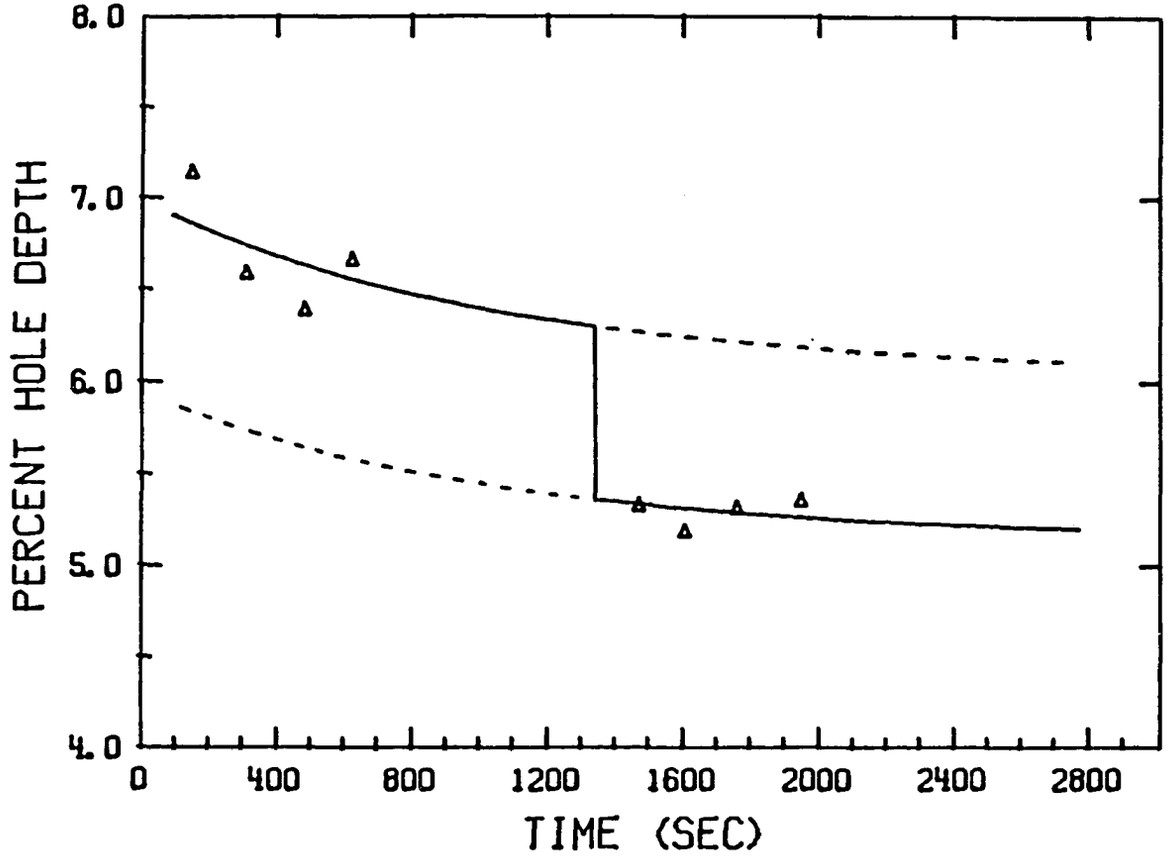

Figure 6. Laser-induced hole filling of Nd^{3+} in PVOH with initial burn (ω_{B_1}) = 579.0 nm and the fill burn (ω_{B_2}) = 578.75 nm, both burns were with 100 mW/cm^2 for 10 minutes. The data points (Δ) indicate the measured holes after each burn. The calculated curves are fits for spontaneous hole filling (see text). The vertical line represents the end of the fill burn where the percent hole fill was measured to be 15%

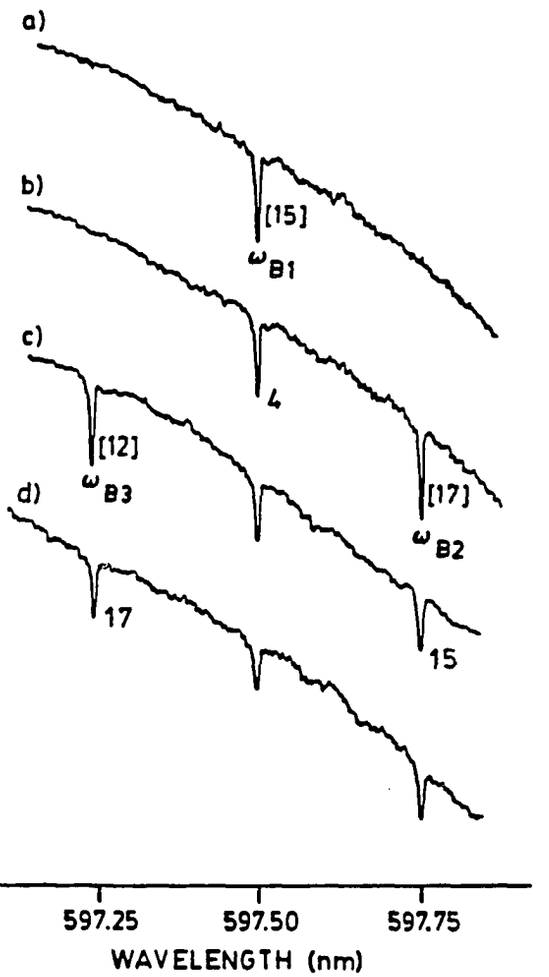

Figure 7. Hole burning and laser-induced hole filling data for Pr^{3+} in PVOH. All burns were performed with a ring dye laser with ~100 mW/cm^2 for 10 minutes. For spectra a-c, all burns were into the lowest energy component of the $^1D_2 \leftarrow {}^3H_4$ crystal field split transition as indicated, i.e., ω_{B_1} = 597.5 nm, ω_{B_2} = 597.75 nm and w_{B_3} = 597.25 nm. For spectrum d, the burn was into the next higher energy component at 594.0 nm. The numbers in brackets refer to the initial percent hole depths while the others indicate the percent hole filling due to a subsequent burn. All samples were in pumped helium at 1.7 K

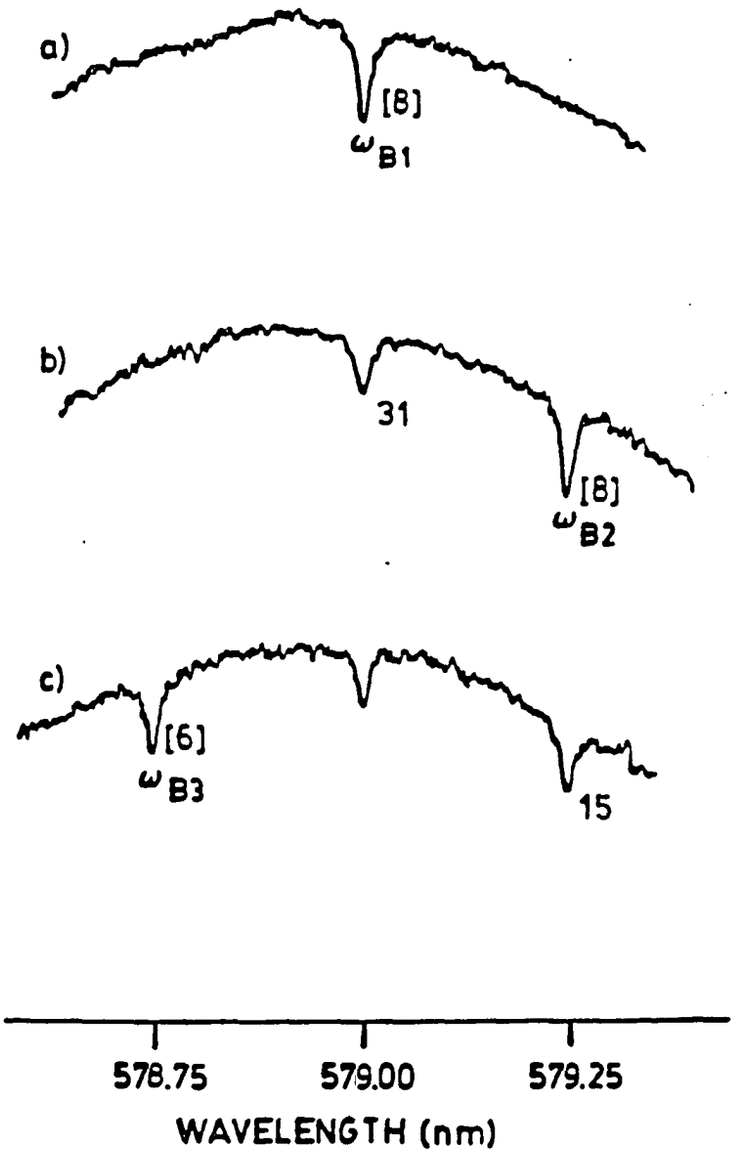

Figure 8. Hole burning and LIHF of Nd^{3+} in PVOH. Burns were into the low energy component of the crystal field split transition of $^2G_{7/2}$, $^4G_{5/2}$ + $^4I_{9/2}$. The sequence of burns is as indicated with the bracketed numbers referring to initial hole depths while the others refer to hole filling. Burns were with ~100 mW/cm^2 for 10 minutes at 1.7 K

at ω_{B_2} by 15%. Trace d) was obtained with secondary irradiation at 594.0 nm into the second J-component of the $^1D_2 \leftarrow {}^3H_4$ transition.

From Fig. 7, we conclude that for Pr^{3+}/PVOH, LIHF is significantly more efficient when the secondary irradiation frequency is displaced to higher energy of the hole being filled, as is the case for R640/PVOH. Another similarity is that the LIHF does not broaden the hole being filled.

The absence of broadening accompanying LIHF is also observed for Nd^{3+}/PVOH. However, this system behaves in a qualitatively different manner than Pr^{3+} or R640 in that the LIHF is more efficient for a secondary irradiation lying to the red of the hole being filled. We return to this point in the following section.

Finally, we have performed preliminary experiments on a binary mixture of Nd^{3+} and Pr^{3+} in PVOH. More extensive measurements are planned, but the results obtained indicate that $Nd^{3+}(^2G_{7/2}, {}^4G_{5/2} \rightsquigarrow Pr^{3+}(^1D_2)$ energy transfer is not an efficient LIHF mechanism for filling of Pr^{3+} holes. This may occur, however, because the $^2G_{7/2}$, $^4G_{5/2}$ states possess a very short lifetime [17].

DISCUSSION

The Puzzle

We begin by summarizing the key results from the preceding section. They are:

1. LIHF of a primary hole at ω_{B_1} occurs for both ω_{B_2} (secondary irradiation) $> \omega_{B_1}$ and $< \omega_{B_1}$.
2. except for Nd^{3+}, the LIHF efficiency for $\omega_{B_2} > \omega_{B_1}$ is significantly higher than for $\omega_{B_2} < \omega_{B_1}$.
3. for R640, the LIHF efficiency exhibits a step behavior at ω_{B_1}. For $\omega_{B_2} > \omega_{B_1}$ and $< \omega_{B_1}$, the dependence of efficiency on $|\omega_{B_2} - \omega_{B_1}|$ is weak.
4. LIHF does not produce any perceptible broadening of the primary hole (for holewidth measurements accurate to ~6%).

In reference to 2 above, the behavior of R640 and Pr^{3+} has also been observed for chlorophyll _a_ [18], chlorophyll _b_ [18,19] and the self-aggregated dimer of chlorophyll _a_ [20] in polystyrene films. With regard to 1 above, the observation that LIHF is operative for $\omega_{B_2} < \omega_{B_1}$ establishes that a mechanism for filling other than intermolecular energy transfer (ET) exists.

Taken as a whole, the above results present an intriguing puzzle. An attempt will be made to explain them but first we argue against a number of possibilities as plausible <u>significant</u> mechanisms for LIHF.

In doing so, we recall that the anti-holes associated with the primary burn can, in principle, lie to higher and lower energy of ω_{B_1} and must be very broad relative to the zero-phonon holewidth [1,21,22]. Furthermore, the conditions of the LIHF experiments (e.g., narrow line excitation) show that the LIHF is surprisingly efficient when the large inhomogeneous profiles in absorption and the large anti-hole width (relative to the laser linewidth) are considered. This, together with the insensitivity of LIHF efficiency to $|\omega_{B_2} - \omega_{B_1}|$, cf. 3 above, precludes direct anti-hole site excitations followed by reversion to original (preburn) configurations as a likely mechanism [2]. This line of argument also eliminates local heating as a plausible mechanism. A third possibility is intermolecular energy transfer. In view of the CV/R560 in PVOH results and the insensitivity of LIHF to ω_{B_2} for $\omega_{B_2} > \omega_{B_1}$, cf. Fig. 3, we are inclined to reject ET as a significant contributor. The CV/R560 results also rule out a trivial emission-reabsorption ("white light erasure") mechanism.

It follows that LIHF cannot be understood by a local (simple) impurity-TLS model. By local, we mean that model which is typically used to explain the phenomenon of nonphotochemical hole production itself [2,6]. In this model, each impurity undergoing hole burning is associated with a single two-level system (TLS) and connectivity (communication) between different impurity-TLS is not considered. It leads naturally to the notion that LIHF is due to a reversion process occur-

ring in isolated impurity-TLS. Nor can the simple impurity-TLS model account for hysteresis effects in NPHB thermal cycle experiments [11].

A Tentative Model for LIHF

The glassy state which we associate with glasses and polymers depends on how that state was prepared. Prior to a burn, there are points in configuration space which are thermally accessible to the initially prepared state. The simple TLS model was designed to model this state of affairs [2,6]. With this in mind, NPHB leading to stable holes can be viewed as a process which produces a glassy state which is thermally inaccessible to the preburn state. In our view, LIHF or thermal erasure of a hole in excitation frequency space should not be viewed as a return of the system to its original preburn state. Rather, both are likely irreversible in nature, given the essential continuum of glassy configurations which exist.

An obvious difficulty with the TLS model as it is applied to most systems is that something as fundamental as the spatial extents of the TLS are not known. Without this knowledge for the host TLS (intrinsic) and those which may be introduced by the impurity (extrinsic), the concept of TLS connectivity is impossible to quantify. Nevertheless, we proceed to explore a model for LIHF which is based on the premise that filling involves communication between impurity sites excited by secondary irradiation (ω_{B_2}) and those which are not and are, therefore, spatially removed from sites in the ω_{B_2} isochromat. In doing so, we pursue the idea that we can divide the TLS distribution into two sets, one

whose members are weakly coupled to the impurity and the other whose members are strongly coupled [23]. For convenience, we refer to the former and latter as intrinsic and extrinsic. The extrinsic TLS would include those which, for example, lead to hole formation by phonon assisted tunneling. Their spatial extent may be considered as localized relative to that of the intrinsic TLS. For polymers, in particular, a large spatial extent for intrinsic TLS is not unreasonable since chain "snaking" along the channel or "tube" formed by its neighbors can presumably occur to some degree even at helium temperatures. Leger and De Gennes [24] and de Gennes [25] have referred to such motion as reptation. Now for each and every extrinsic TLS we associate a potential energy curve $V^j_{ex}(q,\underline{\xi})$ where q is the usual intermolecular double well coordinate associated with the extrinsic (ex) TLS [6]. The superscript j labels the ground or excited electronic state of the impurity. The $\underline{\xi}$ variable denotes the coordinates of the atoms associated with the intrinsic TLS. Within the Born-Oppenheimer approximation, one can view V^j_{ex} as depending parametrically on the $\underline{\xi}$ coordinates. Thus, $\langle V^j_{ex}(q,\underline{\xi})\rangle_{gls}$ represents the extrinsic TLS potential for a particular glassy state (gls). The gls defines the value of $\underline{\xi}$ and is governed by the intrinsic TLS(s) which surround the extrinsic TLS.

LIHF is then viewed as resulting from irreversible gls $\sim\sim>$gls′ glassy state transitions triggered by secondary light absorption by extrinsic impurity-TLS different from those involved in the primary burn. The initial excitation (via secondary irradiation) and coupling between the extrinsic excited impurity-TLS and intrinsic TLS leads to

the irreversible evolution of gls′. The time scale may be long with much of the configurational change associated with gls → gls′ occurring with the impurity in its ground electronic state. The energies V_{ex}^{j} respond adiabatically to the glassy state transition (we have used glassy state interchangeably with the state of the intrinsic TLS which surround an influence the extrinsic TLS). Thus, provided the spatial extent of the intrinsic TLS is large, the excitation frequencies of extrinsic impurity-TLS spatially removed from those excited can be altered. The picture which emerges is that excitation of a spectrally narrow isochromat causes excitation frequency diffusion over a broad segment of excitation frequency space.

We proceed now to discuss the results 1-4 (vide supra) in terms of this model (referred to hereafter as A). Consider first the first part of result 3 and Fig. 3. Our initial response to the step behavior at ω_{B_1} was that there are two LIHF mechanisms, only one of which is operative for $\omega_{B_2} < \omega_{B_1}$. At the present time, this possibility has not been excluded although we are not able to come up with a plausible model (B). Thus, we consider here only model A. We suggest that the behavior of Fig. 3, the results of Figs. 7 and 8 and other LIHF results for polystyrene [18,20] are explicable by one mechanism, i.e., model A. An important clue is provided by Fig. 8 which shows that Nd^{3+} is intriguingly different in the sense that LIHF is more efficient for $\omega_{B_2} < \omega_{B_1}$. This leads us to consider correlation effects between impurity site excitation energies and glassy state (intrinsic TLS) absolute energies. By

positive (negative) correlation, we mean that increasing excitation energy is associated with increasing (decreasing) absolute energy of the intrinsic TLS. Although the zero-point splittings, barrier heights, etc. of extrinsic impurity-TLS may be dominated by interatomic interactions from within their domains, the intrinsic TLS which envelop them may be a major contributor to the determination of excitation frequencies within the inhomogeneously broadened absorption profile. It is reasonable to suggest that the absolute energies of intrinsic TLS are quite insensitive to the state of the impurity due to their assumed large spatial extent. In addition to correlation, we introduce the notion that an arbitrary perturbation (like secondary irradiation of LIHF) is, on average, far more disposed to promote gls $\rightarrow$ gls' configurational transformations in which E(gls') < E(gls). This is not unreasonable for transformations at helium temperatures. Thus, for positive correlation and within the framework of model A, secondary irradiation would cause red shifts of a wide distribution of site excitation energies while for negative correlation, blue shifts would occur. Given the gradient in excitation frequency space due to the primary hole, these shifts lead to hole filling.

With this in mind, one can qualitatively understand the step behavior for R640, Fig. 3, and the results for Pr^{3+}, Fig. 7. For both, there is a significant amount of positive correlation, albeit not perfect since some filling is observed for $\omega_{B_2} < \omega_{B_1}$. On the other hand for Nd^{3+}, Fig. 8, a significant amount of negative correlation is indicated.

Consider next the result 4 which is that the hole broadening accompanying LIHF is imperceptible. The analogous spectral diffusion problem pertaining to thermally induced spectral diffusion (hole broadening) and hysteresis has been treated theoretically by Friedrich et al. [26]. The associated problem for spontaneous hole filling (SPHF) is considered in Paper 5. The theory of Friedrich et al. [26] is, with slight modification, a reasonable starting point for LIHF and model A. If the probability function for an excitation frequency shift $\omega' \rightarrow \omega' + \Delta\omega$ has an effective width σ and is independent of ω', the theory shows that hole broadening would be difficult to observe (at our 6% accuracy and percent fills) for $\sigma \gtrsim 10\ \gamma$, where γ is the width of hole prior to filling. Thus, failure to observe hole broadening is not necessarily in contradiction with model A.

Thus far, this model has qualitatively accounted for all the results listed at the beginning of this section except the second part of 3, see Fig. 3. Although one can understand why LIHF can occur for large $|\omega_{B_2} - \omega_{B_1}|$ (with ω_{B_2} within the absorption profile), it is difficult to explain why for $\omega_{B_2} > \omega_{B_1}$ or $< \omega_{B_1}$, the % LIHF is essentially constant. For the same ω_{B_2} flux and irradiation time, one would reasonably assume that the % filling would mimic the variation in optical density across the absorption profile, Fig. 3. In addition, there is the result from Table 1 (first 2 rows) that ω_{B_2} irradiation of R560 near the peak of its absorption yields a % fill for CV identical to that obtained for the same ω_{B_2} but with R560 absent (for the latter case the optical density

at ω_{B_2} is 0.08 compared to 0.35 when R560 was present). Further experiments are required to understand the above behavior including studies with substantially reduced ($<<$ 1 mW/cm^2) ω_{B_2} fluxes. Given the saturation (bottleneck) behavior for NPHB shown in Fig. 5, it is possible that LIHF itself is being affected by a saturation effect.

CONCLUDING REMARKS

The model presented for LIHF is based on the idea of connectivity or communication between spatially separated (extrinsic) impurity-TLS. For the concentrations used in the R640 and CV/R560 experiments, the average distance between impurities is ~225 Å. The idea that the relatively localized impurity-TLS is enveloped by spatially extended intrinsic TLS and that the impurity excitation frequencies depend in an adiabatic manner on the configuration of the intrinsic TLS is introduced. The latter can be viewed as being a type of embedding glassy state (gls) for each and every impurity-TLS. A possible mechanism for the above long range communication for polymer hosts could involve subtle reptation-type motion of polymer chains. Accepting that a perturbation to the system, like secondary ω_{B_2} irradiation, produces a preponderance of downward (energy lowering) gls transitions, much of the LIHF data presented can be qualitatively explained when one additional ingredient is introduced. It is that some degree of correlation between impurity site excitation energies and the absolute gls energies exists.

The general features of LIHF shown here for R640, Pr^{3+}, Nd^{3+} and CV/560 in PVOH have also been observed for chlorophyll *a* and *b* [18,19] and the chlorophyll *a* dimer [20] in polystyrene. More recently, they have been observed for oxazine 720 in PVOH [27]. Thus, given the range of impurities studied, it may be that the features are general for hole burning in polymers.

The above model, however, should be viewed as a tentative one. There are a number of experiments which can be used to test it; for

example, LIHF as a function of impurity concentration and the determination of the $|\omega_{B_2} - \omega_{B_1}|$ dependence of LIHF in nonpolymeric hosts such as aprotic and alcohol glasses. Such experiments are planned. In addition, the R640 results, Fig. 3, suggest that it will be important to determine how the $|\omega_{B_2} - \omega_{B_1}|$ dependence is affected by reductions in secondary irradiation flux.

REFERENCES

1. B. L. Fearey and G. J. Small, Chem. Phys. 101, 269 (1986).

2. J. M. Hayes and G. J. Small, Chem. Phys. 27, 151 (1978).

3. A. R. Gutierrez, J. Friedrich, D. Haarer, and H. Wolfrum, IBM J. Res. Develop. 26, 198 (1982).

4. T. P. Carter and B. L. Fearey, Iowa State University, Ames, Iowa, unpublished results.

5. J. M. Hayes and G. J. Small, J. Lumin. 18/19, 219 (1979).

6. J. M. Hayes, R. P. Stout, and G. J. Small, J. Chem. Phys. 74, 4266 (1981).

7. R. W. Olson, H. W. H. Lee, M. D. Fayer, R. M. Shelby, D. P. Burum, R. M. Macfarlane, J. Chem. Phys. 77, 2283 (1982).

8. H. W. H. Lee, C. A. Walsh and M. D. Fayer, J. Chem. Phys. 82, 3948 (1985).

9. T. P. Carter, B. L. Fearey, J. M. Hayes, and G. J. Small, Chem. Phys. Lett. 102, 272 (1983).

10. B. L. Fearey, T. P. Carter, and G. J. Small, J. Phys. Chem. 87, 3590 (1983).

11. Specifically, when a sample which had been burned at 1.7 K, was raised rapidly to some higher temperature (T_h) and then promptly recooled to 1.7 K, significant broadening was observed when hole filling was comparable to LIHF. For example, for filling of ~10% ($T_h \approx 10$ K), a broadening of ~20% occurred. This is in marked contrast to the results for LIHF.

12. M. Romagnoli, W. E. Moerner, F. M. Schellenberg, M. D. Levenson, and G. C. Bjorklund, J. Opt. Soc. Am. 1, 341 (1984).

13. S. K. Lyo and R. Orbach, Phys. Rev. B 22, 4223 (1980).

14. P. Reinecke and H. Morawitz, Chem. Phys. Lett. 86, 359 (1982).

15. T. Forster, Ann. Phys. 2, 55 (1948).

16. R. M. Macfarlane and R. M. Shelby, in NATO Workshop on Coherence and Energy Transfer in Glasses, edited by P. A. Fleury and B. Golding (Plenum Press, New York, 1982).

17. J. K. Tyminski, R. C. Powell, and W. K. Zwicker, Phys. Rev. B 29, 6074 (1984).

18. T. P. Carter and G. J. Small, submitted to Chem. Phys. Lett., 1985.

19. J. M. Hayes, B. L. Fearey, T. P. Carter, and G. J. Small, Int. Rev. Phys. Chem., 1986 (in press).

20. T. P. Carter and G. J. Small, J. Chem. Phys. (submitted).

21. B. L. Fearey, R. P. Stout, J. M. Hayes, and G. J. Small, J. Chem. Phys. 78, 7013 (1983).

22. H. F. Childs and A. H. Frances, J. Phys. Chem. 89, 466 (1985).

23. B. Golding, M. V. Schickfus, S. Hunkburger, and K. Dransfeld, Phys. Rev. Lett. 43, 1817 (1979).

24. L. Leger and P.-G. de Gennes, Ann. Rev. Phys. Chem. 33, 49 (1982).

25. P.-G. de Gennes, "Entangled Polymers", Physics Today 33 (June, 1983).

26. J. Friedrich, D. Haarer and R. Silbey, Chem. Phys. Lett. 95, 119 (1983).

27. M. J. Kenney, Iowa State University, Ames, Iowa (unpublished results).

ACKNOWLEDGEMENTS

This work was supported by the National Science Foundation, Grant No. DMR-8400905.

BLF would like to thank the IBM Corporation for fellowship support during the performance of this research.

GENERAL CONCLUSIONS

Conclusions From Thesis Work

Over the course of this research, a wide variety of systems have been examined and a diverse set of studies performed. Over a dozen different molecules have been examined in terms of nonphotochemical hole burning (NPHB) (cf. Experimental). In order to summarize the extent of this work, it is necessary to outline the many and different results in basically a chronological order.

Early in the thesis work, the importance of hydrogen bonding was clearly established as being a crucial element in NPHB [68] (see Paper 1). This was accomplished by performing a deuteration dependent experiment on tetracene in both protonated and deuterated ethanol:methanol glasses. The hole burning efficiency was determined to be ~5 times more efficient for the protonated than for the deuterated samples. However, the observed efficiency was still roughly 10 times weaker dependence than that observed by Olson et al. [45] for NPHB of pentacene in benzoic acid. Recently, this apparently low NPHB efficiency for pentacene in benzoic acid has been found to be due to a triplet bottleneck effect [46] and that, in fact, the hole burning efficiency is "higher" in the deuterated sample. It is important to note that crystalline materials are very impurity dependent (cf. Introduction) making direct comparisons difficult. Lastly, a temperature dependent dephasing study on the deuterated sample (Paper 1) was performed showing that the holewidth dependence on deuteration is weak. These results are consistent with

theory in that TLS involved in the hole burning process are basically distinct from those involved in the dephasing.

The next stage involved the rather fortuitous discovery of a highly efficient class of hole burning systems for study [69] (see Paper 2). These were the ionic dyes, primarily laser dyes, doped into either of two hydroxylated polymers, i.e., poly(acrylic acid) (PAA) or poly(vinyl alcohol) (PVOH). These systems exhibit facile NPHB, relative to most other organic host systems, and exhibit a rich vibronic satellite hole structure. In general, the vibronic structure is observed primarily to lower energy of the burn frequency indicating that the intramolecular Franck-Condon factors are small. This is not in contradiction to the strong low energy vibronic structure [69] (see Paper 2) since the intensities are governed by Franck-Condon factors weighted by the origin site distribution function. Further, these systems are characterized by weak electron-phonon coupling (i.e., weak phonon side bands). Although, as already established (vide supra), the extended hydrogen-bonding network is instrumental in the NPHB efficiency, the ionic dye itself also seems to enhance the hole burning facility for these systems.

After finding that hole burning was extremely facile in the hydroxylated polymers, two rare earth ions (Pr^{+3} and Nd^{+3}) were found to also hole burn very efficiently in the host material PVOH. The efficiency was estimated to be approximately two orders of magnitude more efficient than in hard inorganic glasses [71] (see Paper 4). This was the first demonstration of NPHB of rare earth ions in a soft organic glass.

Having determined that these new facile systems were ideal for examining the glassy state, several quite different and distinct experiments were undertaken. The first was to examine the dephasing temperature dependences in one of the new systems, cresyl violet perchlorate (CV) in PVOH. Due to the fact that the samples were imbedded in easily handled samples (i.e., several identical sections could be mounted simultaneously) [70] (see Paper 3 for details), a new burn-probe sequence was utilized to examine the optical dephasing [70] (see Paper 3 for details). The importance of the new sequence versus previous burn-probe sequences was that the distortion of measured holewidths due to irreversible thermal annealing was eliminated. The observed T-dependence of $T^{1.1\pm0.1}$ was in basic agreement with many other results (within experimental error) and was easily understood in terms of current theories.

In an attempt to fully understand some of the properties of the glassy state, two more sets of experiments were undertaken; spontaneous hole filling (SPHF) and laser induced hole filling (LIHF). The hope was to gain an understanding of the microscopic interactions between different two level systems (TLS). Extensive work was performed on the systems of R640, Nd^{+3} and Pr^{+3} in PVOH.

Important SPHF results were that no line broadening of the zero-phonon hole (ZPH) was observed even over extended periods of time [50] (see Paper 5), in contrast to results observed for some other systems [156,157]. The decay rates of each of the above systems was determined based off a simple exponential fit. The decay rates of the holes were found to be constant for each particular system. A theoretical model

was developed to account for the "uniform" spontaneous hole filling phenomenon. The concept basically involved a feedback from the anti-hole sites [50] (see Paper 5 for details) into the ZPH. Further, in order to account for the lack of spectral diffusion, a correlation between the site excitation energies of the hole and the anti-hole was imposed.

Lastly, LIHF was also performed on the above systems along with the mixed system of R560 and CV in PVOH [51] (see Paper 6). This study provided an interesting insight into the various interactions between different types of TLS. In particular, the relationship between extrinsic TLS (impurity-TLS) and intrinsic TLS (host TLS or glassy state) was interrogated. A tentative (although quite reasonable) model was presented to explain the observed LIHF results. The model for LIHF is based on long range connectivity or communication between spatially separated extrinsic TLS via intrinsic TLS (i.e., the glassy state). The exact communication is envisioned to invoke subtle "reptation-type" motion of the polymer chains [51] (see Paper 6 for details). Several other mechanisms were determined to be insignificant. Note that even the obvious mechanism of energy transfer was found to be unimportant in LIHF as verified via the mixed dye experiment. Additionally, a degree of correlation between the absolute energy of the glassy state and the impurity transition energies was suggested. This was required in order to describe the more efficient hole filling for the secondary red or blue of the initial burn, depending on the system.

Therefore, to summarize this widely diverse set of results and experiments it difficult. However, suffice it to say that this thesis work has established the general versatility of persistent hole burning and has also demonstrated that NPHB is an invaluable tool for the determination of some of the most difficult problems in solid state physics, the understanding of the amorphous state.

The Future of Optical Hole Burning

Throughout the performance of the thesis work, many interesting experiments have been considered. Since only a few detailed experiments can be performed at any one time, many experiments have been passed over. Nevertheless, it seems appropriate at this time to briefly discuss some important and interesting experiments that would contribute to our knowledge of the phenomenon of optical hole burning.

Experimentally, in terms of detection techniques, it is imperative that improved data detection such as some of those discussed in the Introduction be undertaken. These methods would allow for NPHB to be performed and detected with significantly lower powers and would also greatly increase the present dynamic range. These avenues are presently being explored in Dr. G. J. Small's group in terms of either holographic detection [91], highly sensitive transmittance detection [109], or high frequency modulation [83].

Obviously, the study of the various properties of glasses needs to be extended to lower temperatures, this project is in progress by M. J. Kenney. With the Dewar system developed, temperatures $\lesssim 0.3$ should be attained. This lower temperature range should contribute significantly

to the understanding of the microscopic properties as probed via dephasing, SPHF and LIHF studies. Additionally, these low temperature results may prove the acid test for many theories.

Another interesting possibility would be to incorporate a specific heat or thermal conductivity apparatus with the normal hole burning apparatus. If this sort of device could be accomplished, then two data sets under identical conditions could be attained greatly improving the understanding of the TLS of the glassy state. The results could then be used to determine, more accurately, the TLS's parameter distributions via the theory of Jankowiak et al. [154].

In terms of SPHF and LIHF experiments, with improved detection systems, the concentration dependence of these phenomena needs to be studied over at least two orders of magnitude variation in the sample concentration. This would determined whether the proposed theories are an accurate estimation of the interactions occurring in the glassy state.

Several purely "interesting" experiments also could be attempted. The use of CARS (coherent anti-stokes Raman spectroscopy) to detect optically burned hole appears to be possible. S. G. Johnson anticipates attempting this for the system of Pr^{+3} in PVOH. Also, it is known that DECI (cf. Experimental), when at high concentration, forms dimers [158] whose spectra are red shifted from the monomer and are quite sharp (called J-bands). It seems reasonable that hole burning can be performed analogous to the hole burning of Carter and Small [116] on chlorophyll dimers. However, in this case, the molecule being probed would

be significantly simpler. J. K. Gillie expects to attempt this sort of hole burning experiment.

Lastly, based on some somewhat questionable unpublished results by the author [159], the author suggests that hole burning should again be attempted on pentacene in polystyrene. Instead of the low temperature hole burning (cf. Table 3), the hole burning should be performed at elevated temperatures. It appeared in preliminary work that hole burning <u>did</u> occur at approximately 100 K. However, after three scans and a short period of time, the hole disappeared. Nevertheless, hole burning in this system should again be attempted at higher temperatures.

ADDITIONAL REFERENCES

1. T. P. Hughes, Nature 195, 325 (1962).
2. P. Kisliuk and D. J. Walsh, Bull. Am. Phys. Soc. 7, 330 (1962).
3. C. L. Tang, H. Statz, and G. deMars, Appl. Phys. Lett. 2, 222 (1963).
4. C. L. Tang, H. Statz, and G. deMars, J. Appl. Phys. 34, 2289 (1963).
5. W. R. Bennet, Phys. Rev. 126, 580 (1962).
6. W. E. Lamb, Phys. Rev. 134, A1439 (1964).
7. P. H. Lee and M. L. Skolnick, Appl. Phys. Lett. 10, 303 (1967).
8. A. Corney, Atomic and Laser Spectroscopy (Clarendon Press, Oxford, 1977).
9. A. Szabo, Phys. Rev. B. 11, 4512 (1975).
10. R. M. Macfarlane and R. M. Shelby, Opt. Lett. 6, 96 (1981).
11. A. Szabo, Phys. Rev. B. 11, 4512 (1975).
12. R. M. Shelby and R. M. Macfarlane, Opt. Commun. 21, 399 (1978).
13. L. E. Erickson, Phys. Rev. B. 16, 4731 (1977).
14. H. Staerk and G. Czerlinski, Nature 207, 399 (1965).
15. A. Laubereau and W. Kaiser, Opto-electronics 6, 1 (1974).
16. M. R. Topp and H. Lin, Chem. Phys. Lett. 50, 412 (1977).
17. M. Leung and M. A. El-Sayed, Chem. Phys. Lett. 16, 454 (1972).
18. R. A. Avarmaa and K. Kh. Mauring, Opt. Spectrosc. 41, 393 (1976).
19. R. M. Macfarlane and R. M. Shelby, Phys. Rev. Lett. 42, 788 (1979).
20. A. Winnacker, R. M. Shelby, and R. M. Macfarlane, Opt. let. 10, 350 (1985).
21. A. A. Gorokhovskii, R. K. Kaarli, and L. A. Rebane, JETP Lett. 20, 216 (1974).

22. H. deVries and D. A. Wiersma, Phys. Rev. Lett. 36, 91 (1976).

23. B. M. Kharlamov, R. I. Personov, and L. A. Bykovskaya, Opt. Commun. 12, 191 (1974).

24. B. M. Kharlamov, R. I. Personov, and L. A. Bykovskaya, Opt. Spectrosc. 39, 137 (1975).

25. J. M. Hayes and G. J. Small, Chem. Phys. 27, (1978) 151.

26. J. M. Hayes and G. J. Small, Chem. Phys. Lett. 54, 435 (1978).

27. J. M. Hayes and G. J. Small, J. Lumin. 18/19, 219 (1979).

28. J. M. Hayes, R. P. Stout, and G. J. Small, J. Chem. Phys. 73, 4129 (1980).

29. J. M. Hayes, R. P. Stout, and G. J. Small, J. Chem. Phys. 74, 4266 (1981).

30. G. J. Small, "Molecular Spectroscopy", edited by V. M. Agranovich and R. M. Hochstrasser, in Modern Problems in Solid State Physics, V. M. Agronovich and A. A. Maradudin, General Eds. (North Holland, Amsterdam, 1983).

31. R. C. Zeller and R. O. Pohl, Phys. Rev. B 4, 2029 (1971).

32. P. W. Anderson, B. I. Halperin, and C. M. Varma, Phil. Mag. 25, 1 (1972).

33. W. A. Phillips, J. Low Temp. Phys. 7, 351 (1972).

34. F. H. Stillinger, Science 225, 983 (1984).

35. T. A. Weber and F. H. Stillinger, Phys. Rev. B 32, 5402 (1985).

36. F. H. Stillinger and T. A. Weber, Phys. Rev. A 28, 2408 (1983).

37. R. I. Personov, Spectrochim. Acta, 38B, 1533 (1983).

38. J. Friedrich and D. Haarer, Angew. Chem. Int. Ed. Engl. 23, 113 (1984).

39. J. M. Hayes, R. J. Jankowiak, and G. J. Small in Persistent Hole Burning: Science and Applications, edited by W. E. Moerner, (Springer-Verlag, Berlin, 1986), in preparation.

40. J. M. Hayes, B. F. Fearey, T. P. Carter, and G. J. Small, Review, Int. Rev. Phys. Chem., 1986 (in press).

41. G. S. Sim, J. M. Robertson, and T. H. Goodwin, Acta Crysta. 8, 157 (1955).

42. S. Hayashi, J. Umemura, and R. Nakamura, J. Mol. Struct. 123, 123 (1980).

43. S. Nagaoka, T. Terao, F. Imashira, A. Saika, H. Hirota, and S. Hayashi, Chem. Phys. Lett. 92, 581 (1981).

44. F. G. Patterson, H. W. H. Lee, R. W. Olson, and M. D. Fayer, Chem. Phys. Lett. 84, 59 (1981).

45. R. W. Olson, H. W. H. Lee, F. G. Patterson, M. D. Fayer, R. M. Shelby, D. P. Burum, and R. M. Macfarlane, J. Chem. Phys. 77, 2283 (1982).

46. C. A. Walsh and M. D. Fayer, J. Lumin. 34, 37 (1985).

47. R. Casalegno and H. P. Trommsdorff, Photochemistry and Photobiology, in Proceedings of the International Conference, (University of Alexandria, Egypt, 1983).

48. J. M. Clemens, R. M. Hochstrasser, and H. P. Trommsdorff, J. Chem. Phys. 80, 1744 (1984).

49. H. B. Levinsky and D. A. Wiersma, J. Chem. Phys. 79, 2677 (1983).

50. B. L. Fearey and G. J. Small, Chem. Phys. 101, 269 (1986).

51. B. L. Fearey, T. P. Carter, and G. J. Small, Chem. Phys. 101, 279 (1986).

52. R. Jankowiak and H. Bassler, Chem. Phys. Lett. 95, 124 (1983).

53. R. Jankowiak and H. Bassler, Chem. Phys. Lett. 95, 310 (1983).

54. R. Jankowiak and H. Bassler, Chem. Phys. Lett. 101, 274 (1983).

55. R. Jankowiak and H. Bassler, J. Mol. Electr. 1, 73 (1985).

56. R. Eiermann, G. M. Parkinson, H. Bassler, and J. M. Thomas, J. Phys. Chem. 87, (1983) 544.

57. R. Jankowiak, K. D. Rockwitz, and H. Bassler, J. Phys. Chem. 87, 552 (1983).

58. J. Wong and C. A. Angell, Glass Structure by Spectroscopy (Marcel Dekker, New York, 1976), Chap. 1.

59. J. D. Winefordner and P. A. St. John, Anal. Chem. 35, 2211 (1963).

60. A. V. Lesikar, J. Chem. Phys. 66, 4263 (1977).

61. C. A. Angell, J. M. Sare, and E. J. Sare, J. Phys. Chem. 82, 2622 (1978).

62. R. P. Stout, Ph.D. Dissertation, Iowa State University, Ames, Iowa, 1981.

63. D. Turnbull, Contemp. Phys. 10, 473 (1969).

64. A. Szabo, Phys. Rev. Lett. 25, 924 (1970).

65. R. I. Personov, E. I. Al'shits, and L. A. Bykovskaya, JETP Lett. 15, 609 (1972).

66. R. I. Personov, E. I. Al'shits, and L. A. Bykovskaya, Opt. Commun. 6, 169 (1972).

67. J. H. Eberly, W. C. McColgin, K. Kawaoka, and A. P. Marchetti, Nature 251, 215 (1974).

68. B. L. Fearey, R. P. Stout, J. M. Hayes, and G. J. Small, J. Chem. Phys. 78, 7013 (1983).

69. B. L. Fearey, T. P. Carter, and G. J. Small, J. Phys. Chem. 87, 2309 (1983).

70. T. P. Carter, B. L. Fearey, J. M. Hayes, and G. J. Small, Chem. Phys. Lett. 102, 272 (1983).

71. B. L. Fearey, T. P. Carter, and G. J. Small, J. Lumin. 31&32, 792 (1984).

72. U. Bogner, P. Schatz, R. Seel, and M. Maier, Chem. Phys. Lett. 102, 267 (1983).

73. A. P. Marchetti, M. Scozzafava, and R. H. Young, Chem. Phys. Lett. 51, 424 (1977).

74. A. F. Childs and A. H. Francis, J. Phys. Chem. 89, 466 (1985).

75. L. W. Molenkamp and D. A. Wiersma, J. Chem. Phys. 83, 1 (1985).

76. T. P. Carter and G. J. Small, Chem. Phys. Lett. 120, 178 (1985).

77. E. Cuellar and G. Castro, Chem. Phys. 54, 217 (1981).

78. R. M. Macfarlane and R. M. Shelby, Opt. Commun. 45, 46 (1983).

79. R. M. Macfarlane and R. M. Shelby, Proceedings of the NATO Workshop Coherence and Energy Transfer in Glasses (Plenum Press, New York, 1984), p. 189

80. B. L. Fearey and G. J. Small, Chem. Phys. 101, 269 (1986).

81. G. C. Bjorkland, M. D. Levenson, W. Lenth, and C. Ortiz, Appl. Phys. B 32, 145 (1983).

82. W. Lenth, C. Ortiz, and G. C. Bjorkland, Opt. Lett. 6, 351 (1981).

83. M. Romagnoli, W. E. Moerner, F. M. Schellenberg, M. D. Levenson, and G. C. Bjorkland, J. Opt. Soc. Am. B 1, 341 (1984).

84. M. Romagnoli, M. D. Levenson, and G. C. Bjorkland, Opt. Lett. 8, 635 (1983).

85. M. Romagnoli, M. D. Levenson, and G. C. Bjorkland, J. Opt. Soc. Am. B 1, 571 (1984).

86. H. Lengfellner, T. R. Gosnell, R. W. Tkach, and A. J. Sievers, Appl. Phys. Lett. 43, 437 (1983).

87. A. L. Huston and W. E. Moerner, J. Opt. Soc. Am. B. 1, 349 (1984).

88. O. N. Korotaev, S. M. Surin, A. I. Yurchenko, V. I. Glyadkovsky, and E. I. Donskoi, Chem. Phys. Lett. 110, 533 (1984).

89. H. P. H. Thijssen, R. Van den Berg, S. Volker, and J. H. Van der Waals, Chem. Phys. Lett. 111, 11 (1984).

90. A. Rosencwaig, Advan. Electron. Electron Phys. 53, 517 (1981).

91. A. Renn, A. J. Meixner, U. P. Wild, and F. A. Burkhalter, Chem. Phys. 93, 157 (1985).

92. Chr. Brauchle and D. M. Burland, Angew. Chem. Intern. Ed. 22, 582 (1983).

93. K. K. Rebane and V. V. Palm, Opt. Spectrosc. 57, 229 (1984).

94. K. K. Rebane and V. V. Palm, Eest. NSV Tead. Akad. Toim., Fuus. Mat. 33, 461 (1984).

95. Ya. V. Kikas, dissertation abstract, Tartu, USSR, 1979.

96. H. W. H. Lee, M. Gehrtz, E. E. Marinero, and W. E. Moerner, Chem. Phys. Lett. 118, 611 (1985).

97. W. E. Moerner, F. M. Schellenberg, G. C. Bjorkland, P. Kaipa, and F. Luty, Phys. Rev. B 32, 1270 (1985).

98. P. Kaipa and F. Luty, Phys. Rev. B 32, 1264 (1985).

99. U. Bogner, P. Schatz, and M. Maier, Chem. Phys. Lett. 119, 335 (1985).

100. A. K. Rebane, R. K. Kaarli, P. Saari, A. Anijalg, and K. Timpmann, Opt. Commun. 47, 173 (1983).

101. A. K. Rebane, R. K. Kaarli, and P. M. Saari, JETP Lett. 38, 384 (1983).

102. T. W. Mossberg, Opt. Lett. 7, 77 (1982).

103. W. Richter, G. Schulte and D. Haarer, Opt. Commun. 51, 412 (1984).

104. T. Tani, H. Namikawa, K. Arai, and A. Makiskima, J. Appl. Phys. 58, 3559 (1985).

105. H. Dislish, Angew. Chem. Int. Ed. 10, 363 (1971).

106. S. Sakka and K. Kamiya, J. Non-Cryst. Solids 42, 403 (1980).

107. A. Makishima and T. Tani, National Institute for Research in Inorganic Materials, Sakura-mura, Japan, 1985 (unpublished results).

108. W. E. Moerner, A. J. Sievers, R. H. Silsbee, A. R. Chraplyvy, and D. K. Lambert, Phys. Rev. Lett. 49, 398 (1982).

109. W. E. Moerner, A. R. Chraplyvy, A. J. Sievers, and R. H. Silsbee, Phys. Rev. B 28, 7244 (1983).

110. T. B. Gosnell, A. J. Sievers, and R. H. Silsbee, Phys. Rev. Lett. 52, 303 (1984).

111. R. T. Harley, M. J. Henderson, and R. M. Macfarlane, J. Phys. C: Sol. St. Phys. 17, L233 (1984).

112. B. A. Leland, A. D. Joran, P.M. Felker, J. J. Hopfield, A. H. Zewail, and P. B. Dervan, J. Phys. Chem. 89, 5571 (1985).

113. C. K. Johnson, research proposal, University of Kansas, Lawrence, KS, 1984.

114. R. A. Avarmaa, K. Mauring, and A. Suisalu, Chem. Phys. Lett. 77, 88 (1981).

115. R. A. Avarmaa and K. K. Rebane, Chem. Phys. 68, 2309 (1982).

116. T. P. Carter and G. J. Small, submitted to J. Chem. Phys, 1985.

117. S. R. Meech, A. J. Hoff, and D. A. Wiersma, Chem. Phys. Lett. 121, 287 (1985).

118. S. G. Boxer, D. J. Lockhart, and T. R. Middendorf, Chem. Phys. Lett., 1986 (in press).

119. A. Szabo, "Frequency selective optical memory", U.S. Patent No. 3,896,420 (1975).

120. G. Castro, D. Haarer, R. M. Macfarlane, and H. P. Trommsdorff, "Frequency selective optical data storage systems", U.S. Patent No. 4,101,976 (1978).

121. A. R. Gutierrez, J. Friedrich, D. Haarer, and H. Wolfrum, IBM J. Res. Develop. 26, 198 (1982).

122. G. C. Bjorkland, W. Lenth, and C. Ortiz, SPIE 298, 107 (1981).

123. W. E. Moerner, Photonics Spectra, February, 59 (1985).

124. W. E. Moerner and M. D. Levenson, J. Opt. Soc. Am. B 2, 915 (1985).

125. P. Pokrowsky, W. Zapka, F. Chu, and G. C. Bjorkland, SPIE, 395, 35 (1983).

126. U. Bogner, K. Beck, and M. Maier, Appl. Phys. Lett. 46, 534 (1985).

127. U. P. Wild, S. E. Bucher, and F. A. Burkhalter, Appl. Opt. 24, 1526 (1985).

128. J. Hegarty and W. H. Yen, Phys. Rev. Lett. 84, 215 (1981).

129. J. D. Macomber, The Dynamics of Spectroscopic Transitions (Wiley-Interscience, New York, 1976), p. 166.

130. P. M. Selzer, D. L. Huber, D. S. Hamilton, W. M. Yen, and M. J. Weber, Phys. Rev. Lett. 36, 813 (1976).

131. T. L. Reinecke, Sol. St. Commun. 32, 1103 (1979).

132. S. K. Lyo and R. Orbach, Phys. Rev. B 22, 4223 (1980).

133. S. K. Lyo, Phys. Rev. Lett. 48, 688 (1982).

134. S. K. Lyo, in Electronic Excitation and Interaction Processes in Organic Molecular Aggregates. edited by P. Reinecker, H. Haken, and H. C. Wolf (Springer-Verlag, Berlin, 1983), Vol. 49 of Springer Series in Solid State Sciences.

135. D. L. Huber, M. M. Broer, and B. Golding, Phys. Rev. Lett. 52, 2281 (1984).

136. P. Reineker and H. Morawitz, Chem. Phys. Lett. 86, 359 (1982).

137. P. Reineker, H. Morawitz, and K. Kassner, Phys. Rev. 29, 4546 (1984).

138. S. K. Lyo and R. Orbach, Phys. Rev. B 29, 2300 (1984).

139. G. J. Small, Iowa State University, Ames, Iowa (unpublished results).

140. B. Jackson and R. Silbey, Chem. Phys. Lett. 99, 331 (1983).

141. H. P. H. Thijssen, A. I. M. Dicker, and S. Volker, Chem. Phys. Lett. 92, 7 (1982).

142. H. P. H. Thijssen, S. Volker, M. Schmidt, and H. Port, Chem. Phys. Lett. 94, 537 (1983).

143. H. P. H. Thijssen, R. Van den Berg, and S. Volker, Chem. Phys. Lett. 97, 295 (1983).

144. H. P. H. Thijssen, R. Van den Berg, and S. Volker, Chem. Phys. Lett. 120, 503 (1985).

145. J. Friedrich, H. Wolfrum, and D. Haarer, J. Chem. Phys. 77, 2309 (1982).

146. M. M. Broer, B. Golding, W. H. Haemmerle, J. R. Simpson, and D. L. Huber, 1986 (submitted for publication).

147. J. M. Pellegrino, W. M. Yen, and M. J. Weber, J. Appl. Phys. 51, 6332 (1981).

148. R. B. Stephens, Phys. Rev. B 8, 2896 (1973).

149. J. Jackle, Z. Phys. 257, 212 (1972).

150. J. L. Black and B. I. Halperin, Phys. Rev. B 16, 2879 (1977).

151. J. Jackle, K.-L. Jungst, Z. Phys. B30, 243 (1978).

152. P. J. Anthony and A. C. Anderson, Phys. Rev. B 20, 763 (1979).

153. R. Schilling, Phys. Rev. Lett. 53, 763 (1984).

154. R. Jankowiak, K. Athreya, and G. J. Small, 1986 (submitted for publication).

155. M. Kasha, J. Opt. Soc. Am. 38, 929 (1948).

156. W. Breinl, J. Friedrich, and D. Haarer, Chem. Phys. Lett. 106, 487 (1984).

157. W. Breinl, J. Friedrich, and D. Haarer, J. Chem. Phys. 81, 3915 (1984).

158. Z. X. Yu, P. Y. Lu, and R. R. Alfano, Chem. Phys. 79, 289 (1983).

159. B. L. Fearey, Iowa State University, Ames, Iowa (unpublished results).

160. J. M. Hayes and G. J. Small, Chem. Phys. 27, 151 (1978).

161. A. A. Gorokhovskii, Ya. V. Kikas, V. V. Palm, and L. A. Rebane, Sov. Phys. Solid State 23, 602 (1981).

162. H. P. H. Thijssen, R. Van den Berg, and S. Volker, Chem. Phys. Lett. 120, 503 (1985).

163. M. Edelson, J. M. Hayes, and G. J. Small, Chem. PHys. Lett. 60, 307 (1979).

164. M. J. McGlade, Iowa State University, Ames, Iowa (unpublished results).

165. A. A. Gorokhovskii and V. V. Palm, JETP Lett. 5, 238 (1983).

166. B. M. Kharlamov, L. A. Bykovskaya, and R. I. Personov, Opt. Spectrosc. 42, 445 (1977).

167. B. M. Kharlamov, L. A. Bykovskaya, and R. I. Personov, Chem. Phys. Lett. 50, 407 (1977).

168. U. Bogner, G. Roska, and F. Graf, Thin Sol. Films 99, 257 (1983).

169. M. Fujiwara, R. Kuroda, and H. Nakatsuka, J. Opt. Soc. Am. B 2, 1643 (1985).

170. D. M. Burland and H. Haarer, IBM J. Res. Develop. 23, 534 (1979).

171. F. Graf, H.-K. H ong, A. Nazzal, and D. Haarer, Chem. Phys. Lett. 59, 217 (1978).

172. R. M. Macfarlane, R. M. Shelby, A. Z. Genack, and D. A. Weitz, Opt. Lett. 5, 462 (1980).

173. N. B. Manson, Opt. Commun. 44, 32 (1982).

174. A. J. Silversmith and N. B. Manson, J. Phys. C: Sol. St. Phys. 17, L97 (1984).

175. R. L. Cone, R. T. Harley, and M. J. M. Leask, J. Phys. C: Sol. St. Phys. 17, 3101 (1984).

176. R. M. MacFarlane and R. M. Shelby, in Laser Spectroscopy VI, edited by H. P. Weber and W. Luty (Springer-Verlag, Berlin, 1983), Vol. 40.

177. D. P. Burum, R. M. Shelby, and R. M. Macfarlane, Phys. Rev. B 25, 3009 (1982).

178. R. M. Macfarlane and R. M. Shelby, Opt. Lett. 6, 96 (1981).

179. R. M. Shelby, D. P. Burum, and R. M. Macfarlane, Opt. Commun. 52, 283 (1984).

180. R. M. Shelby, A. C. Tropper, R. T. Harley, and R. M. Macfarlane, Opt. Lett. 8, 304 (1983).

181. R. M. Macfarlane and R. S. Meltzer, Opt. Commun. 52, 320 (1985).

182. H. P. H. Thijssen, R. E. Van den Berg, and S. Volker, Chem. Phys. Lett. 103, 12 (1983).

183. H. P. H. Thijssen and S. Volker, Chem. Phys. Lett. 120, 496 (1985).

184. S. Volker and R. M. Macfarlane, IBM J. Res. Develop. 23, 547 (1979).

185. A. I. M. Dicker and S. Volker, Chem. Phys. Lett. 87, 481 (1982).

186. S. Volker, R. M. Macfarlane, A. Z. Genack, and H. P. Trommsdorff, J. Chem. Phys. 67, 1759 (1977).

187. A. I. M. Dicker, J. Dobkowski, and S. Volker, Chem. Phys. Lett. 84, 415 (1981).

188. V. G. Maslov, Opt. Spectrosc. 50, 599 (1981).

189. M. N. Sapozhnikov and V. I. Aleeksev, Chem. Phys. Lett. 107, 265 (1984).

190. A. I. M. Dicker, L. W. Johnson, S. Volker, and J. H. van der Waals, Chem. Phys. Lett. 100, 8 (1983).

191. R. M. Shelby and R. M. Macfarlane, Chem. Phys. Lett. 64, 545 (1979).

192. Ya. V. Kikas and R. V. Yaniso, Sov. Phys. Solid State 26, 1128 (1984).

193. F. A. Burkhalter, G. W. Suter, U. P. Wild, V. D. Samoilenko, N. V. Rasumova, and R. I. Personov, Chem. Phys. Lett. 94, 483 (1983).

194. V. D. Samoilenko, N. V. Razumova, and R. I. Personov, Opt. Spectrosc. 52, 346 (1982).

195. S. Volker and R. M. Macfarlane, J. Phys. Chem. 73, 4476 (1980).

196. V. G. Maslov, Opt. Spectrosc. 45, 718 (1978).

197. H. W. H. Lee, A. L. Huston, M. Gehrtz, and W. E. Moerner, Chem. Phys. Lett. 114, 491 (1985).

198. A. Gutierrez, G. Catro, G. Schulte, and D. Haarer, in Organic Molecular Aggregates: Electronic Excitation and Interaction Processes, edited by P. Reinecker, H. Haken, and H. C. Wolf (Springer-Verlag, Berlin, 1983), Vol. 49, p. 206.

199. A. A. Gorokhovskii and J. Kikas, Opt. Commun. 21, 272 (1977).

200. A. A. Gorokhovskii and L. A. Rebane, Opt. Commun. 20, 144 (1977).

201. A. R. Gutierrez, Chem. Phys. Lett. 74, 293 (1980).

202. V. G. Maslov, A. S. Chunaev, and V. V. Tugarinov, Molekuly. Biol. 15, 1016 (1981).

203. J. Friedrich, H. Scheer, B. Zickendraht-Wendelstadt, and D. Haarer, J. Chem. Phys. 74, 2260 (1981).

204. J. Friedrich, H. Scheer, B. Zickendraht-Wendelstadt, and D. Haarer, J. Lumin. 24/25, 815 (1981).

205. J. Friedrich, H. Scheer, B. Zickendraht-Wendelstadt, and D. Haarer, J. Am. Chem. Soc. 103, 1030 (1981).

206. R. M. Macfarlane and R. M. Shelby, Phys. Rev. Lett. 64, 788 (1979).

207. R. T. Harley and R. M. Macfarlane, J. Phys. C: Sol. St. Phys. 16, 1507 (1983).

208. R. T. Harley and R. M. Macfarlane, J. Phys. C: Sol. St. Phys. 16, L395 (1983).

209. P. Porkrowsky, W. E. Moerner, F. Chu, and G. C. Bjorkland, Opt. Lett. 8, 280 (1983).

210. M. Dubs and Hs. H. Gunthard, Chem. Phys. Lett. 64, 105 (1979).

211. M. Dubs and Hs. H. Gunthard, J. Mol. Struc. 60, 311 (1980).

212. M. Dubs and Hs. H. Gunthard, J. Mol. Spectrosc. 93, 458 (1982).

213. M. Dubs, L. Ermanni, and Hs. H. Gunthard, J. Mol. Spectrosc. 91, 458 (1982).

214. P. Felder and Hs. H. Gunthard, Chem. Phys. Lett. 88, 473 (1982).

215. S. L. Hager and J. E. Willard, J. Chem. Phys. 61, 3244 (1974).

ACKNOWLEDGEMENTS

I would like to express my thanks to a number of persons who have aided me in the performance of various stages of this research project. I am particularly grateful to my research advisor, Professor Gerald J. Small, who not only initiated my interest in the phenomenon of nonphotochemical hole burning but also created an atmosphere in which I felt comfortable discussing with him many different aspects of research and theory. It is through his insight that I was able to gain an understanding of the amorphous state along with the mechanisms involved in NPHB and how the two relate to one another. In addition, I want to thank him for the many squash games, in which he offered me not only strong competition, but did not retaliate when I would happen to beat him every once in a while. I never did believe in the adage: "Let your boss win."

I am greatly indebted to Dr. John M. Hayes for his interest, guidance and knowledge of both experimental procedures and practical jokes. His suggestions were surely some of the most helpful and devious in each respect. I also am appreciative of Dr. Sylvia H. Stevenson, who helped me greatly in the solving and understanding of many of my so called "simple" problems which arose during the beginning of my project. The two turkey dinners were great. Doug's shooting was greatly appreciated since that was the only game in town.

I would like to thank T. P. Carter for his contributing work on NPHB, along with his patience in showing me much of the basics of experimental apparatuses and the various improvements which can be made to

improve signal to noise. Also, I would like to acknowledge his effort put forth in the building of the double beam absorption setup.

Further, several persons who have helped me retain my sanity over the past few years deserve considerable thanks. In particular, Dr. Jonathan A. Warren, whose friendship made much of the drudgery bearable. Also, my squash partners who have helped me get rid of much of my aggression by hitting the "heck" out of a little defenseless ball.

I also need to thank J. Kevin Gillie for his aid in the proofing of this thesis.

Additionally, I thank Iowa State University and the Ames Laboratory-USDOE for funding and support during this work. The support of the National Science Foundation is appreciated. Importantly, I want to express my appreciation for the honor of being awarded a predoctoral fellowship from the IBM Corporation during the two consecutive years 1984-1985.

Lastly, I would like to thank some of the persons most dear in my life. I am especially grateful to my parents, Mr. Evan J and Mrs. Darlene L. Fearey, for their encouragement and support throughout my educational experience. Most importantly, I want to thank my wife and fellow researcher, Maureen, who not only provided late night (or early morning) lab help and "gourmet" take-out dinners but also provided the warmth, love and security that only a wife and best friend can.

APPENDIX

The purpose of this section, as stated in the Introduction, is to give a semi-comprehensive table of the majority of hole burning systems found to date (given in Table 4). Although it is impossible to ever be totally inconclusive, this table includes an extensive number of systems. References are given to one or more of the papers referring to that particular system, however, only a partial list is given, in general, for the systems. Further, the author attempts to classify the system as nonphotochemical or photochemical either based upon statements in the pertinent paper or based purely on an informed intuitive guess. When there appears to be contradiction in the literature or the appropriate mechanism is unclear, question marks are indicated. The hope of the author is that this table (Table 4) will be used as a starting point for the new student initiating studies in hole burning and also as a quick reference to hole burning systems by other authors.

Table 4. Tabulation of persistent hole burning systems

Impurity (class)	Host system	Type HB	Reference
aromatic hydrocarbons			
naphthalene	EtOH[a]/MeOH[b]	N[c]	Hayes and Small (160)
anthracene	EtOH/MeOH	N	Hayes and Small (160)
tetracene	EtOH/MeOH	N	Hayes and Small (160)
	isopropanol/ether	N	Gorokhovskii et al. (161)
	amor.[d] anthracene	N	Jankowiak and Bassler (52,53)
	amor. 9,10-diphenylanthracence	N	Jankowiak and Bassler (54,55)
	amor. 2,3-dimethylanthracene	N	Jankowiak and Bassler (55)
	amor. 9-phenylanthracene	N	Jankowiak and Bassler (55)
	tetradecane	N	Gorokhovskii et al. (161)
	benzoic acid	N	Levinsky et al. (49)
pentacene	PMMA[e]	N	Molenkamp & Wiersma (75), Thijssen et al. (162)
	PS[f]	N?	Fearey (159)
	benzoic acid	N or P[g]	Olson et al. (45), Casalegno and Trommsdorff (47)
phenanthrene	EtOH/MeOH	N	Edelson, Hayes and Small (163)
phenanthrene	EtOH/MeOH	N	Edelson, Hayes and Small (163)

[a] EtOH ≡ ethanol.
[b] MeOH ≡ methanol.
[c] N ≡ nonphotochemical hole burning.
[d] Amor. ≡ amorphous.
[e] PMMA ≡ polymethylmethacrylate.
[f] PS ≡ polystyrene.
[g] P ≡ photochemical hole burning.

Table 4. Continued

Impurity (class)	Host system	Type HB	Reference
aromatic hydrocarbons			
pyrene	gly[h]/DMSO[i]/DMF[j]	N	McGlade (164)
	butyl bromide (triplet HB)	N	Gorokhovskii and Palm (165)
3,4,8,9-dibenzpyrene	EtOH	N	Kharlamov et al. (166,167)
perylene	EtOH	N	Kharlamov et al. (23,24)
	LBR[k]-Cd arachidate	N	Bogner et al. (168)
	PVB[l]	N	Bogner et al. (72)
	sapphire surface	N	Bogner et al. (99)
	quartz surface	N	Bogner et al. (99)
	γ-alumina surface	N	Bogner et al. (99)
	anodized Al	N	Bogner et al. (99)
perylene butyric acid	PVB	N	Bogner et al. (99)
	sapphire surface	N	Bogner et al. (99)
	quartz surface	N	Bogner et al. (99)
	γ-alumina surface	N	Bogner et al. (99)
	anodized Al	N	Bogner et al. (99)
azulene	EtOH/MTHF[m]	N	Stout (62)
2-phenyl-1-azaazulene	gly/EtOH/H_2O[n]	N	Stout (62)
2-phenyl-1,3-diazaazulene	EtOH/MeOH	N	Stout (62)

[h]Gly ≡ glycerol.
[i]DMSO ≡ dimethylsulfoxide.
[j]DMF ≡ dimethyl formamide.
[k]LBF ≡ Langmuir-Blogett film.
[l]PVB ≡ poly(vinyl butyral).
[m]MTHF ≡ methyltetrahydrofuran.
[n]H_2O ≡ water.

Table 4. Continued

Impurity (class)	Host system	Type HB	Reference
aromatic hydrocarbons			
dimethyl-s-tetrazine	PMMA, PEG[o]	N	Thijssen et al. (143)
	PVK[p]	N & P	Cuellar and Castro (77), Thijssen et al. (143)
	durene mixed crystal	N	de Vries and Wiersma (22)
diphenyltetrazine	EtOH/MeOH	N	Hayes and Small (160)
carbazole	boric acid	P	Lee et al. (96)
organic dyes			
R560[q]	PVOH[r]	N	present work, Fearey et al. (51)
R640[s]	PVOH, PAA[t]	N	present work, Fearey et al. (51,71)
	PMMA	N	Stout (62)
CV[u]	PVOH	N	present work, Fearey et al. (69), T. P. Carter et al. (70)
	PAA	N	present work, Hayes et al. (40), Fearey et al. (51,69)
	PVK	N	present work, Hayes et al. (40)
	PMMA	P?	Thijssen et al. (162)
	EtOH/MeOH	N	Small (30)
	Gly/EtOH/H_2O	N	present work, Fearey et al. (69)
	EtOH	P?	Thijssen et al. (162)

[o]PEG ≡ poly(ethylene glycol).
[p]PVK ≡ poly(vinyl carbazole).
[q]R560 ≡ rhodamine 560 chloride.
[r]PVOH ≡ poly(vinyl alcohol).
[s]R640 ≡ rhodamine 640 perchlorate.
[t]PAA ≡ poly(acrylic acid).
[u]CV ≡ cresyl violet perchlorate.

Table 4. Continued

Impurity (class)	Host system	Type HB	Reference
organic dyes			
cresyl fast violet	cellulose	N	Fujiwara et al. (168)
nile blue	PVOH, PAA	N	present work, Hayes et al. (40), Fearey et al. (69)
Ox720[v]	PVOH, PAA	N	present work, Fearey and Small (50), Fearey et al. (69,71)
Ox725[w]	PVOH, PAA	N	present work, Hayes et al. (40)
Ox750[x]	PAA	N	present work, Hayes et al. (40)
MCI[y]	PVOH	N	present work, Hayes et al. (40)
malachite green	PAA	N?	present work, Hayes et al. (40)
methylene blue	PAA	N	present work, Hayes et al. (40)
indigo carmine	PAA	N?	present work, Hayes et al. (40)
thioindigo	benzoi acid	N	Clemens et al. (48)
resorufin	PMMA	N or P?	Childs and Francis (75), Thijssen et al. (162)
	EtOH	P?	Thijssen et al. (162)
9-aminoacridine	EtOH	N	Kharlamov et al. (23,24)
	PVB	N	Bogner et al. (126)

[v]Ox720 ≡ oxazine 720 perchlorate.
[w]Ox725 ≡ oxazine 725 perchlorate.
[x]Ox750 ≡ oxazine 750 perchlorate.
[y]MCI ≡ 1,1'-methylene-2,2'-cyanine iodide (donated by Alfred Marchetti, Eastman Kodak Co.).

Table 4. Continued

Impurity (class)	Host system	Type HB	Reference
organic dyes			
quinizarin	EtOH/MeOH	P	Burland and Haarer (170)
	EtOH	P	Graf et al. (171)
	EtOH	P	Graf et al. (171)
	P^{z}:MP^{aa}:MC^{bb}	P	Stout (62)
	boric acid	P	Friedrich et al. (145)
	amor. silica	P	Tani et al. (104)
tetraflourodihyroxy-tetracenequinone	EtOH	P	Graf et al. (171)
	PMMA	P	Graf et al. (171)
rare earth ions			
Eu^{+3}	EuP_5O_{14} glass	N	Macfarlane et al. (172)
	$NaEu(WO_4)_2$	N	Manson (173)
	$KNaEu(WO_4)_2$	N	Silversmith and Manson (174)
	$EuVO_4$	N	Cone et al. (175)
Nd^{+3}	PVOH	N	present work, Fearey and Small (50), Fearey et al. (51,71)
	silicate glass	N	Macfarlane and Shelby (78,79)
	phosphate, BeF_2 glasses	N	Macfarlane and Shelby (77)
Pr^{+3}	PVOH	N	present work, Fearey and Small (50), Fearey et al. (51,71)
	silicate glass	N	Macfarlane and Shelby (78,79)
	CaF_2	N	Macfarlane and Shelby (176)
	CaF_3	N	Burum, Shelby and Macfarlane (177)
	LaF_3	N	Macfarlane and Shelby (178)
	YPO_4 (crystal)	N	Shelby et al. (179)
	YAG	N	Shelby et al. (180)

[z] P ≡ pentane.
[aa] MP ≡ methylpentane.
[bb] MCP ≡ methylcyclopentane.

Table 4. Continued

Impurity (class)	Host system	Type HB	Reference
rare earth ions			
Sm^{+2}	BaClF	N	Winnacker et al. (20)
	SrF_2	N	Macfarlane and Meltzer (181)
biomolecules			
free-base porphin	EtOH, glycol, glycerol	P	Thijssen et al. (141)
	gly/EtOH, diglycerol	P	Thijssen et al. (143)
	MTHF	P	Thijssen et al. (141)
	PMMA	P	Thijssen et al. (143)
	PVK, PS, PC[cc], PVOH, PEG[dd]	P	Thijssen et al. (143)
	PE[ee]	P	Thijssen et al. (182)
	PMA[ff], PP[gg], PBA[hh]	P	Thijssen and Volker (183)
	hexane	P	Volker and Macfarlane (184)
	heptane	P	Dicker and Volker (185)
	octane	P	Gorokhovskii et al. (21), Volker et al. (186)
	decane	P	Dicker et al. (187)
tetrabenzoporphin	THF[ii]/ether	P	Maslov (188)
free-base porphin dimer	glycerol, MTHF	P	Thijssen et al. (141)
Mg^{+2}-tetraazaporphin	EtOH	N?	Sapozhnikov and Alekseev (189)
Mg^{+2}-porphin:pyridine complex	octane	N?	Dicker et al. (190)

[cc] PC ≡ polycarbonate.
[dd] PEG ≡ polyethylene glycol.
[ee] PE ≡ polyethylene.
[ff] PMA ≡ polymethacrylate.
[gg] PP ≡ polypropylene.
[hh] PBA ≡ polybutylacrylate.
[ii] THF ≡ tetrahydrofuran.

Table 4. Continued

Impurity (class)	Host system	Type HB	Reference
biomolecules			
Zn^{+2} porphin	octane	N	Shelby and Macfarlane (191)
Zn^{+2}-tetraphenylporphine	EtOH	N	Kharlamov et al. (170)
	diethyl ether/butanol	N	Kikas and Yaniso (192)
chlorin	PS, PVB	P	Burkhalter et al. (193), Samoilenko et al. (194)
	PMMA	P	Thijssen et al. (143), Burkhalter et al. (193)
	hexane, octane	P	Volker and Macfarlane (184)
	decane	P	Volker and Macfarlane (195)
octaethylchlorin	PMMA	P	Korotaev et al. (88)
	PS	P	Rebane and Palm (93)
Cd^{+2}-etiochlorin:pyridine	THF/ether	N	Maslov (196)
free-base phthalocyanine	concentrated sulfuric acid	P	Lee et al. (197)
	PE	P	Romagnoli et al. (93), Richter et al. (103)
	PMMA	P	Richter et al. (103), Gutierrez et al. (121)
	PS	P	Gutierrez et al. (198)
H_2-tetra-4-tert-butylphthalocyanin	nonane	P	Gorokhovskii and Kikas (199)
	tetradecane	P	Gorokhovskii and Rebane (200)
Ru^{+2}-phthalocyanine	3MP[jj]/EtOH/MTHF	N	Gutierrez (201)
	EtOH/Pyridine	N	Gutierrez (201)
	MTHF/Pyridine	N	Gutierrez (201)
bacteriochlorophyll-a	gly/H_2O	N?	Meech et al. (117)
	PVA	N?	Boxer et al. (118)

[jj] 3MP ≡ 3-methylpentane

Table 4. Continued

Impurity (class)	Host system	Type HB	Reference
biomolecules			
chlorophyll-a	ether	N	Avarmaa et al. (114), Rebane and Avarmaa (115)
	PS	N	Hayes et al. (40), Carter and Small (76)
chlorophyll-b	ether	N	Avarmaa et al. (114), Rebane and Avarmaa (115)
	PS	N	Hayes et al. (40), Carter and Small (76)
chlorophyll-a dimers	PS	N	Carter and Small (116)
protochlorophyll-a	ethyl ether/EtOH/H_2O	N	Avarmaa et al. (114), Rebane and Avarmaa (115)
chlamydomonas reinhardii w/ chlorophyll-a & P700	acetate suspension	N?	Maslov et al. (202)
pheophytin-a	ether,ether butanol	N	Avarmaa et al. (114)
	heptane	N	Avarmaa et al. (114)
phycoerythrin	gly/buffer	P	Friedrich et al. (203,204)
C-phycocyanin	gly/buffer	P	Friedrich et al. (204, 205)
porphyrazine	PS	N?	Rebane et al. (101)
color centers			
F_3^+	NaF (crystal)	N	Macfarlane and Shelby (206)
607 nm (aggr.[kk] center)	NaF (crystal)	N	Harley and Macfarlane (207)
577 nm (aggr. center)	NaF(crystal)	N	Harley and Macfarlane (208)

[kk] Aggr. ≡ aggregate.

Table 4. Continued

Impurity (class)	Host system	Type HB	Reference
color centers			
F_4^-	NaF:OH^-	N	Moerner et al. (97)
R' color center	LiF: Mg^{+2}	N	Pokrowsky et al. (209)
defect centers (GR1, N-V, H4, N3)	diamond	N	Harley et al. (111)
vibrational transition			
ReO_4^-	KI,RbI (crystals)	N	Moerner et al. (108, 109), Gosnell et al. (110)
difluoroethane	Ar matrix	P	Dubs and Gunthard (210-212), Dubs et al. (213)
	Kr matrix	P	Dubs and Gunthard (211-212), Dubs et al. (213)
	N_2 matrix	P	Dubs and Gunthard (212), Dubs et al. (213)
diflouroethane aggr.	Ar, Kr, N_2 matrix	P	Dubs et al. (213)
methyl nitrite aggr.	N_2 and Ar matixes	P	Felder and Gunthard (214)
methanol aggr.	Ar matrix	P	Felder and Gunthard (214)
other			
trapped electrons (e_t^-)	3MP, MTHF	N	Hager and Willard (215)